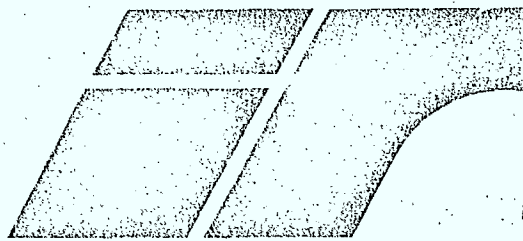


17-309

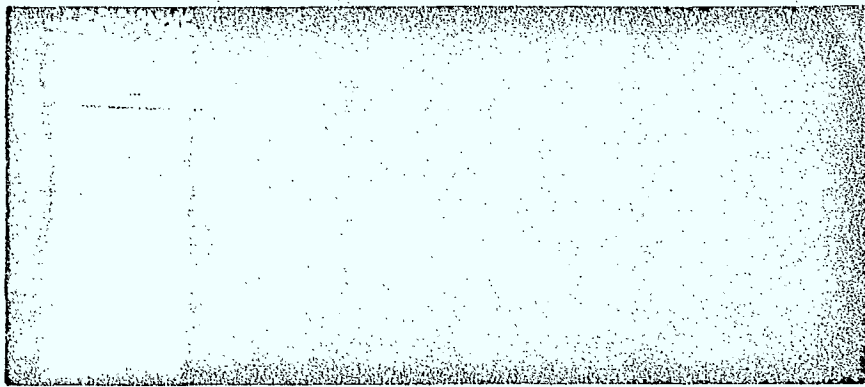
G1

P
91
C655
S4333
1978



Industry Canada
LIBRARY
JUL 20 1998
BIBLIOTHEQUE
Industrie Canada

OFFICE OF INDUSTRIAL RESEARCH



COMMUNICATIONS CANADA
OCT 11 1984
LIBRARY - BIBLIOTHÈQUE



The University of Manitoba, Winnipeg, Manitoba, Canada R3T 2N2

checked 11/83

INVESTIGATION AND DESIGN OF OFFSET
PARABOLOID ANTENNAS FOR LOW CROSS-POLAR RADIATION

FINAL REPORT

Submitted by: Dr. L. Shafai
Dept. of Electrical
Engineering

February 28, 1978

②
INVESTIGATION
AND
DESIGN OF OFFSET
PARABOLOID ANTENNAS
FOR
LOW CROSS-POLAR RADIATION ^o_b

final report

DSS FILE 06SU 36100-7-9517

CONTRACT SERIAL OSU 77-00188

FINAL REPORT

Submitted by: Dr. *L. Shafai*^①
Dept. of Electrical Engineering

FEBRUARY 28, 1978

SUMMARY

This section summarizes the objectives and the results of this report. The objectives were to investigate the performance of an offset paraboloidal antenna and design a suitable feed. Antenna parameters were set at:

Frequency: 11.7 - 12.2 GHz_z

Polarization: Linear and orthozonal-linear

Antenna efficiency > 65

Antenna size: 10 to 15 ft

Side lobe level: lower than $32 - 25 \log \theta$ dB_i for $1^\circ < \theta < 48^\circ$

- 10 dB_i $48^\circ < \theta < 180^\circ$

Cross-polarization level: lower than -25 dB below Copol.

In the course of this investigation certain parameters were modified to facilitate the analysis. As an example, the size of the antenna was somewhat reduced (100λ) to reduce the computational time. This reduction of the antenna size does not affect the antenna performance as far as the polarization or the side lobe levels are concerned. It only reduces the gain as the ratio of the reflector areas. Also, the experimental work on the design of the feed were carried out at 10GHz_z, instead of 12GHz_z. This frequency was selected to facilitate the investigation of the feed performance and its bandwidth. The dimensions of the feed for the above frequency range can be obtained, simply by reducing the dimensions of our feed by a factor of 1.20.

The materials in the next sections present the results of our investigations. The performance of the offset paraboloidal reflectors is investigated first. It is shown that when an offset reflector is illuminated by a

linearly polarized plane wave, its focal region field can be approximated by the field distribution of two waveguide modes. The mixing ratio of these two modes depends on the parameters of the reflector. The main parameters are the offset angle and the f/D of the reflector. Thus, by selecting the proper mixing ratio the cross-polar radiation can be reduced considerably. Furthermore, it is shown that the antenna gain factor normally decreases as the offset angle increases.

From above discussion it is evident that, if the goals of the contract are met by a system with a large offset angle and a small f/D , the performance of any system with smaller offset angles or larger f/D will be more superior. For this reason we have selected our parameters for a "worse case analysis". For the feed a simple circular waveguide is selected. Its geometry is simple and is inexpensive to fabricate. For the reflector a large offset angle of 50° is assumed and its f/D ratio is selected to be small, so that it will have inherently small gain factor and large cross-polarization. With these assumptions the mixing ratio of the TE_{21} to TE_{11} modes needs to be large, so that the cross-polar radiation can be reduced to small values. This large mixing ratio also complicates drastically the design of the feed system. Any system with smaller offset angle and larger f/D will have smaller cross-polar radiation and its feed design will be much simpler, since it requires much smaller excitation level of the TE_{21} mode.

It is shown in the report that for a 50° reflector offset angle and $f/D = 0.4773$ (aperture angle = 45° , $D = 100\lambda$), the original -17 dB cross-polar radiation of the reflector without TE_{21} mode, can be reduced to better

than -36 dB by introducing TE_{21} mode with 0.3 mixing ratio ($d = TE_{21}/TE_{11} = 0.3$). The overall efficiency of the antenna however, drops from 63.12% to 62.81%. This is due to the fact that the introduction of the TE_{21} mode modifies the feed patterns and the above aperture angle is not the optimum one. It is shown that by increasing the aperture angle from 45° to 50° (test case 1) the efficiency increases to 65.597%. That is, the performance of the original reflector with the cross-polar radiation of -17 dB, and the efficiency of 63.12% improves to the cross-polar radiation and efficiency of -37 dB and 65.597%, by introducing the TE_{21} mode with the mixing ratio of $\alpha = 0.3$. It should be noted however, that the above mixing ratio of 0.3 is not the optimum one and is a selected number to show that both the cross-polar radiation and the antenna efficiency can be improved by introducing the TE_{21} mode. The optimum value of α is near 0.3 and will yield much better performance of the cross-polar radiation. The radiation patterns of the reflector is repeated here for convenience, figure a. The required level of side lobes ($32 - 25 \log \theta$ dB₁) is also indicated on the figure, which shows the side lobe levels are considerably lower.

As a second example figure (b) shows the radiation patterns of a reflector with offset angle 30° and $f/D = 0.833$. Here, the required mixing ratio α of TE_{21} and TE_{11} modes is 0.07, which is much smaller than that of the previous case. The figure also shows that the level of the cross-polar radiation has dropped to around -50 dB of the CO-polar field. In addition, the antenna efficiency is much larger and with the above $\alpha = 0.07$ mixing ratio is about 75%. We, therefore, conclude that for better performance of the offset system the offset angle must be small and f/D of the

reflector must be as large as possible. These conditions require smaller mixing ratio of the modes α and the design of the feed becomes much simpler.

To investigate the feed experimentally, we selected the case of $\alpha = 0.3$. This case requires larger component of the TE_{21} mode and its design is more complex. Various ways for exciting this mode were attempted, some of which are indicated in the report. It was found that the excitation of the TE_{21} mode for any of the orthogonal polarizations was in most cases possible, but its excitation with the same α for both polarizations simultaneously was a difficult task. A geometry which could achieve this was finally obtained and its radiation patterns are shown in figures (c) and (d). The performance of this feed over the band is shown to be good. However, the feed requires large aperture obstructions to generate the required mixing ratio of $\alpha = 0.3$.

From above discussions we conclude that generally it is possible to design a feed to give a proper mixing of the TE_{21} and TE_{11} modes to improve the performance of the offset reflector. However, for all above reasons it is recommended that the geometry of the reflector be selected to have small offset angles and large f/D ratios. This geometry will yield a high antenna efficiency and will require a smaller mixing ratio α . The smaller mixing ratio requires smaller obstacles in the waveguide, which improves its frequency performance and simplifies its design.

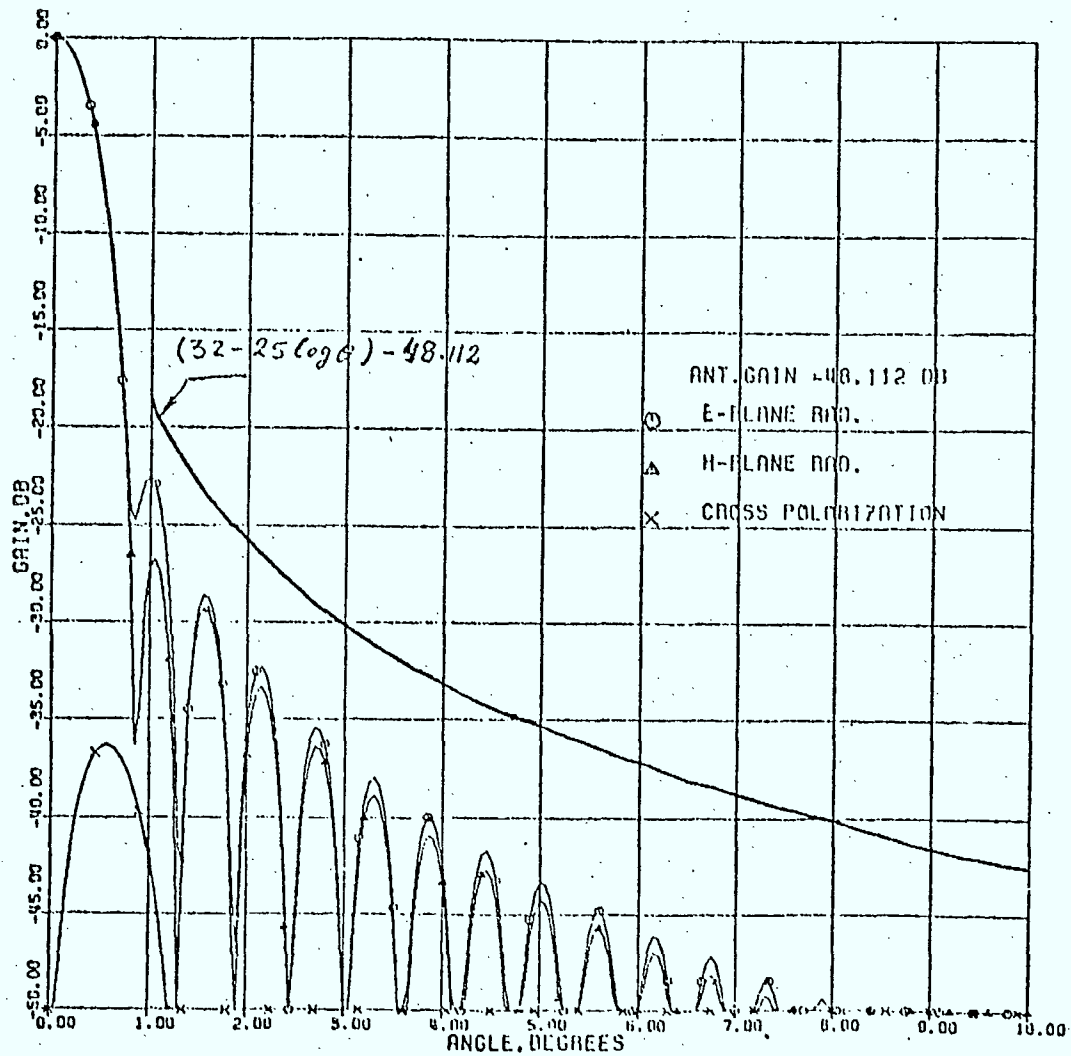


Fig. a) Copolar and cross-polar radiation of an offset reflector with a matched feed, $\alpha=0.3$, $D=100\lambda$, $f=41.95\lambda$, $\theta_0=50^\circ$, $\theta_c=50^\circ$.

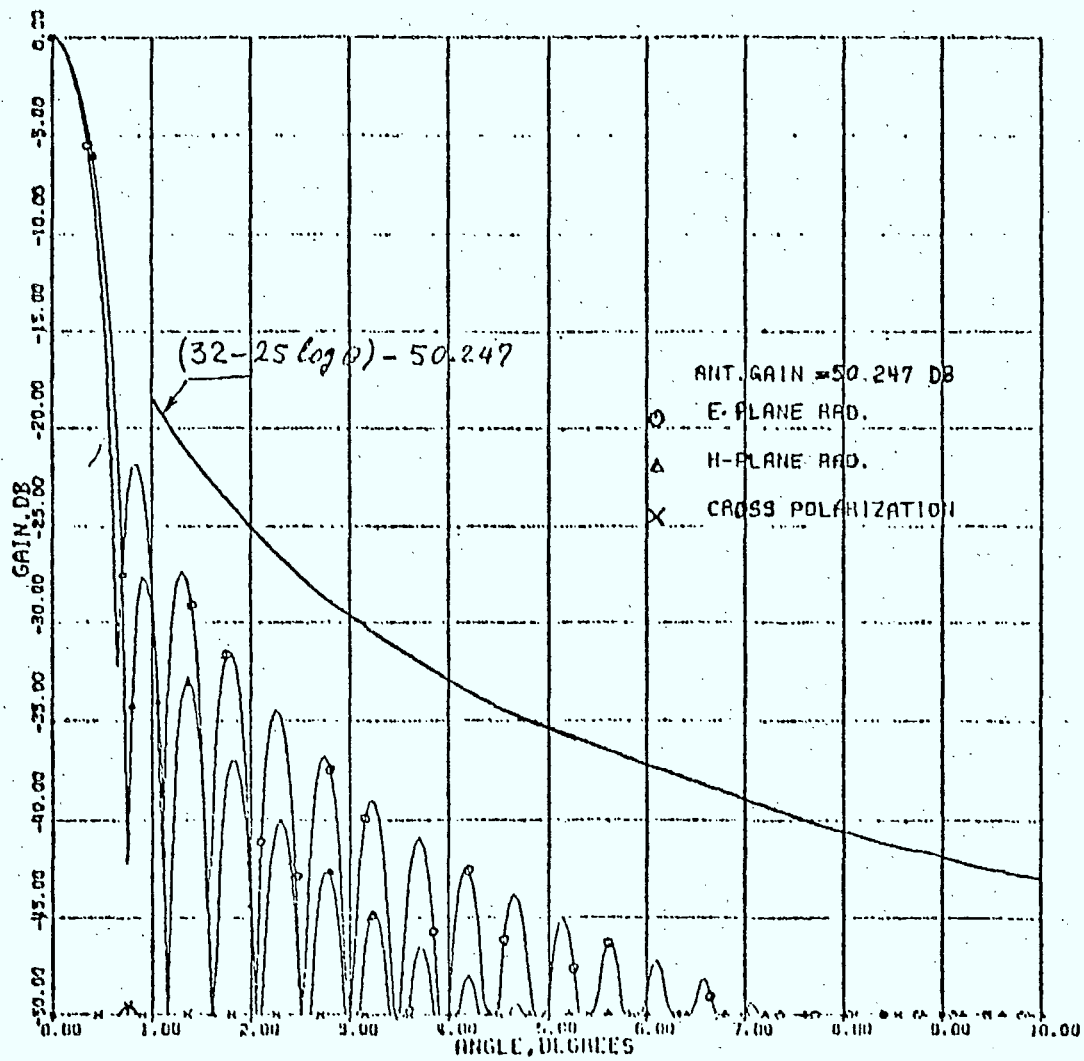


Fig. b) Copolar and cross-polar radiation of an offset reflector with a matched feed, $\alpha=0.07$, $D=120 \lambda$, $f=103.92 \lambda$, $\theta_0=30^\circ$, $\theta_c=30^\circ$.



Fig. c) E-plane radiation patterns of the matched feed, $\alpha=0.3$.

d,

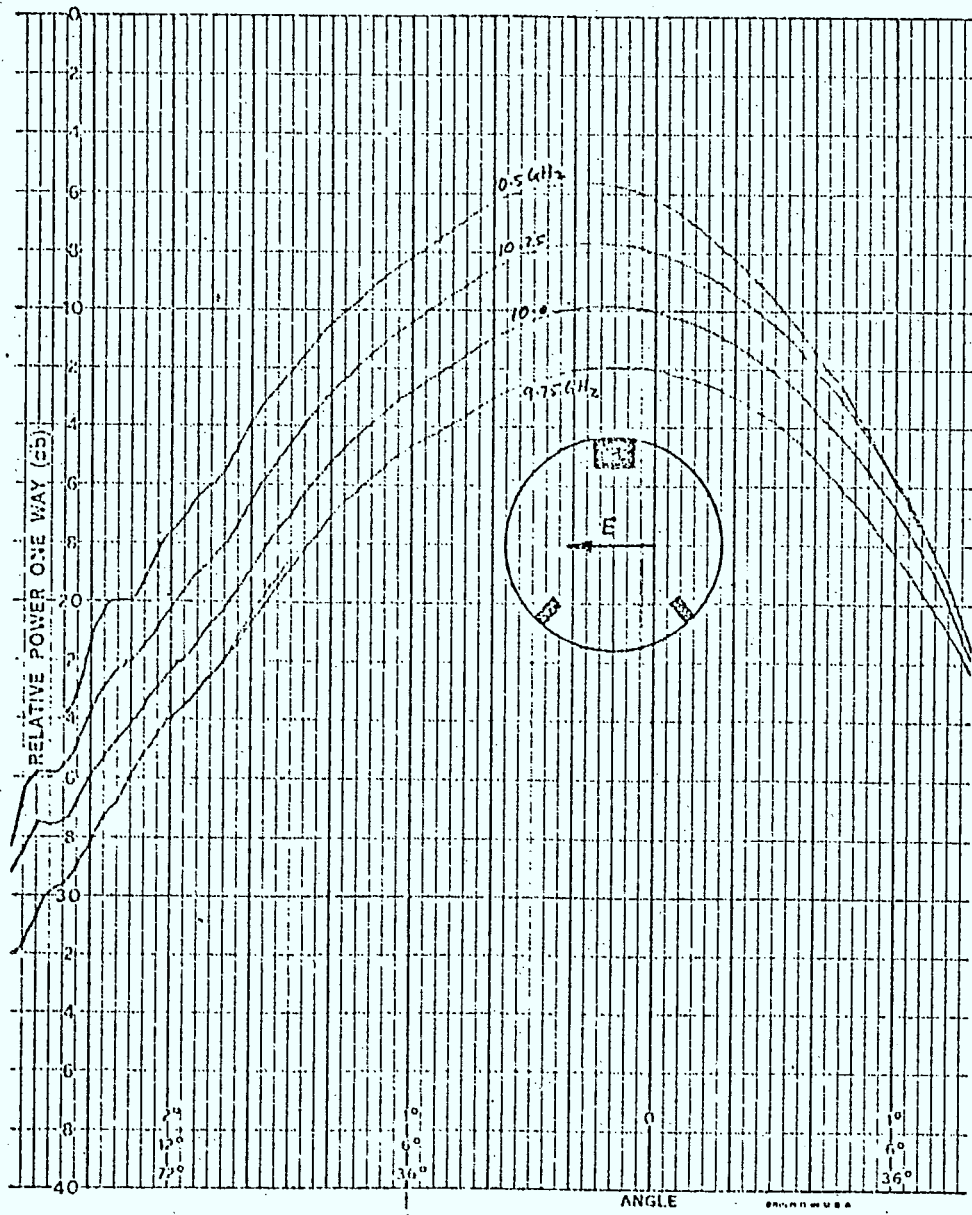


Fig. d) H-plane radiations patterns of the matched feed, $\alpha=0.3$.

ACKNOWLEDGEMENTS

The research for this project was supported by the Communication Research Centre (Res. Cont. DSS-06SU.36100-7-9517) and the National Research Council of Canada (Grant A7702).

Authors would like to thank Dr. R.W. Breithaupt and A.K.C. Kong of Communication Research Centre for initiating this project and many useful discussions, throughout this investigation. They also acknowledge with thanks the assistance of their colleagues at the Electrical Engineering Department of the University of Manitoba. Special thanks are due to Professor E. Bridges for his discussions and encouragement and to Mr. K. Iskander for helping in computer plots.

TABLE OF CONTENTS

	Page Number
ACKNOWLEDGEMENTS	i
ABSTRACT	1
INTRODUCTION	3
GEOMETRICAL PARAMETERS	6
APERTURE FIELD DISTRIBUTION	10
THE VECTOR RADIATION PATTERN	14
MATCHED PRIMARY-FEED	23
METHOD OF STATIONARY PHASE	36
BASIC PARAMETERS	48
NUMERICAL VERIFICATION	53
EXPERIMENTAL RESULTS	59
CONCLUSIONS	65
APPENDIX	165
PLOT PROGRAM	175

ABSTRACT

It is known that the offset parabolic reflector antennas can offer certain advantages over their axisymmetric full-paraboloidal counterpart. Their main advantages are in less or no aperture blockage, less mutual reaction between the reflector and the primary feed and a reduction in the astigmatism for off-axis feed locations. Although these advantages are quite important, the asymmetry of the offset configuration also introduces undesirable characteristics, that is, it deteriorates the polarization property of the antenna and introduces beam squinting effect when a circular polarization is employed. To overcome these inherent disadvantages recently the concept of matched primary feed is introduced, which by matching the depolarization of the offset reflector minimizes the overall depolarization of the antenna. It considers the particular field distribution in the focal plane of the offset reflector, in the receiving mode, when it is illuminated by a linearly-polarized uniform plane wave. By invoking the reciprocity principle, a feed that exactly synthesizes this focal plane field would produce, upon transmission a linearly polarized uniform aperture field distribution. In practice the design of such a feed is not a simple task. However, it is shown in the literature that by exciting two proper waveguide-modes one may approximately obtain the focal plane field and to partially match the primary feed to the offset reflector. Such a feed will then improve the performance of the offset reflector, but the degree of improvement on the performance will depend on the degree of field match between the primary feed and the offset reflector.

This report investigates the improvements in the polarization properties of the offset reflectors using these types of matched feeds. The main interest is in the near-axis fields of the total radiation patterns where a straight use of the stationary phase method for the field computation is not applicable. However, to reduce the computational labour a modified version, suggested in the literature is utilized. That is, the stationary phase method is used to carry out the integration for the azimuthal coordinate, but the results are modified to be more exact by recognizing the asymptotic forms and replacing them by the exact expressions. The remaining integral is carried out numerically. The vector radiation patterns presented here reduce to known exact expressions of the offset reflectors with the fundamental mode primary feeds, or to those of symmetric paraboloid antennas.

1. INTRODUCTION

The vector-radiation fields of offset parabolic antennas and their depolarization properties have previously been examined by Cook et al. [1] and more recently by Chu and Turrin [2] and Rudge [3], [4]. The mathematical model that provides the prediction of both copolar and cross-polar radiations from the offset parabolic reflectors, illuminated by a conventional linearly polarized primary feed, has been given by Shafai and Aboul-Atta [5], [6]. The electric field distribution in the focal region of an offset reflector and for a normally incident linearly polarized plane wave is investigated by Bem [7] and the polarization losses due to dipole and Huggen-source primary feeds is calculated by Dijk et al [8].

The above investigations show the performance limitations of the offset reflectors. When illuminated by a linearly polarized feed they generate a high degree of cross-polar radiation, which increases with an increase of the offset angle. They also generate a relatively large beam-squint angle, when illuminated by a circularly polarized feed. These limitations have let Rudge [10] to develop the "offset reflector matched feed concept" and design [11] a new class of primary feeds [Applied for a British patent], which makes use of a higher order waveguide modes to compensate for the reflector generated cross polar radiation.

Compared to its full-paraboloidal counterpart, the offset reflector avoids the aperture blocking, reduces the reflector reaction on the primary feed and offers a reduction in the astigmatism for the off-

axis feed location [12] and [13]. The fact that in such an antenna the aperture blockage by the primary feed and its support structure is avoided makes the side-lobe and the gain performance of the offset antenna significantly better than those of an equivalent axisymmetric reflector with similar illumination characteristics [14] and [15]. The major drawback of these antennas, which can be attributed directly to the asymmetrical nature of the offset geometry [2], has been their poor polarization performance. This can now be alleviated by the use of non-conventional dimode or trimode, linear or circularly polarized, primary feeds described by Rudge [10] and [11]. Hence, the offset paraboloidal reflector with a projected circular aperture becomes an attractive design for the satellite or earth station antennas, when low side-lobe and low cross-polarization performances are desirable features. Since the aperture field of this new class of primary feeds effectively matches the focal plane field of the offset reflector when illuminated (in the receiving mode) by a linearly polarized uniform plane wave, they have been termed "matched feeds".

The research described in this report essentially considers the theoretical potential of these matched feed devices with dual linear polarization. It examines the feasibility of their use for illuminating offset parabolic reflectors to meet certain design goals of low side-lobe and low cross-polarization levels. A simple mathematical model is developed, which provides the prediction of both copolar and cross-polar radiation of the offset antennas illuminated by these matched feeds. The model is developed with the prime objective of producing sufficiently accurate results with relatively small computation cost.

It utilizes a modified stationary phase approximation [16] to eliminate one integration, while retaining a good accuracy as compared with the results of double integration techniques. This is achieved by detecting the asymptotic expressions of the Bessel functions in the results of the stationary phase approximation for the integral and replacing them by their exact form. The net outcome of the method is a single integral, which can be carried out numerically to yield the radiation patterns of the reflector. The expressions for the vector radiation patterns reduce to the exact expressions, obtained by other [5] and [6], for the offset antennas illuminated by conventional primary feeds. They also become identical to those of symmetrical paraboloidal antennas, obtained by direct integration process.

2. GEOMETRICAL PARAMETERS

Fig. 1 shows the geometry of the offset reflector under discussion. This type of geometry is typically characterised by three basic parameters f , θ_0 , and θ_c , where (f) is the focal length of the parent paraboloid, θ_0 is the offset angle and θ_c is the semi-angle subtended by the reflector periphery at the geometrical focus. The physical contour of the reflector is elliptical, but its projection into the focal plane ($z = 0$) produces a true circle. In terms of the above mentioned reflector characteristics, the following parameters, that are of interest to the present work can be usefully expressed in a concise form. These parameters are the diameter D of the parent paraboloid, the clearance distance d_c between the negative z -axis and the lower edge of the aperture, the position x_0 of the projected-aperture center relative to the geometric focus, the diameter d of the projected-aperture, the position vector $\bar{p}' \equiv (p', \theta', \phi')$ of an arbitrary point on the reflector surface, and its projected radial vector \bar{r} in the focal plane. Their mathematical expressions are given by

$$D = 4 f \text{ TAN } (\frac{1}{2}[\theta_0 + \theta_c])$$

$$d_c = 2 f \text{ TAN } (\frac{1}{2}[\theta_0 - \theta_c])$$

$$x_0 = 2 f \text{ SIN } \theta_0 / (\text{COS } \theta_0 + \text{COS } \theta_c)$$

$$d = 4 f \text{ SIN } \theta_c / (\text{COS } \theta_0 + \text{COS } \theta_c)$$

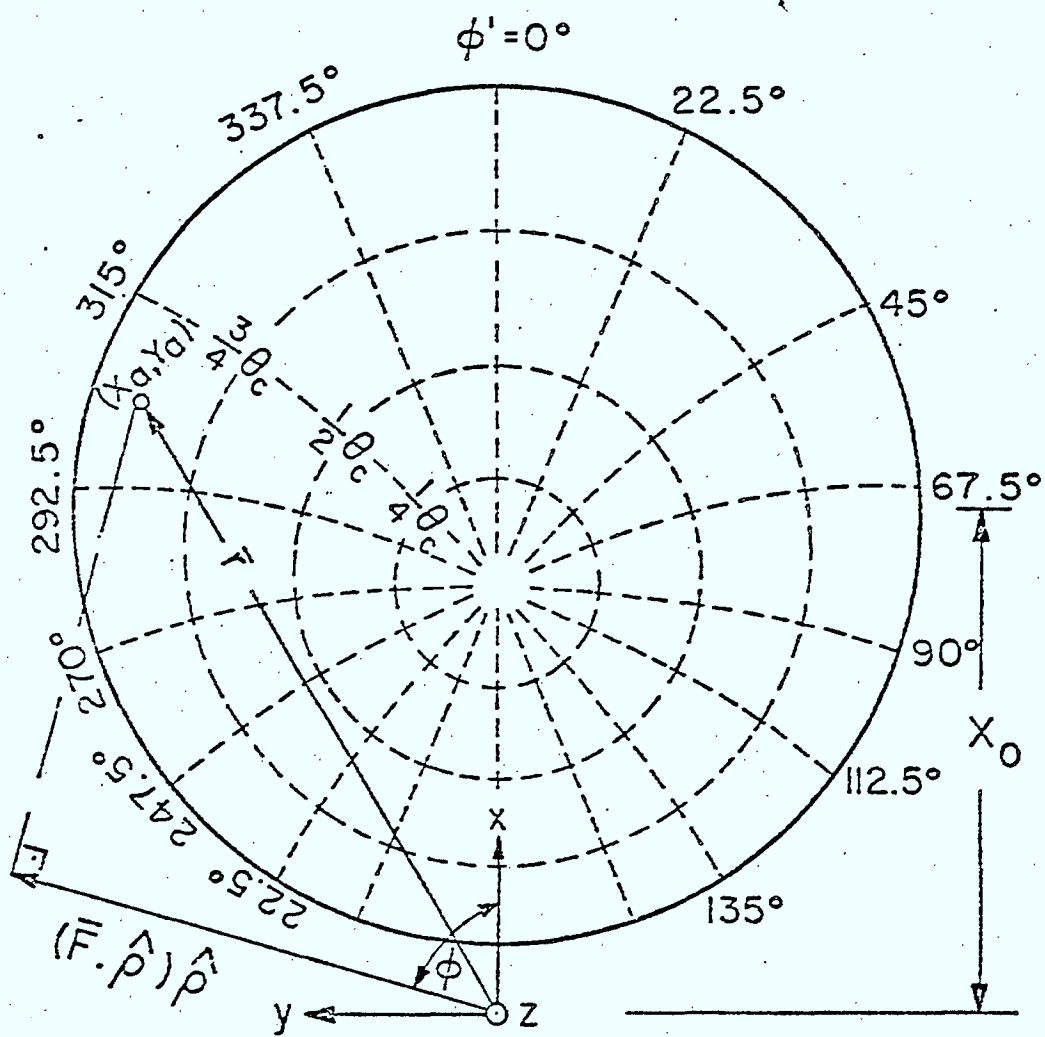
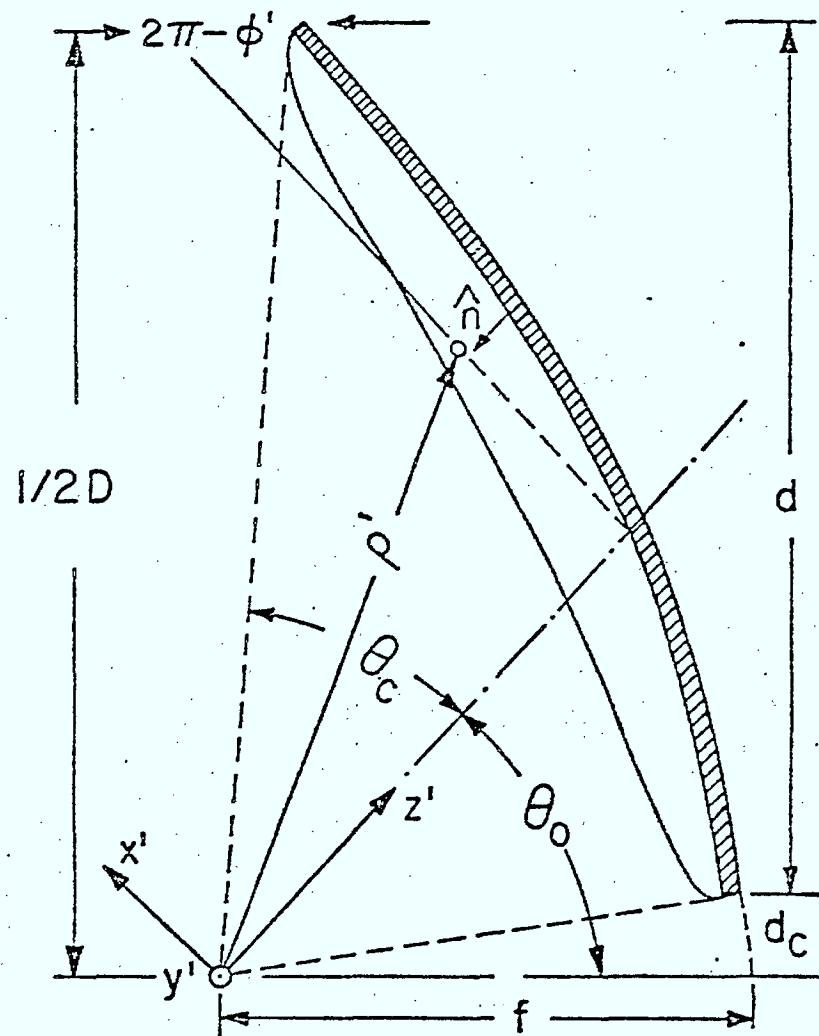


Fig. 1 Front view of the projected aperture in the focal plane



Cross sectional view in the plane of symmetry

$$\rho' = 2 f/t \quad , \quad t = 1 + \cos \theta' \cos \theta_0 - \sin \theta' \sin \theta_0 \cos \phi'$$

$$\bar{r} = \hat{x} \rho' [\cos \theta' \sin \theta_0 + \sin \theta' \cos \theta_0 \cos \phi'] - \hat{y} \rho' [\sin \theta' \sin \phi']$$

It has been shown previously [1] that the projection of $\bar{\rho}'$, for a constant θ' , on the focal plane describes a circle as ϕ' varies from 0 to 2π this circle can be defined by the equation

$$\left(x - \frac{2 f \sin \theta_0}{\cos \theta_0 + \cos \theta'}\right)^2 + y^2 = \left(\frac{2 f \sin \theta'}{\cos \theta_0 + \cos \theta'}\right)^2$$

and a family of such circles is shown in Fig. 1. This figure also shows the projections of $\bar{\rho}'$ for various values of ϕ' . As seen in the figure, the antenna is best described by two coordinate systems. The primed coordinates $\bar{R}' \equiv (x', y', z') \equiv (R', \theta', \phi')$ which has its best use in describing the primary-feed radiation field \underline{E}_f as well as some properties of the reflector surface and the main coordinates $\bar{R} \equiv (x, y, z) \equiv (R, \psi, \Phi)$ often used to describe the vector-radiation field of the offset antenna at an arbitrary observation point P relative to the boresight ($z = 0$). For a surface point S on the reflector, $\bar{R}_s \equiv \bar{\rho}' \equiv (x'_s, y'_s, z'_s) \equiv (\rho', \theta', \phi')$ $\bar{R}_s = \bar{\rho}_s \equiv (x_a, y_a, z_s) \equiv (\rho', \theta, \phi)$, $\hat{n} = (\hat{z} - \beta)/\sqrt{2t}$, and its projection on the aperture $\bar{r} \equiv (x_a, y_a) \equiv (r, \frac{1}{2}\pi, \phi)$ the following relations can be easily varified [17]

$$(x_a^2 + y_a^2) = 4 f (z_s + f)$$

$$\hat{n} = \hat{x} n_x + \hat{y} n_y + \hat{z} n_z$$

$$n_x = -\cos \phi \sin \frac{1}{2} \theta$$

$$n_y = -\sin \phi \cos \frac{1}{2} \theta$$

$$n_z = \sin \frac{1}{2} \theta$$

and ds , the differential surface element is given by,

$$ds = (dx_a dy_a) / \sin \frac{1}{2} \theta = (\rho'^2 \sin \theta' d\theta' d\phi') / \sin \frac{1}{2} \theta$$

with reference to those coordinates, the transformation of the unit vectors $(\hat{\rho}', \hat{\theta}', \hat{\phi}') \rightarrow (\hat{x}', \hat{y}', \hat{z}') \rightarrow (\hat{x}, \hat{y}, \hat{z})$ can be summarized as follows [2].

$$\hat{\rho}' = \sin \theta' \cos \phi' \hat{x}' + \sin \theta' \sin \phi' \hat{y}' + \cos \theta' \hat{z}'$$

$$\hat{\theta}' = \cos \theta' \cos \phi' \hat{x}' + \cos \theta' \sin \phi' \hat{y}' - \sin \theta' \hat{z}'$$

$$\hat{\phi}' = -\sin \phi' \hat{x}' + \cos \phi' \hat{y}', \quad \hat{z}' = \sin \theta_0 \hat{x} - \cos \theta_0 \hat{z}$$

$$\hat{x}' = \cos \theta_0 \hat{x} + \sin \theta_0 \hat{z}$$

$$\hat{y}' = -\hat{y}$$

$$\hat{z}' = \sin \theta_0 \hat{x} - \cos \theta_0 \hat{z}$$

In the prime coordinates the following unit vectors can be easily recognized in their spherical representation,

$$\hat{\rho}' \equiv (1, \theta', \phi') \quad , \quad \hat{\theta}' \equiv (1, \frac{\pi}{2} + \theta', \phi') \quad , \quad \hat{\phi}' \equiv (1, \frac{1}{2}\pi, \frac{1}{2}\pi + \phi')$$

$$\hat{x} \equiv (1, \frac{1}{2}\pi - \theta_0, 0) \quad , \quad \hat{y} \equiv (1, \frac{\pi}{2}, \frac{3\pi}{2}) \quad , \quad \hat{z} \equiv (1, \pi - \theta_0, 0)$$

$$\hat{x}' \equiv (1, \frac{1}{2}\pi, 0) \quad , \quad \hat{y}' \equiv (1, \frac{1}{2}\pi, \frac{1}{2}\pi) \quad , \quad \hat{z} \equiv (1, 0, 0)$$

where the standard inner product of any two of the above unit vectors becomes

$$\hat{e}_i \cdot \hat{e}_j = \cos \gamma_{ij} = \cos \theta'_i \cos \theta'_j + \sin \theta'_i \sin \theta'_j \cos(\phi'_i - \phi'_j).$$

To be more precise the following inner products are required in the formulation of the aperture-field dependence on the primary-feed radiation pattern,

$$\hat{x} \cdot \hat{\rho}' = \cos \theta' \sin \theta_0 + \sin \theta' \cos \theta_0 \cos \phi'$$

$$\hat{x} \cdot \hat{\theta}' = -\sin \theta' \sin \theta_0 + \cos \theta' \cos \theta_0 \cos \phi'$$

$$\hat{x} \cdot \hat{\phi}' = -\cos \theta_0 \sin \phi'$$

$$\hat{y} \cdot \hat{\rho}' = -\sin \theta' \sin \phi'$$

$$\hat{y} \cdot \hat{\theta}' = -\cos \theta' \sin \phi'$$

$$\hat{y} \cdot \hat{\phi}' = -\cos \phi'$$

$$\hat{z} \cdot \hat{\rho}' = -\cos \theta' \cos \theta_0 + \sin \theta' \sin \theta_0 \cos \phi'$$

$$\hat{z} \cdot \hat{\theta}' = \sin \theta' \cos \theta_0 + \cos \theta' \sin \theta_0 \cos \phi'$$

$$\hat{z} \cdot \hat{\phi}' = -\sin \theta_0 \sin \phi'$$

3. APERTURE FIELD DISTRIBUTION

The distribution of the tangential electric field on the focal plane projected aperture region is determined by the use of the physical optics approximation. This method is preferred over the surface current method, since within a 30° cone angle, it predicts far field results with no significant difference with those of the surface current method. In addition, the aperture-field method leads to simpler mathematical expressions and offers the possibility of a significant reduction in the required computational effort. The electric field \underline{E}_r reflected from

the offset reflector is obtained from [12], [13]

$$(1) \quad \underline{E}_r = 2(\hat{n} \cdot \underline{E}_i)\hat{n} - \underline{E}_i$$

where \underline{E}_i is the incident electric field at the reflector surface and \hat{n} is the surface unit normal. The incident electric field \underline{E}_i is taken as the radiation field of the primary-feed with the following representation in the spherical coordinate system (R', θ', ϕ')

$$\underline{E}_f = E_f^{\theta'} \hat{\theta}' + E_f^{\phi'} \hat{\phi}'$$

A direct substitution of \underline{E}_f , in equation (1) and utilizing \hat{n} as given in section 2, yields

$$\begin{aligned} \underline{E}_r &= \hat{x}[2(\hat{n} \cdot \underline{E}_f)(\hat{n} \cdot \hat{x}) - (\hat{x} \cdot \underline{E}_f)] + \hat{y}[2(\hat{n} \cdot \underline{E}_f)(\hat{n} \cdot \hat{y}) - (\hat{y} \cdot \underline{E}_f)] \\ &= -\hat{x}[(\hat{z} \cdot \underline{E}_f)(\hat{x} \cdot \hat{\rho}') \frac{1}{t} + (\hat{x} \cdot \underline{E}_f)] - \hat{y}[(\hat{z} \cdot \underline{E}_f)(\hat{y} \cdot \hat{\rho}') \frac{1}{t} + (\hat{y} \cdot \underline{E}_f)] \\ &= -\frac{\hat{x}}{t} \{[(\hat{z} \cdot \hat{\theta}')(\hat{x} \cdot \hat{\rho}') + (\hat{x} \cdot \hat{\theta}')t] E_f^{\theta'} + [(\hat{z} \cdot \hat{\phi}')(\hat{x} \cdot \hat{\rho}') + (\hat{x} \cdot \hat{\phi}')t] E_f^{\phi'}\} \\ &\quad - \frac{\hat{y}}{t} \{[(\hat{z} \cdot \hat{\theta}')(\hat{y} \cdot \hat{\rho}') + (\hat{y} \cdot \hat{\theta}')t] E_f^{\theta'} + [(\hat{z} \cdot \hat{\phi}')(\hat{y} \cdot \hat{\rho}') + (\hat{y} \cdot \hat{\phi}')t] E_f^{\phi'}\} \end{aligned}$$

Therefore,

$$\begin{aligned} \underline{E}_r &= \frac{\hat{x}}{t} \{[\sin \theta' \sin \theta_0 - \cos \phi'(1 + \cos \theta' \cos \theta_0)] E_f^{\theta'} + \\ &\quad [\sin \phi'(\cos \theta' + \cos \theta_0)] E_f^{\phi'}\} \\ &\quad + \frac{\hat{y}}{t} \{[\sin \phi'(\cos \theta' + \cos \theta_0)] E_f^{\theta'} - [\sin \theta' \sin \theta_0 - \cos \phi' \\ &\quad (1 + \cos \theta' \cos \theta_0)] E_f^{\phi'}\} \end{aligned}$$

In this report, the same abbreviations previously used by Shafai [5] and others [16] have been adopted to simplify the above expression for the reflected field. That is

$$a = 1 + \cos\theta' \cos\theta_0$$

$$b = \sin\theta' \sin\theta_0$$

$$c = \cos\theta' + \cos\theta_0, \quad c^2 = a^2 - b^2$$

and,

$$\begin{bmatrix} E_r^x \\ E_r^y \end{bmatrix} = \frac{1}{t} \begin{bmatrix} (b-a \cos\phi') & c \sin\phi' \\ c \sin\phi' & -(b-a \cos\phi') \end{bmatrix} \begin{bmatrix} E_f^{\theta'} \\ E_f^{\phi'} \end{bmatrix}$$

When the phase center of the primary-feed is located at the reflector geometric focus, the incident field at the surface of the reflector can be expressed in the form

$$(2) \quad \underline{E}_f = (A_{\theta'} \hat{\theta}' + A_{\phi'} \hat{\phi}') \frac{e^{-jk\rho'}}{\rho'}$$

where $A_{\theta'}$ and $A_{\phi'}$ are functions of (θ', ϕ') and describe the variation of the primary-feed radiation pattern on a sphere of constant radius and k is the propagation constant $(2\pi/\lambda)$. This facilitates the writing of the aperture field \underline{E}_A in terms of the primary-feed radiation pattern, which in the matrix forms:

$$(3) \begin{bmatrix} E_A^x \\ E_A^y \end{bmatrix} = \frac{e^{-j2kf}}{2f} \begin{bmatrix} (b-a \cos \phi') & c \sin \phi' \\ c \sin \phi' & -(b-a \cos \phi') \end{bmatrix} \begin{bmatrix} A_{\theta'} \\ A_{\phi'} \end{bmatrix}$$

4. THE VECTOR RADIATION PATTERN

The far field radiation arising from a known tangential electric field distribution on an infinite plane can be determined exactly [13]. In dealing with the offset reflectors, the infinite surface is chosen as the focal plane (xy -plane, $z=0$) and the tangential electric field outside the projected-aperture region is assumed to be negligible. Neglecting the electric field outside the projected aperture region is acceptable [4] provided that the dimension of the aperture area is large compared to the electrical wave length λ . By invoking the spatial Fourier transform formulation [12], and making use of the Ludwig's definition of the polarization [18], the principal and cross-polarized components of the antenna far fields can be expressed in terms of the resolved principal and cross-polarized components of the reflector aperture electric field distributions. The mathematical expression that relates the above mentioned quantities involve a pair of two dimensional integrals, which can be evaluated, at least numerically, for each field observation point $P \equiv [R, \Psi, \Phi]$. This expression which is based on the above mentioned tangential aperture field distribution has in the past proved successful in providing accurate and computationally economic prediction of both the principal and the cross-polarized radiation fields from high gain offset reflectors over a moderate range of angles about the boresight [10]. Within these ranges, the mathematical expression for the antenna vector-radiation pattern, based on the projected-aperture model, has been given previously by Silver [12]

$$(4) \quad \underline{E}(P) = \left(\frac{jke^{-jkR}}{4\pi R} \right) \int_A ([\hat{R} + \hat{Z}] \times \underline{E}_A] \times \hat{R}) e^{jk\bar{r} \cdot \hat{R}} dA$$

where

\underline{r} = is the radial vector from the origin of the projected-aperture to the integration point in the aperture

\hat{R} = is the unit vector which specifies the direction of the observation point $P \equiv (R, \Psi, \Phi)$ relative to the origin of the aperture.

A = is the area of the projected-aperture.

In terms of two arbitrary, yet spatially orthogonal, unit vectors \hat{p} and \hat{q} ($\hat{p} \times \hat{q} = \hat{z}$) in the projected area, equation (4) can be written by defining two functions ϵ_p and ϵ_q as the spatial Fourier transforms of the (p, q) - components of the tangential electric field \underline{E}_A respectively. That is,

$$(5) \quad \underline{E}(P) = \left(\frac{j e^{-jkR}}{\lambda R} \right) \left(\frac{1 + \cos \Psi}{2} \right) [\hat{e}_p \epsilon_p + \hat{e}_q \epsilon_q] = \hat{e}_p E^p + \hat{e}_q E^q$$

where,

$$\hat{e}_p = \cos(\Phi - \Phi_p) \hat{\Psi} - \sin(\Phi - \Phi_p) \hat{\Phi}$$

$$\hat{e}_q = \sin(\Phi - \Phi_p) \hat{\Psi} + \cos(\Phi - \Phi_p) \hat{\Phi}$$

$$\epsilon_p = \int_A (\hat{p} \cdot \underline{E}_A) e^{jk\bar{r} \cdot \hat{R}} dA$$

$$\epsilon_q = \int_A (\hat{q} \cdot \underline{E}_A) e^{jk\bar{r} \cdot \hat{R}} dA$$

Φ_p = is the angle of the unit vector \hat{p} with the positive x-axis

The (E^Ψ, E^Φ) - components of the antenna vector-radiation field in the spherical coordinate system (R, Ψ, Φ) can be related to the (p, q) - components of the measured field of the antenna (E^p, E^q) , as well as the two spatial Fourier transforms of the aperture field distribution (ϵ_p, ϵ_q) in the following matrix forms,

$$(6) \begin{bmatrix} E^p \\ E^q \end{bmatrix} = \begin{bmatrix} \cos(\Phi - \Phi_p) & -\sin(\Phi - \Phi_p) \\ +\sin(\Phi - \Phi_p) & \cos(\Phi - \Phi_p) \end{bmatrix} \begin{bmatrix} E^\Psi \\ E^\Phi \end{bmatrix}$$

$$(7) \begin{bmatrix} E^\Psi \\ E^\Phi \end{bmatrix} = \left(\frac{je^{-jkR}}{\lambda R} \right) \left(\frac{1 + \cos \Psi}{2} \right) \begin{bmatrix} \cos(\Phi - \Phi_p) + \sin(\Phi - \Phi_p) \\ -\sin(\Phi - \Phi_p) & \cos(\Phi - \Phi_p) \end{bmatrix} \begin{bmatrix} \epsilon_p \\ \epsilon_q \end{bmatrix}$$

Therefore,

$$(8) \begin{bmatrix} E^p \\ E^q \end{bmatrix} = \left(\frac{je^{-jkR}}{\lambda R} \right) \left(\frac{1 + \cos \Psi}{2} \right) \begin{bmatrix} \epsilon_p \\ \epsilon_q \end{bmatrix}$$

That is, the magnitude of the electric field can be directly related to the spatial Fourier transform by the use of equation (8)

$$||E|| = \frac{1}{\lambda R} \left(\frac{1 + \cos \Psi}{2} \right) \sqrt{|\epsilon_p|^2 + |\epsilon_q|^2}$$

Since, according to equation (3), the projected aperture field distribution is

$$(9) \begin{bmatrix} p \\ E_A \\ q \\ E_A \end{bmatrix} = \left(\frac{e^{-j2kf}}{2f} \right) \begin{bmatrix} \cos \phi_p & \sin \phi_p \\ -\sin \phi_p & \cos \phi_p \end{bmatrix} \begin{bmatrix} c_1 & s_1 \\ s_1 & -c_1 \end{bmatrix} \begin{bmatrix} A_{\theta'} \\ A_{\phi'} \end{bmatrix}$$

where,

$$\underline{E}_A = \hat{p} E_A^p + \hat{q} E_A^q$$

$$c_1 = b - a \cos \phi'$$

$$s_1 = c \sin \phi'$$

Then, the spatial Fourier transforms (ϵ_p, ϵ_q) becomes

$$\epsilon_p = 2f e^{-j2kf} \int_0^{2\pi} \int_0^{\theta_c} [\cos \phi_p (c_1 A_{\theta'} + s_1 A_{\phi'}) + \sin \phi_p (s_1 A_{\theta'} - c_1 A_{\phi'})] \frac{\sin \theta'}{t^2} e^{jk\bar{r} \cdot \hat{R}} d\theta' d\phi'$$

$$\epsilon_q = 2f e^{-j2kf} \int_0^{2\pi} \int_0^{\theta_c} [-\sin \phi_p (c_1 A_{\theta'} + s_1 A_{\phi'}) + \cos \phi_p (s_1 A_{\theta'} - c_1 A_{\phi'})] \frac{\sin \theta'}{t^2} e^{jk\bar{r} \cdot \hat{R}} d\theta' d\phi'$$

This indicates the dependence of (ϵ_p, ϵ_q) on the primary-feed radiation pattern $(A_{\theta'}, A_{\phi'})$ through the following two specific spatial Fourier transform (γ, δ)

$$\begin{bmatrix} \gamma \\ \delta \end{bmatrix} = \int_0^{2\pi} \int_0^{\theta_c} (c_1 A_{\theta'} \pm s_1 A_{\phi'}) \frac{\text{SIN } \theta'}{r^2} e^{jk\bar{r} \cdot \hat{R}} d\theta' d\phi'$$

$$\epsilon_p = 2f e^{-j2kf} [\gamma \text{COS } \phi_p + \delta \text{SIN } \phi_p]$$

$$\epsilon_c = 2f e^{-j2kf} [-\gamma \text{SIN } \phi_p + \delta \text{COS } \phi_p]$$

The literature survey [2], [10] indicates that when the offset antenna is used in conjunction with a conventional linearly polarized primary-feed with balanced and well suppressed cross-polarized radiation (i.e. of the type constructed by Shafai [5] and Potter [9]) of the form

$$\underline{E}_f = F(\theta') [\text{COS}(\phi' - \phi_p) \hat{\theta}' - \text{SIN}(\phi' - \phi_p) \hat{\phi}'] \frac{e^{-jkR'}}{R'}$$

the overall radiation pattern of the antenna exhibits cross-polarized components which is directly attributed to the depolarization properties of the offset reflector geometry. The radiated cross-polar energy forms a pair of characteristic lobes in the plane of asymmetry of the reflector (i.e. yz-plane of Fig. 1). The peak level of these lobes, as compared to the peak level of the copolar main beam, are strongly dependent upon the reflector angular parameters θ_0 and θ_c and is comparatively insensitive to the illumination taper introduced by the primary-feed. The above can be obtained directly from equation (9) in the form

$$\begin{bmatrix} p \\ E_A \\ q \\ E_A \end{bmatrix} = - \frac{e^{-j2kf} F(\theta')}{2f} \left(\frac{a+c}{2} \begin{bmatrix} +\text{COS}(\phi_p + \phi'_p) \\ -\text{SIN}(\phi_p + \phi'_p) \end{bmatrix} + \frac{a-c}{2} \begin{bmatrix} \text{COS}[2\phi' - (\phi_p + \phi'_p)] \\ \text{SIN}[2\phi' - (\phi_p + \phi'_p)] \end{bmatrix} \right. \\ \left. - b \begin{bmatrix} \text{COS}[\phi' - (\phi_p + \phi'_p)] \\ \text{SIN}[\phi' - (\phi_p + \phi'_p)] \end{bmatrix} \right)$$

Although the choice of \hat{p} is considered arbitrary, the previous relation shows that the preference is usually given to $\phi_p = -\phi'_p$ (when the symmetry of the aperture around $\phi = \phi' = 0$ prevails) to enhance the even/odd property of E_A^p/E_A^q respectively with respect to $\phi' = 0$. The same can be generalized for unbalanced conventional primary-feeds of the type

$$\underline{E}_f = [EP(\theta') \text{COS}(\phi' - \phi'_p) \hat{\theta}' - HP(\theta') \text{SIN}(\phi' - \phi'_p) \hat{\phi}'] \frac{e^{-jkR'}}{R'}$$

by a direct substitution in equation (9) while observing the specific choice $\phi_p = -\phi'_p$

$$\begin{bmatrix} p \\ E_A \\ q \\ E_A \end{bmatrix} = - \frac{e^{-j2kf}}{2f} \left(\frac{a+c}{2} \begin{bmatrix} A + B \text{COS}(2\phi' - 2\phi'_p) \\ 0 - B \text{SIN}(2\phi' - 2\phi'_p) \end{bmatrix} + \frac{a-c}{2} \begin{bmatrix} A \text{COS} 2\phi' + B \text{COS} 2\phi'_p \\ A \text{SIN} 2\phi' + B \text{SIN} 2\phi'_p \end{bmatrix} \right. \\ \left. - b \begin{bmatrix} A \text{COS} \phi' + B \text{COS}(\phi' - 2\phi'_p) \\ A \text{SIN} \phi' - B \text{SIN}(\phi' - 2\phi'_p) \end{bmatrix} \right).$$

where, $A = \frac{1}{2}(EP + HP)$ and $B = \frac{1}{2}(EP - HP)$

To retain the same symmetry mentioned before, ϕ'_p must be limited only to the special cases $\phi'_p = r \frac{\pi}{2}$. That is, the main polarizations of the primary-feed are best considered in the x' and y' direction as follows

$$(10) \begin{bmatrix} p \\ E_A \\ q \\ E_A \end{bmatrix} = -\frac{e^{-jkR}}{2f} \begin{bmatrix} [A(\frac{a+c}{2}) + (-1)^r B(\frac{a-c}{2})] - [b(A + (-1)^r B)] \cos \phi' + \\ - [b(A - (-1)^r B)] \sin \phi' + \\ [A(\frac{a-c}{2}) + (-1)^r B(\frac{a+c}{2})] \cos 2\phi' \\ [A(\frac{a-c}{2}) - (-1)^r B(\frac{a+c}{2})] \sin 2\phi' \end{bmatrix}$$

Of interest to the present work are the multi-mode feeds of the type

$$(11) \quad E_f = \frac{e^{-jkR'}}{R'} \sum_{\ell=1}^n [E^\ell \cos(\gamma\phi' - \phi'_p) \hat{\theta}' - H^\ell \sin(\gamma\phi' - \phi'_p) \hat{\phi}']$$

which leads to the following aperture field distributions

$$E_A^p = -K \sum_0^{n+1} (S_m^+ \cos[m\phi' - (\phi'_p + \phi_p)] + S_m^- \cos[m\phi' - (\phi'_p - \phi_p)])$$

$$E_A^q = -K \sum_0^{n+1} (S_m^+ \sin[m\phi' - (\phi'_p + \phi_p)] - S_m^- \sin[m\phi' - (\phi'_p - \phi_p)])$$

where

$$K = e^{-j2kf/2f}$$

$$S_m^{\pm} = \left[\left(\frac{E^{m+1} \pm H^{m+1}}{2} \right) \left(\frac{a \pm c}{2} \right) - b \left(\frac{E^m \pm H^m}{2} \right) + \left(\frac{E^{m-1} \pm H^{m-1}}{2} \right) \left(\frac{a \mp c}{2} \right) \right]$$

The evidence that S_m^- coefficients are identically zero for highly balanced feeds, suggests the definition of \hat{p} to be $\phi_p = -\phi_p'$ in order to bring about the even/odd symmetries previously mentioned. In that context, the p-component becomes known as the copolar component of the aperture field, while the q-component becomes the cross-polar part. Because the different modes in the given primary-feed are not always balanced, it is better to restrict the primary-feed polarizations to the x' or y' axis ($\phi_p' = r \frac{\pi}{2}$) to retain the symmetry and its accompanied mathematical simplifications. That is,

$$(12) \quad E_{-A} = -K \left[\hat{p} \sum_0^{n+1} p_m \cos m\phi' + \hat{q} \sum_1^{n+1} q_m \sin m\phi' \right]$$

where

$$p_m = S_m^+ + (-1)^{\ell} S_m^-$$

$$q_m = S_m^+ - (-1)^{\ell} S_m^-$$

For the case of only one mode, say n , the above summation starts at $(n-1)$ and end at $(n+1)$, while the E, H parameters for the other modes are taken to be zero. For example, the case of single mode ($n=2$) gives the following cross-polarized component of the aperture field distribution.

$$\begin{aligned}
 (13) \quad E_{\Lambda}^q = & -K \left[\left(\frac{E^2 + H^2}{2} \right) \left(\frac{a+c}{2} \right) - (-1)^{\ell} \left(\frac{E^2 - H^2}{2} \right) \left(\frac{a-c}{2} \right) \right] \text{SIN } \phi' - b \left[\frac{E^2 + H^2}{2} - (-1)^{\ell} \frac{E^2 - H^2}{2} \right] \text{SIN } 2\phi' \\
 & + \left[\left(\frac{E^2 + H^2}{2} \right) \left(\frac{a-c}{2} \right) - (-1)^{\ell} \left(\frac{E^2 - H^2}{2} \right) \left(\frac{a+c}{2} \right) \right] \text{SIN } 3\phi'
 \end{aligned}$$

It can be seen that the addition of this mode (n=2) to the conventional feed of equation (10) reduces the effect of the dominant term (sin ϕ') of the cross-polar component of the aperture field on the total cross-polarization of the antenna.

5. MATCHED PRIMARY FEEDS

In the preceding sections of this report we have established most of the needed background to examine the performance and limitation of an offset parabolic reflector antenna when operated in conjunction with conventional primary-feeds. Special emphasis was given to the depolarization properties due to the offset reflector geometry, since, it has been identified as the principal limiting factor in using such systems. Equations (10) and (13) show that the mixing of the extra mode ($n=2$) to the conventional feed provides a means to alter the cross-polarization properties of the vector-radiation pattern and hopefully overcomes the inherent disadvantage of the offset system.

A class of improved primary-feed devices has recently been introduced [10] and [11], which confirm the above mentioned possibility and offers the means to enhance the use of the offset parabolic reflector in many applications. The design concept of these "Matched-feed" devices and their feasibility for a single-linear or dual-linear polarization are best explained by the study of the offset focal-plane fields. In the reception mode, a linearly polarized and uniform plane wave incident normally upon a paraboloidal metallic surface induces a surface-current which in turn gives rise to a particular field distribution in the focal region of the reflector. By reciprocity, any primary-feed that can synthesizes the entire focal-plane field distribution would, upon transmission, produce a linearly polarized and uniform plane wave field distribution in the projected-aperture with 100% aperture efficiency. This is why the

concept is known in the literature as the "Matched-feed concept". Since it identifies the focal-fields as those corresponding to an optimum feed aperture-field distribution, in the sense of achieving maximum aperture efficiency. The concept has been utilized with considerable success in the development of high efficiency feeds for both the axisymmetric paraboloid [18], as well as for offset systems [7], [10] and [19].

Bem's analysis [7] for the focal region field has the particular merit that the transverse focal-plane field components for a reflector with long focal length can be described by simple closed form expressions. For an incident wave polarized in the plane of symmetry, the focal fields are

$$(14-a) \quad E_{x'} = K' \left[\frac{J_1(u)}{u} + j \frac{d \sin \theta_0}{4f} \frac{J_2(u)}{u} \cos \phi' \right]$$

$$(14-b) \quad E_{y'} = K' \left[-j \frac{d \sin \theta_0}{4f} \frac{J_2(u)}{u} \sin \phi' \right]$$

where,

$$u = \frac{kr'}{4f} (1 + \cos \theta_0)$$

r' = is the radial distance of the point from the z' -axis.

$J_n(u)$ = is the Bessel function of order n .

The solution for the wave polarization in the plane of asymmetry is achieved from the above equations by interchanging x' and y' and replacing ϕ' by $(2\pi - \phi')$. That is,

$$(15-a) \quad E_{x'} = K' \left[j \frac{d \sin \theta_0}{4f} \frac{J_2(u)}{u} \sin \phi' \right]$$

$$(15-b) \quad E_{y'} = K' \left[\frac{J_1(u)}{u} + j \frac{d \sin \theta_0}{4f} \frac{J_2(u)}{u} \cos \phi' \right]$$

A simple inspection of the above two cases shows that the cross-polar component is an asymmetrical function of ϕ' with a magnitude which decreases with the decrease of the offset angle θ_0 . It also is in a phase-quadrature with respect to the principal axisymmetric copolar component. The axisymmetric copolar term is also modified by the presence of the quadrature component, which is identical to the cross-polar term in all but its dependence on ϕ' . The focal-plane field is shown in Fig. 2, as a superposition of two configurations of the "symmetric" and the "antisymmetric" field distributions of two polarizations. In order that the primary-feed provides a match to these incoming fields, its aperture-field must exhibit similar linear-polarization properties. It is a fact that conventional high performance axisymmetric feeds provide an excellent match to only the copolar component, which leads to poor cross-polar radiation characteristics of the antenna. Rudge et al [10] and [11] explained how the asymmetric component can be well matched by making use of higher-order asymmetrical waveguide modes. To illustrate the general principle, the desired aperture-field distribution for the primary-feed can be approximated by an appropriate combination of a fundamental and a higher order mode. Fig. 3 shows geometries for obtaining linear-polarization in the plane of symmetry using either rectangular or circular structures. It

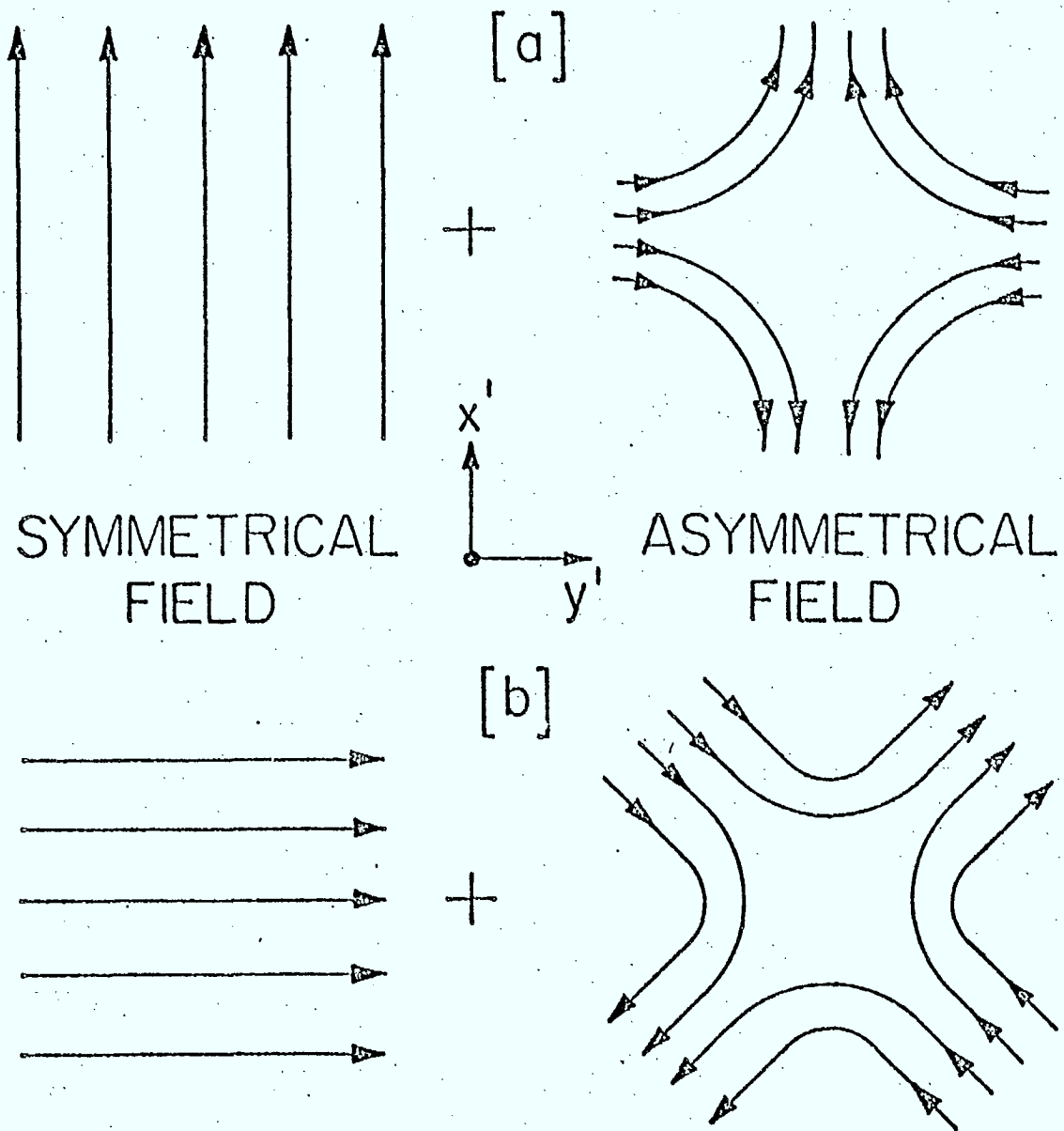


Fig. 2 Symmetric and asymmetric components of the offset reflector focal-plane field.

[a] Polarization in the plane of symmetry.

[b] Polarization in the plane of asymmetry.

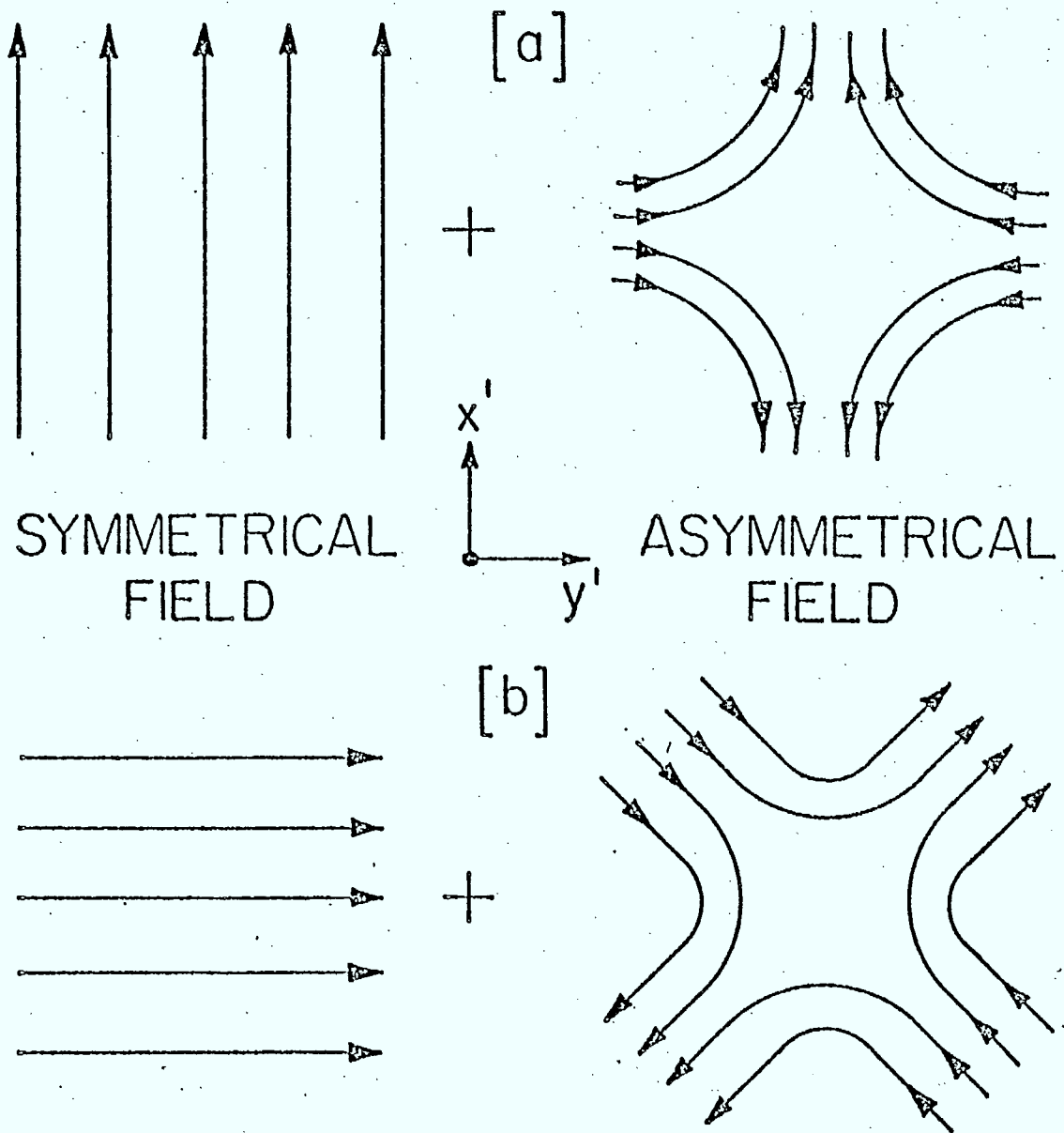


Fig. 2 Symmetric and asymmetric components of the offset reflector focal-plane field.

[a] Polarization in the plane of symmetry.

[b] Polarization in the plane of asymmetry.

is also possible to match the orthogonal linear polarization with circular structures by the same principle shown in Fig. 3. The higher order mode in each situation provides the necessary asymmetric cross-polar field distribution to compensate for the one generated by the offset geometry.

This wave-guide mode is the TE_{21} mode for the smooth-walled guides or the HE_{21} hybrid mode in the cylindrical corrugated structures. As the unbalanced smooth-walled structures radiate a cross-polarization field into the diagonal planes of the far field, the third mode, TM_{11} , can be employed to improve the axisymmetry of the feed. The transverse electric modes in the circular wave-guide aperture (TE_{mn}) have the transverse electric field configuration of the form [20],

$$E_{Af}^{mn}(\phi'_p) = K_{mn} \left[m \frac{J_m(u')}{u'} \cos(m\phi' - \phi'_p) \hat{r}' - J'_m(u') \sin(m\phi' - \phi'_p) \hat{\phi}' \right],$$

$$u' = p'_{mn} \left(\frac{r'}{a} \right)$$

$$= \frac{1}{2} K_{mn} \left[J_{m-1}(u') \cos[(m-1)\phi' - \phi'_p] + J_{m+1}(u') \cos[(m+1)\phi' - \phi'_p] \right] \hat{x}'$$

$$- \left[J_{m-1}(u') \sin[(m-1)\phi' - \phi'_p] - J_{m+1}(u') \sin[(m+1)\phi' - \phi'_p] \right] \hat{y}'$$

where, p'_{mn} is the n -th root of $\frac{d}{du'} J_m(u') = 0$ and K_{mn} is a constant factor, proportional to the complex amplitude of the TE_{mn} mode. The TE_{21} - mode exhibits the following properties for the specific polarization $\phi'_p = 0$,

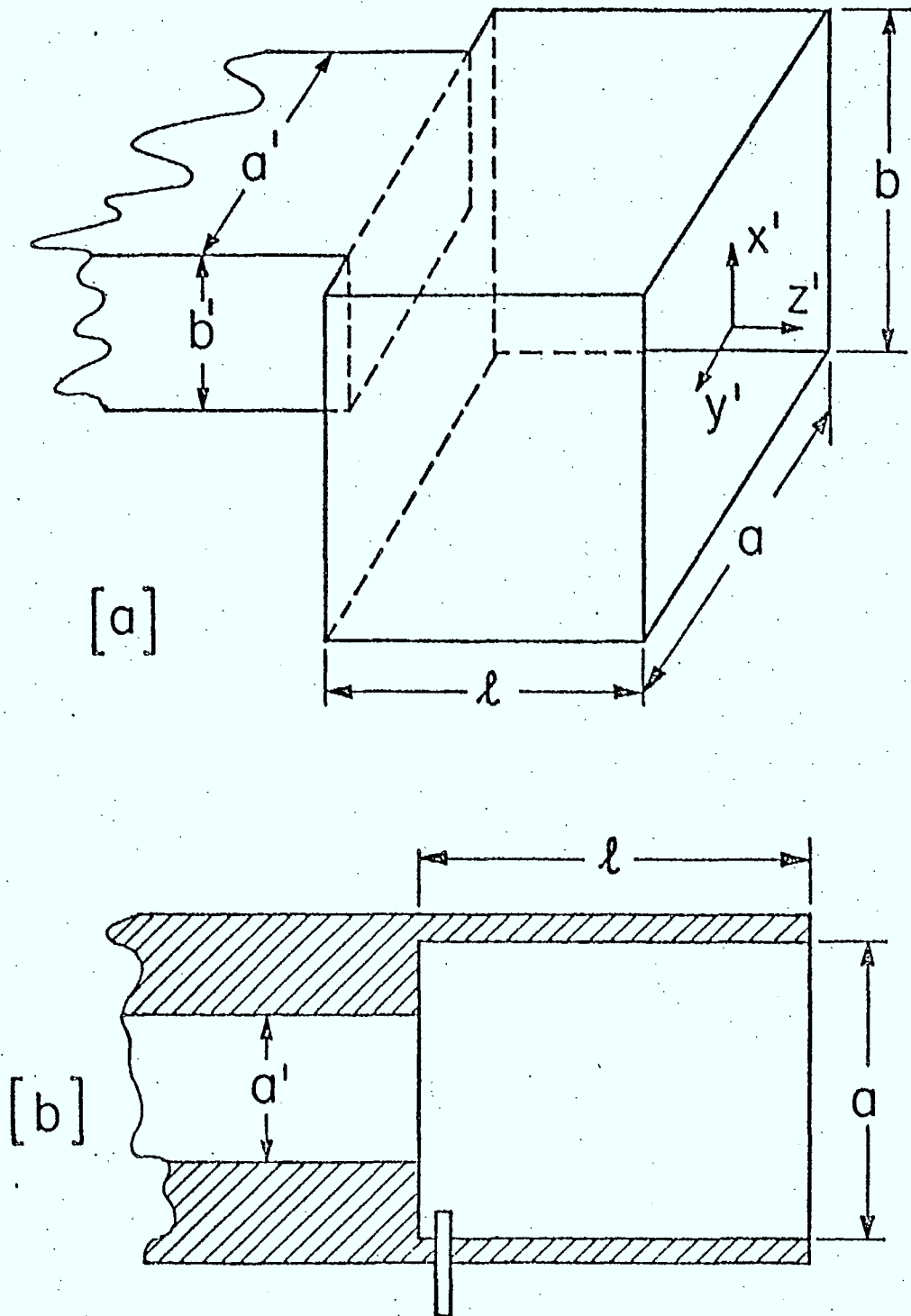


Fig. 3 Matched-feed configuration for linear polarization in the plane of symmetry.
 [a] Rectangular mixing of TE_{01} and TE_{11} .
 [b] Circular mixing of TE_{11} plus TE_{21} .

$$E_{Af}^{21}(0) = 2K_{21} \frac{J_2(u')}{u'} \hat{x}' \quad \text{at } \phi'_p = 0, \quad \text{and}$$

$$E_{Af}^{21}(0) = 2K_{21} \frac{J_2(u')}{u'} \hat{y}' \quad \text{at } \phi' = \frac{\pi}{2},$$

which provides an excellent match to both copolar and cross-polar asymmetric components of the focal-plane field due to the incident plane wave with linear polarization in the plane of symmetry (See equations (14-a) and (14-b)). It is worth noting that the coefficient K_{21} must be in phase-quadrature with respect to K_{11} coefficient to comply with the matching criteria. For the other (orthogonal) polarization, the substitution $\phi'_p = \frac{\pi}{2}$ leads to

$$E_{Af}^{21}\left(\frac{\pi}{2}\right) = K_{21} J_2'(u') \hat{y}' = K_{21} \left(2 \frac{J_2(u')}{u'} - J_3(u')\right) \hat{y}' \quad \text{at } \phi' = 0, \quad \text{and}$$

$$E_{Af}^{21}\left(\frac{\pi}{2}\right) = K_{21} J_2'(u') \hat{x}' = K_{21} \left(2 \frac{J_2(u')}{u'} - J_3(u')\right) \hat{x}' \quad \text{at } \phi' = \frac{\pi}{2},$$

which has the same trend of matching equations (15-a) and (15-b). For corrugated structures in which the fields satisfy anisotropic boundary conditions, it is still possible to show that the effect of HE_{21} mode of the guide plays the same role of matching the asymmetric component of the incoming wave and hence it must be mixed with the fundamental HE_{11} corrugated mode to match both principal polarization. By direct analogy, one should expect the mixing of the TE_{11} rectangular waveguide mode to provide similar compensation, suited for the polarization in the plane of symmetry, when used with the corresponding fundamental TE_{01} rectangular

waveguide mode. On the other hand, it is obvious that the matching of the other (orthogonal) polarization in the plane of asymmetry can not be met in the rectangular configuration. Since it is not feasible to rotate the TE_{01} -mode by $\frac{\pi}{4}$ (45°).

Emerging requirements, from the previous analysis of the focal-plane field, is that the improved class of primary-feed devices must be at least a bimodal in the sense of radiating (in transmission mode) a fundamental $E^{(1)}$ mode plus a compensating mode $E^{(2)}$. The necessary condition is that these two modes be in phase-quadrature at the aperture of the device. Since the compensating mode has a skew-symmetric field distribution in the aperture, then upon radiating its generated $E^{(2)}$ becomes in phase with the fundamental radiation $E^{(1)}$. Hence the total vector-radiation field from a matched-feed device E_T may be expressed, at a distance R' , by,

$$(16) \quad E_T = (E^{(1)} + E^{(2)}) \frac{e^{-jkR'}}{R'}$$

where $E^{(1)}$ and $E^{(2)}$ are real quantities representing the angular variation (θ', ϕ') of the respective radiation of the fundamental and the compensating modes. The mathematical expressions for $E^{(1)}$ and $E^{(2)}$ can be derived as seen in previous sections by taking the Fourier transform of the respective aperture field distributions. The general trend of the bimodal feed radiation behaviours can be detected and recognized. For example, Silver's results [12] for the TE_{11} and TE_{21} circular waveguide modes are of the same form as the vector-radiation patterns described by equation (11) with $n=2$. The $E^1(\theta')$ and $H^1(\theta')$ describe

the E and H-plane radiation-pattern functions of the fundamental mode and for the TE_{11} circular waveguide mode are

$$E^1(\theta') = \frac{J_1(u)}{u} (1 + \cos \theta'), \quad H^1(\theta') = (1 + \cos \theta') J_1'(u) / [1 - (\frac{u}{P_{11}})^2]$$

while for the compensating TE_{21} mode the functions take the form

$$E^2(\theta') = \alpha \frac{2J_2(u)}{u} (1 + \cos \theta'), \quad \alpha = K_{21}/K_{11}$$

$$H^2(\theta') = \alpha (1 + \cos \theta') J_2'(u) / [1 - (\frac{u}{P_{21}})^2]$$

where the parameter u is equal to $(\pi \frac{d'}{\lambda} \sin \theta')$ and d' is the diameter of the primary-feed aperture. Note also that there exist a class of tri-mode structures which radiate a balanced fundamental by having the right combinations of TE_{11} and TM_{11} modes, together with the compensating TE_{21} mode. In these cases the radiation fields of the device can be approximated by setting E^1 to be equal to H^1 . Thus equation (6) can be applied to equation (11) to resolve the improved primary-feed radiation fields into copolar and cross-polar components. For linearly polarized radiation the results take the form

$$(17) \begin{bmatrix} p \\ E_f \\ q \\ E_f \end{bmatrix} = \frac{e^{-jkR'}}{R'} \begin{bmatrix} \sum_{\ell=1}^2 1/2(E^\ell + H^\ell) \cos(\ell - 1)\phi' + 1/2(E^\ell - H^\ell) \cos \\ \sum_{\ell=1}^2 -1/2(E^\ell + H^\ell) \sin(\ell - 1)\phi' + 1/2(E^\ell - H^\ell) \sin \end{bmatrix}$$

$$\begin{bmatrix} I(\ell + 1) \phi' - 2\phi'_p \\ I(\ell + 1) \phi' - 2\phi'_R \end{bmatrix}$$

Thus, in the principal planes ($\phi = 0, \pi/2$) the radiation patterns of a matched feed device, when the polarization vector \hat{p} is aligned along the x' -axis ($\phi'_p = 0$), are

$$E_f^p(\phi' = 0) = \frac{e^{-jkR'}}{R'} [E^1(\theta') + E^2(\theta')] \quad , \quad E_f^q(\phi' = 0) = 0$$

$$E_f^p(\phi' = \frac{\pi}{2}) = \frac{e^{-jkR'}}{R'} E^1(\theta') \quad , \quad E_f^q(\phi' = \frac{\pi}{2}) = -\frac{e^{-jkR'}}{R'} E^2(\theta')$$

Therefore, in the plane of symmetry ($\phi' = 0$) the primary-feed radiates a pure copolar component (which is the algebraic sum of the two individual E-plane radiation patterns) with a squint due to the skew-symmetry of $E^2(\theta')$. This is the desirable feature that compensates for the asymmetrical attenuation factor ($1/R'$) at the parabolic reflector surface. The demonstrated principles of the matched-feed indicate that the cancellation of the reflector generated cross-polar radiation requires the field of the above mentioned two modes to be in phase-quadrature at the aperture of the primary-feed. In addition, the relative amplitude of the compensating mode must be dependent upon the parameters of the reflector. If we assume that the compensating mode is generated at the asymmetric junction and then is allowed to propagate together with the fundamental mode, the length of the waveguide reaction for the phase criterion is given by (Fig. 3)

$$l = \frac{\pi}{2} / (\beta_1 - \beta_2) \quad \text{with} \quad \beta_r = \frac{2\pi\sqrt{\epsilon_r}}{\lambda} \sqrt{1 - \left(\frac{\lambda}{\sqrt{\epsilon_r} \lambda_c}\right)^2}$$

The aperture dimension permits the propagation of only these two modes.

The diameter of the first section ($2a'$), in the circular structure of Fig. 3, is usually adjusted for the operating frequency (f^0) to be above the fundamental cutoff frequency and below the next higher order mode (i.e. in the middle range). In the λ -section, the diameter ($2a$) is taken such that the operating frequency is midway between the compensating mode cutoff-frequency and its next higher order mode. As an example, the circular structure of Fig. 4 is adjusted to operate at a frequency of 10 GHz with the following geometrical parameters.

$$\text{Fundamental TE}_{11}: (a/\lambda_c) = (af^c/c) = 0.3043, \lambda^c = 3.412a$$

$$\text{Next mode TM}_{01}: (a/\lambda_c) = (af^c/c) = 0.38314, \lambda^c = 2.613a$$

$$\text{Compensating mode TE}_{21}: (a/\lambda_c) = (af^c/c) = 0.48614, \lambda^c = 2.057a$$

$$\text{Next mode TM}_{11}: (a/\lambda_c) = (af^c/c) = 0.6097, \lambda^c = 1.64a$$

That is,

$$(a'f^0/c) = 0.34, (af^0/c) = 0.55, (a/a') = 1.62$$

It is worth mentioning that increasing the radius a to $1.62a'$, in order to allow the propagation of the compensating mode, can also be achieved by loading the original waveguide by a dielectric material of $\epsilon_r = 2.625$. Fig. 5. Shows one such design, which is equivalent to that of Fig. 4, but the dielectric constant is assumed to be 2.0.

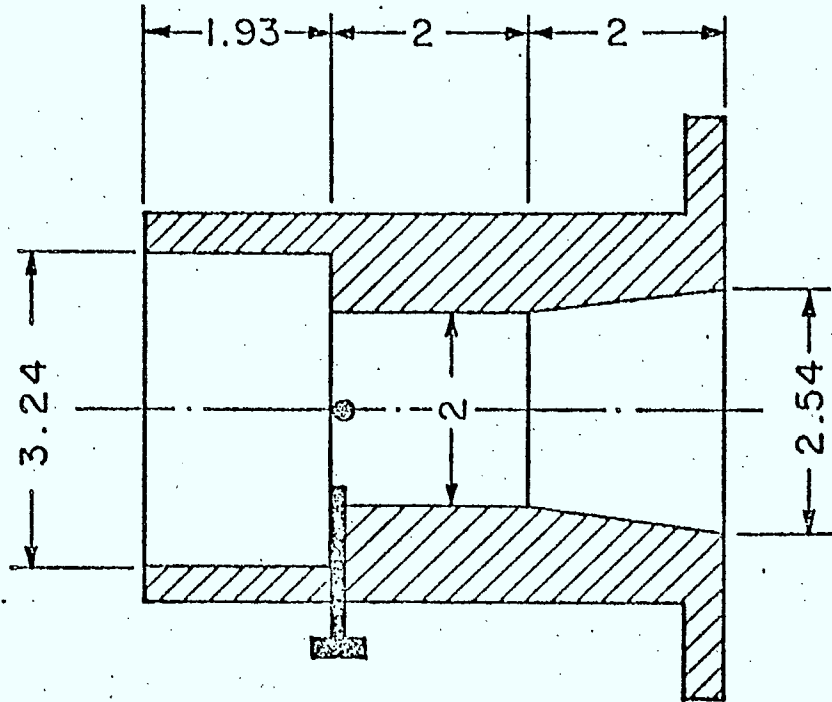


Fig. 4 Matched-primary feed to be tested at central frequency of 10 GHz.

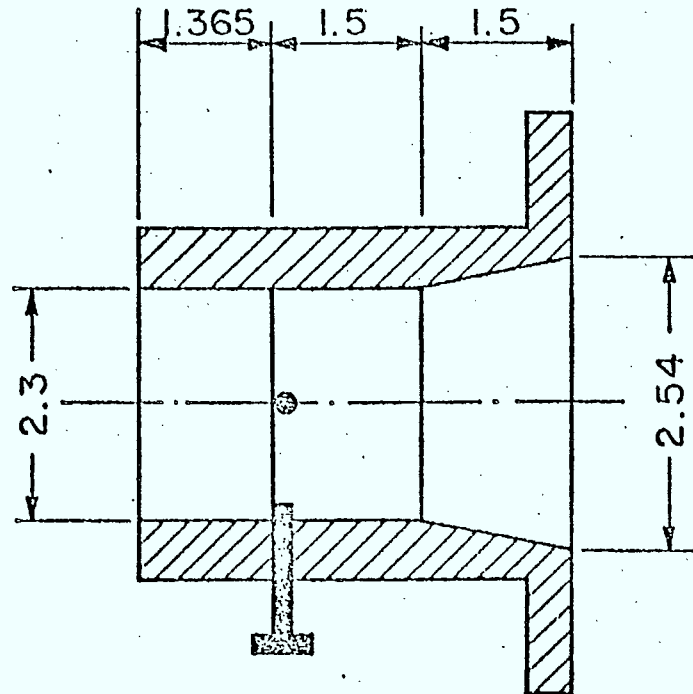


Fig. 5 The use of dielectric in matched-feed device to be tested at 10 GHz.

6. METHOD OF STATIONARY PHASE

The computation of the far field vector-radiation patterns of the offset reflector antennas are needed here to predict the performance of the matched-feed devices and to examine the characteristics of the antenna such as the side lobe levels and cross-polarization. The computation of the radiation patterns could be performed by the precise computation of the appropriate diffraction integrals, which require double numerical integration. Such direct computations require considerable computation time, specially for large off-axis angles, where the integral form is suitable for approximation by the method of stationary phase. The method of stationary phase is usually applied to eliminate the azimuthal ϕ' integration. In application of the method it was subsequently recognized [16] that some of the terms in the approximation are related to the asymptotic expansions of the Bessel functions. Therefore, the same stationary phase approximation, used for large angles, has been modified in [5] and [16] so that it can also be used to compute the far field with good accuracy in the immediate vicinity of the main beam. For the symmetric paraboloidal antennas, the results of the above mentioned modifications reduce to the exact expressions obtained by direct integration techniques, which can be used to examine the validity of the modified technique.

To summarize the approximation technique, let us consider the integral

$$(18) \quad G[g(\phi')] = \int_a^b g(\phi') e^{j2kf \text{ SIN}\theta\psi(\phi')} d\phi'$$

where $(2kf \sin \theta)$ is large, $\Psi(\phi')$ is real, and $g(\phi')$ is a slowly varying function. The integral can be approximated to $\theta(1/2 kf \sin \theta)$ by the method of stationary phase, which considers only the integral contribution in the vicinity of the stationary points of the function $\Psi(\phi')$. That is,

$$(19) \quad G[g(\phi')] \approx \sum_i g(\phi'_i) \sqrt{\frac{j2\pi}{akf \sin \theta \Psi''(\phi'_i)}} \exp [j 2kf \sin \theta \Psi(\phi'_i)]$$

If we write $\bar{r} \cdot \hat{R}$ as $2f\Psi(\phi')$, then two stationary points, ϕ'_1 and ϕ'_2 become evident from the exact nature of the $\Psi(\phi')$ function

$$\Psi(\phi') = [(\cos \theta' \sin \theta_0 + \sin \theta' \cos \theta_0 \cos \phi') \cos \phi - \sin \theta' \sin \phi' \sin \phi] / t$$

$$\Psi'(\phi') = -\sin \theta' [c \sin \phi' \cos \phi + (a \cos \phi' - b) \sin \phi] / t^2$$

$$\Psi''(\phi') = -\frac{\sin \theta'}{t^2} [c \cos \phi' \cos \phi - a \sin \phi' \sin \phi - \frac{2b \sin \phi'}{t}$$

$$(c \sin \phi' \cos \phi + [a \cos \phi' - b])]$$

Therefore,

$$\sin \phi'_{1,2} = \frac{+c \sin \phi}{a \mp b \cos \phi}, \quad \cos \phi'_{1,2} = \frac{b \mp a \cos \phi}{a \mp b \cos \phi}$$

$$t_{1,2} = c^2 / (a \mp b \cos \phi), \quad \Psi(\phi'_{1,2}) = (\sin \theta_0 \cos \phi \mp \sin \theta') / c$$

$$\Psi''(\phi'_{1,2}) = \pm \sin \theta' (a \mp b \cos \phi)^2 / c^3$$

A direct substitution of these in the summation approximation yields

$$G[g(\phi')] \approx \frac{c\pi e^{j\beta}}{a^2 - b^2 \cos^2 \phi} [T_1 \sqrt{\frac{c^2}{\pi\alpha}} \cos(\alpha - \frac{\pi}{4}) - j T_2 \sqrt{\frac{c^2}{\pi\alpha}} \sin(\alpha - \frac{\pi}{4})]$$

where,

$$\alpha = \frac{2kf}{c} \sin \theta' \sin \theta, \quad \beta = \frac{2kf}{c} \sin \theta_0 \sin \theta \cos \phi$$

$$T_{1,2} = a[g(\phi'_1) \pm g(\phi'_2)] + b[g(\phi''_1) \mp g(\phi''_2)] \cos \phi$$

The above expression exhibits singularity at $\theta=0$ or $\theta'=0$ and is applicable only for large values of $(2kf \sin \theta)$. However, upon examination of the terms $\sqrt{\frac{2}{\pi}} \cos(\alpha - \frac{\pi}{4})$ and $\sqrt{\frac{2}{\pi\alpha}} \sin(\alpha - \frac{\pi}{4})$ it becomes obvious that they contain the asymptotic behaviour of the Bessel functions $(-1)^l J_{2l+1}(\alpha)$ respectively. By identifying and replacing these terms by their equivalent and actual Bessel functions, the singularity at the origin ($\alpha=0$) can be removed and the approximation near small angles θ and θ' would improve. There is however no unique method of identifying the exact order l of the needed Bessel functions in the replacement process, and the method previously chosen and tested [16] in the literature was dictated by the requirement that for the symmetric case ($\theta_0=0$) the approximation must reduce to the exact expression. The technique is understood as an association of $J_n(\alpha)$ with $\cos n\phi$ and $\sin n\phi$ terms in the expansion of T_1 and T_2 . Therefore

$$(20) \quad G[g(\phi')] \approx \frac{c\pi e^{j\beta}}{a^2 - b^2 \cos^2 \phi} \sum_r \left(\frac{1}{j}\right)^r (c_g^r \cos r\phi + s_g^r \sin r\phi) J_r(\alpha)$$

where the coefficients C_g^n and S_g^r are defined as

$$C_g^r = (1 + \delta_{r,1}) b g_e^{r-1} + 2 a g_e^r + b g_e^{r+1}$$

$$S_g^r = b g_0^{r-1} + 2a g_0^r + b g_0^{r+1}$$

and g_e and g_0 coefficients are either independent or slowly varying function of Φ and given by

$$g(\phi_1') = \sum_r (g_e^r \cos r \Phi + g_0^r \sin r \Phi)$$

The above expressions reduce to those obtained by the method of stationary phase (equations (18) and (19)) for large values of $(2kf \sin \theta)$ and avoid the singularity at $\alpha=0$. Hence, the new approximation extends considerably the range of approximated ϕ' integration, beyond the applicability of the stationary phase method. For the multi-mode primary-feeds, the two spatial Fourier transform integrals ϵ_p and ϵ_q , defined by equation (5), can now be evaluated in the following form

$$(21) \quad \epsilon_{p,q} = \int_0^{\theta_c} \sin \theta' I_{p,q} d\theta'$$

where

$$I_p = -2fe^{-j2kf \sum_m} \int_0^{2\pi} \left(\frac{p_m \cos m\phi'}{t^2} \right) e^{jkr \cdot \hat{R}} d\phi'$$

$$I_q = -2fe^{-j2kf} \sum_m \int_0^{2\pi} \left(\frac{q_m \text{SIN } m\phi'}{t^2} \right) e^{jk\vec{r} \cdot \hat{R}} d\phi'$$

Equation (20) can be used to evaluate the coefficients C_m^r and S_m^p from

$$G \left[\frac{\text{COS } m\phi'}{t^2} \right] \sim \frac{\pi e^{j\beta}}{c^3 (a^2 - b^2 \text{COS}^2 \phi)} \sum_r \left(\frac{1}{j} \right)^r C_m^r \text{COS } r\phi J_r(\infty)$$

$$G \left[\frac{\text{SIN } m\phi'}{t^2} \right] \sim \frac{\pi e^{j\beta}}{c^3 (a^2 - b^2 \text{COS}^2 \phi)} \sum_r \left(\frac{1}{j} \right)^r S_m^r \text{SIN } r\phi J_r(\infty)$$

which are tabulated in tables (I) and (II). Thus, for the matched-feed of the previous section I_p and I_q becomes

$$(22) \quad I_p = - \frac{2\pi f e^{j(\beta - 2kf)}}{c^3 (a^2 - b^2 \text{COS}^2 \phi)} \sum_{r=0}^5 \left(\frac{1}{j} \right)^r \left(\sum_0^3 p_m C_m^r \right) \text{COS } r\phi J_r(\infty)$$

$$(23) \quad I_q = - \frac{2\pi f e^{j(\beta - 2kf)}}{c^3 (a^2 - b^2 \text{COS}^2 \phi)} \sum_{r=1}^5 \left(\frac{1}{j} \right)^r \left(\sum_1^3 q_m S_m^r \right) \text{SIN } r\phi J_r(\infty)$$

For a balanced primary-feed of the Type used by Shafai [5] that is linearly-polarized in the \hat{y} -direction, the above technique reduces the result to

$$p_0 = q_0 = \left(\frac{a+c}{2} \right) F(\theta'), \quad p_1 = q_1 = -bF(\theta'), \quad p_2 = q_2 = \left(\frac{a-c}{2} \right) F(\theta')$$

$$I_p = - \frac{2\pi f e^{j(\beta - 2kf)}}{c(a^2 - b^2 \cos^2 \phi)} F(\theta') \left[\begin{array}{l} \{c(a+c) J_0(\alpha) + c(a-c) \cos 2\phi J_2(\alpha)\} \\ + j \frac{b}{2}(a-c) \{\cos \phi J_1(\alpha) + \cos 3\phi J_3(\alpha)\} \end{array} \right]$$

$$I_q = - \frac{2\pi f e^{j(\beta - 2kf)}}{c(a^2 - b^2 \cos^2 \phi)} F(\theta') \left[\begin{array}{l} c(a-c) \sin 2\phi J_2(\alpha) \\ + j \left\{ \frac{1}{2} b(3a+c) \sin \phi J_1(\alpha) + \frac{1}{2} b(a-c) \right. \\ \left. \sin 3\phi J_3(\alpha) \right\} \end{array} \right]$$

TABLE (I)

$C_0^0 = a(a^2+c^2), C_1^0 = b(a^2+c^2), C_2^0 = ab^2$		
$C_3^0 = -3b(a^2+c^2) + b(6a^4-7a^2b^2+4b^4)/F$		
<hr/>		
$C_0^1 = -\frac{1}{2}b(a^2+3c^2), C_1^1 = -\frac{1}{2}a(a^2+3c^2), C_2^1 = -\frac{1}{2}b(6c^2+b^2)$		
$C_3^1 = \frac{3}{2}a(a^2+3c^2) - a(6a^4-7a^2b^2+2b^4)/F$		
<hr/>		
$C_0^2 = -ab^2, C_1^2 = -b^3, C_2^2 = +a(2c^2-b^2)$		
$C_3^2 = 3b^3 - 4b(c^4-a^2b^2)/F$		
<hr/>		
$C_0^3 = \frac{1}{2}b^3, C_1^3 = \frac{1}{2}ab^2, C_2^3 = \frac{1}{2}b(a^2+c^2)$		
$C_3^3 = -\frac{3}{2}ab^2 - \frac{a}{2}(4a^4-19a^2b^2+12b^4)/F$		
<hr/>		
$C_0^4 = 0, C_1^4 = 0, C_2^4 = 0$		
$C_3^4 = a^2b(b^2-2c^2)/F$		
<hr/>		
$C_0^5 = 0, C_1^5 = 0, C_2^5 = 0$		
$C_3^5 = -\frac{1}{2}a^3b^2/F$		

$$F = a^2 - b^2 \cos^2 \phi$$

TABLE II

$S_1^1 = \frac{1}{2} C(3a^2 + c^2) \quad , \quad S_2^1 = 3 abc$ $S_3^1 = \frac{3}{2} C(3a^2 + c^2) - c^3(6a^2 + b^2)/F$
$S_1^2 = 0 \quad , \quad S_2^2 = -2C^3$ $S_1^3 = -4 abc^3/F$
$S_1^3 = -\frac{1}{2} b^2 c \quad , \quad S_2^3 = -abc$ $S_3^3 = -\frac{3}{2} b^2 c + \frac{1}{2} c^3(3a^2 + c^2)/F$
$S_1^4 = 0 \quad , \quad S_2^4 = 0$ $S_3^4 = 2 abc^3/F$

$$S_r^0 = S_0^r = 0$$

Matched Feed

For a matched-feed with the main linear-polarization taken in the symmetrical plane the final results are

$$I_p = A \begin{bmatrix} C_0 J_0(\alpha) + C_2 J_2(\alpha) \cos 2\phi + C_4 J_4(\alpha) \cos 4\phi \\ +j [C_1 J_1(\alpha) \cos \phi + C_3 J_3(\alpha) \cos 3\phi + C_5 J_5(\alpha) \cos 5\phi] \end{bmatrix}$$

$$I_q = C^2 A \begin{bmatrix} S_2 J_2(\alpha) \sin 2\phi + S_4 J_4(\alpha) \sin 4\phi \\ +j [S_1 J_1(\alpha) \sin \phi + S_3 J_3(\alpha) \sin 3\phi + S_5 J_5(\alpha) \sin 5\phi] \end{bmatrix}$$

where

$$A = -2\pi f e^{j(\beta-2kf)} / [c^3 (a^2 - b^2 \cos^2 \phi)]$$

$$C_0 = c^3 (aH_1 + cE_1) - \frac{ab}{2} [4a^2 - (6a^4 - 7a^2b^2 + 4b^4)/F] E_2 + \frac{bc}{2} [4(a^2 + c^2) - (6a^4 - 7a^2b^2 + 4b^4)/F] H_2$$

$$C_1 = \frac{c^2 b}{2} (aE_1 - cH_1) - \frac{b^2}{2} (6c^2 + b^2) + \frac{a^2}{2} [(a^2 + 3c^2) - (6a^4 - 7a^2b^2 + 2b^4)/F]$$

$$E_2 + \frac{ac}{2} [2(a^2 + 3c^2) - (6a^4 - 7a^2b^2 + 2b^4)/F] H_2$$

$$C_2 = c^3 (aH_1 - cE_1) + 2ab [c^2 - b^2 + (c^4 - a^2b^2)/F] E_2 + 2bc [b^2 - (c^4 - 2a^2b^2)/F] H_2$$

$$C_3 = \frac{bc^2}{2}(aE_1 - cH_1) - \left[\frac{b^2}{2}(a^2 + c^2) + \frac{a^2}{2} \{2b^2 + (4a^4 - 18a^2b^2 + 12b^4)/F\} \right] E_2 + \frac{ac}{2} [2b^2 + (4a^4 - 18a^2b^2 + 12b^4)/F] H_2$$

$$C_4 = [a^2b(b^2 - 2c^2)/2F](aE_2 - cH_2)$$

$$C_5 = [a^3b^2/4F](aE_2 - cH_2)$$

$$S_1 = \frac{b}{2}(3aE_1 + cH_1) - 4ac[1 - (6a^2 + b^2)/8F]H_2 + \left[\frac{1}{2}(3a^2 + c^2) - c^2(6a^2 + b^2)/2F \right] E_2$$

$$S_2 = c(aH_1 - cE_1) - 2bc[(1 - a^2/F)H_2 + ac/F E_2]$$

$$S_3 = \frac{b}{2}(aE_1 - cH_1) + [ac(3a^2 + c^2)/4F]H_2 + \frac{1}{2}[b^2 - c^2(3a^2 + c^2)/2F]E_2$$

$$S_4 = [abc/F](aH_2 - cE_2)$$

$$S_5 = [-b^2c/4F](aH_2 - cE_2)$$

For the other orthogonal linear polarization the result can be obtained from the above by just interchanging E_m and H_m . It is important at this stage to emphasize that \hat{e}_p and \hat{e}_q are two unit vectors that are perpendicular to each other as well as to the radial unit vector \hat{R} .

$$\hat{e}_p = \cos(\Phi - \Phi_p) \hat{\Psi} - \sin(\Phi - \Phi_p) \hat{\Phi}$$

$$\hat{e}_q = \sin(\Phi - \Phi_p) \hat{\Psi} + \cos(\Phi - \Phi_p) \hat{\Phi}$$

$$\hat{e}_p \cdot \hat{e}_q = \hat{e}_p \cdot \hat{R} = \hat{e}_q \cdot \hat{R} = 0, \quad \hat{e}_p \times \hat{e}_q = \hat{R}$$

where Φ_p is angle that specifies the \hat{p} direction relative to the x-axis of a right handed coordinates. That means if we choose a new cartesian coordinate p, q and z such that $p \times q = z$ then the representation of the copolar and cross-polar unit vectors (e_p, e_q) becomes,

$$\hat{e}_p = \left(\frac{1+\cos \Psi}{2}\right) [1-t^2 \cos 2(\Phi - \Phi_p)] \hat{p} - t^2 \sin 2(\Phi - \Phi_p) \hat{q} - 2t \cos(\Phi - \Phi_p) \hat{z}$$

$$\hat{e}_q = \left(\frac{1+\cos \Psi}{2}\right) [-t^2 \sin 2(\Phi - \Phi_p)] \hat{p} + [1+t^2 \cos 2(\Phi - \Phi_p)] \hat{q} - 2t \sin(\Phi - \Phi_p) \hat{z}$$

where,

$$t = \tan \frac{1}{2} \Psi$$

Hence the projection of the electric far field on the xy -plane

$$\underline{E} - (\hat{z} \cdot \underline{E}) \hat{z} = \hat{p} E^{pp} + \hat{q} E^{qp}$$

leads to the following matrix definition of this projected field in terms of the copolar and cross-polar components,

$$\begin{bmatrix} E^{pp} \\ E^{qp} \end{bmatrix} = \left(\frac{1+\cos \Psi}{2}\right) \begin{bmatrix} 1 - t^2 \cos[2(\Phi - \Phi_p)] & -t^2 \sin[2(\Phi - \Phi_p)] \\ -t^2 \sin[2(\Phi - \Phi_p)] & [1+t^2 \cos[2(\Phi - \Phi_p)]] \end{bmatrix} \begin{bmatrix} E^p \\ E^q \end{bmatrix}$$

That is, the dependence on the spatial Fourier transform componets ϵ_p and ϵ_q becomes

$$\begin{bmatrix} E^{pp} \\ E^{qp} \end{bmatrix} = \frac{j e^{-jkR}}{\lambda R} \left(\frac{1 + \cos \psi}{2} \right) \begin{bmatrix} 1 - t^2 \cos[2(\phi - \phi_p)] & -t^2 \sin[2(\phi - \phi_p)] \\ -t^2 \sin[2(\phi - \phi_p)] & 1 + t^2 \cos[2(\phi - \phi_p)] \end{bmatrix} \begin{bmatrix} \epsilon_p \\ \epsilon_q \end{bmatrix}$$

7. BASIC PARAMETERS

The physical optics approximation

$$\underline{E}_r = 2(\hat{n} \cdot \underline{E}_i) - \underline{E}_i$$

used at the paraboloidal surface, does preserve the norm of the electric field transformation in the sense that $||\underline{E}_r|| = ||\underline{E}_i||$ where the norm is defined in terms of the standard scalar product according to

$$||\underline{E}||^2 = \underline{E} \cdot \underline{E}^*$$

That is, the norm of the incident electric field at a point $P_s \equiv (P', \theta', \phi')$ on the reflector surface is identical to the norm of the aperture electric field at the projection point $P_a \equiv (r, \frac{\pi}{2}, \phi_a) \equiv (x_a, y_a, 0) \equiv \bar{r}$, See Fig. 1., and hence

$$||E_A(P_a)|| = ||E_f(P_s)||$$

For Harmonic wave solution, the average power per unit area

$$\bar{P} = \frac{1}{2} \underline{E} \times \underline{H}^* = \frac{1}{2} \sqrt{\frac{\epsilon}{\mu}} ||\underline{E}||^2 \hat{R}, \quad \underline{H} = \sqrt{\frac{\epsilon}{\mu}} \hat{R} \times \underline{E}$$

suggests the following representation of the radiated power angular distribution to a given point source (radiation intensity)

$$U(\psi, \phi) = R^2 ||\bar{P}|| = \frac{1}{2} \sqrt{\frac{\epsilon}{\mu}} R^2 ||\underline{E}||^2$$

where the radiated power becomes,

$$P_r = \int_0^{4\pi} U(\Psi, \Phi) d\Omega$$

and, accordingly, a gain function is usually defined as

$$G(\Psi, \Phi) = \frac{4\pi}{P_r} U(\Psi, \Phi).$$

Since the electric far field of the projected aperture is to be calculated according to

$$||E|| = \frac{1}{\lambda R} \left(\frac{1 + \cos\Psi}{2} \right) \left| \int_{\underline{A}} \underline{E}_A e^{jk\bar{r} \cdot \hat{R}} dA \right|$$

then the reflector radiation intensity becomes

$$U(\Psi, \Phi) = \frac{1}{2} \sqrt{\frac{\epsilon}{\mu}} \frac{1}{\lambda^2} \left(\frac{1 + \cos\Psi}{2} \right)^2 \left| \int_{\underline{A}} \underline{E}_A e^{jk\bar{r} \cdot \hat{R}} dA \right|^2$$

Also the primary-feed radiation power P_T has the form

$$P_T = \frac{1}{2} \sqrt{\frac{\epsilon}{\mu}} \int_0^{4\pi} ||\underline{E}_f||^2 R^2 d\Omega = \frac{1}{2} \sqrt{\frac{\epsilon}{\mu}} \left(\frac{1}{n_s} \right) \int_0^{\Omega} ||\underline{E}_f||^2 R^2 d\Omega$$

where

$$n_s = \left(\int_0^{\Omega} ||\underline{E}_f||^2 R^2 d\Omega \right) / \left(\int_0^{4\pi} ||\underline{E}_f||^2 R^2 d\Omega \right)$$

represents the efficiency with which the reflector collect the primary-feed radiation power and Ω is the solid angle of the illumination cone.

Therefore,

$$G(\Psi, \Phi) = \eta_s \frac{4\pi}{\lambda^2} \left(\frac{1 + \cos \Psi}{2} \right)^2 \frac{\left| \int_A \frac{\underline{E}_A}{\lambda} e^{jk\bar{r} \cdot \hat{R}} dA \right|^2}{\int_A \left| \frac{\underline{E}_A}{\lambda} \right|^2 dA}$$

The specific value of the gain function along the boresight $G(0, 0)$ defines the antenna gain [12]

$$G_A = \frac{4\pi}{\lambda^2} \left(\frac{\left| \int_A \frac{\underline{E}_A}{\lambda} dA \right|^2}{\int_0^{4\pi} \left| \frac{\underline{E}_A}{\lambda} \right|^2 R^2 d\Omega} \right) = \frac{4\pi \Lambda}{\lambda^2} \eta_s \eta_a$$

where

$$\eta_a = \frac{\left| \int_A \frac{\underline{E}_A}{\lambda} dA \right|^2}{\int_A \left| \frac{\underline{E}_A}{\lambda} \right|^2 dA} \quad \text{is the aperture efficiency}$$

In an explicit form the antenna gain function is in the form

$$G(\Psi, \Phi) = 4 \left(\frac{1 + \cos \Psi}{2} \right)^2 \frac{\left| \frac{1}{\lambda} \int_A \hat{p} \cdot \underline{E}_A e^{jk\bar{r} \cdot \hat{R}} dA \right|^2 + \left| \frac{1}{\lambda} \hat{q} \cdot \underline{E}_A e^{jk\bar{r} \cdot \hat{R}} dA \right|^2}{\int_0^\pi (E_1^2 + E_2^2 + H_1^2 + H_2^2) \sin \theta' d\theta'}$$

where the two integrals

$$\frac{1}{\lambda} \int \hat{p} \cdot \underline{E}_A e^{jk\bar{r} \cdot \hat{R}} dA \quad \text{and} \quad \frac{1}{\lambda} \int \hat{q} \cdot \underline{E}_A e^{jk\bar{r} \cdot \hat{R}} dA$$

are evaluated by two complex functions PISIN (THTPR) and QISIN (THTPR) using the complex function INTEG (0, THTCR, FUNCT) for the θ' integration. The latter function is a subroutine generated using the 40 interval Gaussian quadrature method. For an analytic matched-feed of the type described in the previous section the subroutine PFRPT (THTPR, DN,

ALFA, E1, H1, E2, H2) is written to generate the required E- and H-plane field patterns for both the fundamental and the compensating modes in circular waveguide structures. The normalization factor

$$\int_0^{\pi} (E_1^2 + E_2^2 + H_1^2 + H_2^2) \sin \theta' d\theta'$$

is to be calculated with the aid of the subroutine FACTR(FCT). By calling this subroutine only once, the different values of the primary-feed radiation pattern (E_1, H_1, E_2, H_2) at 0.5° intervals is stored in the common arrays EI (361), HI(361), EII(361), and HII (361), respectively.

The error introduced by the modified stationary phase approximation has been investigated by others[16] and found to be quite small for the off-axis radiation pattern. For the on-axis gain ($\psi=0$), the difference between the exact and approximate value for some specific cases indicates an over estimation in the E-plane calculation and an under estimation in the H-plane that can run between 4% to 7% which is the largest error encountered. For that precise reason, the ϕ' -integration in the bore-sight case is treated here, exactly by the use of the residue theorem of the complex integrations. Four of the essential integrals give the following final results

$$\int_0^{2\pi} \frac{d\phi'}{t} = 2\pi/\sqrt{a^2 - b^2} = 2\pi/c$$

$$\int_0^{2\pi} \frac{\sin^2 \phi'}{t^2} d\phi' = \frac{2\pi}{b} \left(\frac{a}{\sqrt{a^2 - b^2}} - 1 \right) = \frac{2\pi}{b^2 c} (a - c)$$

$$\int_0^{2\pi} \frac{\cos \phi'}{t} d\phi' = \frac{2\pi}{bc} (a - c)$$

$$\int_0^{2\pi} \frac{\sin^2 \phi' \cos \phi'}{t^2} d\phi' = \frac{2\pi}{b^3 c} (a - c)^2$$

Accordingly, the ϕ' -integration for the two needed integrals

$$\left| \int_A \underline{E}_A dA \right|^2 \quad \text{and} \quad \int_A \left| \underline{E}_A \right|^2 dA$$

are carried out for the case of the matched feed that is required for the present work. Therefore, the exact expression for the antenna gain G_A

becomes

$$(24) \quad G_A = 4 \left(\frac{4\pi f}{\lambda} \right)^2 \frac{\int_0^{\theta_c} \text{SIN} \theta' \Sigma_1(\theta') d\theta']^2}{\int_0^{\pi} \text{SIN} \theta' \Sigma_2(\theta') d\theta'}$$

where

$$\Sigma_1(\theta') = \frac{1}{a+b} [E_1 + H_1 + \frac{2b}{a+c} (E_2 + H_2)]$$

$$\Sigma_2(\theta') = [E_1^2 + H_1^2 + E_2^2 + H_2^2]$$

The result is the same if E and H are interchanged which means that, for an identical level of excitation, the gain stays the same for the x and y polarization.

If the feed radiation pattern is normalized such that

$$\frac{1}{4} \int_0^{\pi} [(E_1^N)^2 + (H_1^N)^2 + (E_2^N)^2 + (H_2^N)^2] \text{SIN} \theta' d\theta' = 1,$$

then the antenna gain, equation (24), can be rewritten as

$$(25) \quad G_A = F \left(\frac{\pi d}{\lambda} \right)^2 \text{COT}^2 \frac{\theta_c}{2} \left| \int_0^{\theta_c} \text{TAN} \frac{\theta'}{2} G_f^2(\theta') d\theta' \right|^2$$

where

$$(26) \quad G_f(\theta') = \left[\left(\frac{E_1^N + H_1^N}{2} \right) + 2 \text{TAN} \frac{\theta_o}{2} \text{TAN} \frac{\theta'}{2} \left(\frac{E_2^N + H_2^N}{2} \right) \right]^2$$

$$F = \left[\frac{2(\text{COS} \theta_o + \text{COS} \theta_c)}{(1 + \text{COS} \theta_o)(1 + \text{COS} \theta_c)} \right]^2$$

This final form of equation (25) renders itself useful for the specific case of $\theta_o = 0$, and $E_2^N = H_2^N = 0$ where the factor F becomes unity and the result shows the identical equation of Silver[12] for the symmetrical

paraboloidal reflector. Also the case of $\theta_0 \neq 0$ and $E_2^N = H_2^N = 0$ yields the identical results previously obtained by Ierly and Zucker[16]. It is imperative at this point to illustrate how an off-set antenna has less gain than its symmetrically fed counterpart, for the same feed, because of the factor F which is less than one for $\theta_0 \neq 0$. As the main objective of the off-setting process is to remove the feed from the projected aperture of the antenna, let us consider the limiting case of $\theta_0 = \theta_c$. That is

θ_c	F
20	0.998
25	0.995
30	0.989
35	0.980
40	0.965
45	0.942
50	0.907
55	0.858
60	0.790

This illustrates beyond doubt that for θ_c greater than 50° the effort of avoiding aperture blockage, which causes 15% to 20% reduction in the gain of the symmetrically fed reflector, by the use of the offset system is not that fruitful as the factor F deteriorates even faster for θ_c greater than 60° . On the other hand, if we consider the compensating mode in the matched feed then the situation becomes less pessimistic than previously described. This is apparent from the expression of $G_f(\theta')$ in equation (25) where the second term can now play a part in improving the gain situation beside its essential contribution in minimizing the cross-polarization.

8. NUMERICAL VARIFICATION

To test the preceding analytical investigation by the aid of a

computerized numerical calculation, the analytical feed as given in section (5) is generated in the developed program by the SUBROUTINE PFRPT (THTPR, DN, ALFA, E1, H1, E2, H2). The parameters given to the subroutine are the angle $\theta' = \text{THTPR}$, DN is the normalized aperture diameter of the cylindrical feed in wave length, and ALFA is the mixing ratio of the compensating mode. A numerical listing for E_1 , E_2 , H_1 , and H_2 every half a degree for the first 90° interval of the primary feed radiation pattern is provided as an output of the program. The choice of $\text{DN} = 1.1$ is taken for testing and the listing of five case for ALFA equal 0, 0.1, 0.2, 0.3, and 0.4 are shown below. For the purpose of identifying the corresponding ALFA from experimental results a graphical display of the asymmetrical feed radiation pattern in decibels for those cases are shown in fig. 6 and fig. 7 immediately following the numerical listing mentioned above. Fig. 6 yields the required display for a polarized electric field in the plane of symmetry according to the equation

$$(26) \quad P(\theta') = 20 \log |E_1 \pm E_2| \text{ db}$$

where the positive sign is for $\phi' = 0$ and the minus sign is for $\phi' = \pi$. This equation is a direct consequence of the matched feed radiation pattern which has the analytical form

$$\underline{E}_f = \frac{e^{-jkR'}}{R'} [(E_1 \cos \phi' + E_2 \cos 2\phi') \hat{\theta}' - (H_1 \sin \phi' + H_2 \sin 2\phi') \hat{\phi}']$$

that was discussed in earlier sections. At the same time, if the H-plane ($\phi' = \frac{\pi}{2}$ and $\phi' = \frac{3}{2}\pi$) is considered for the same equation

$$\underline{E}_f = \frac{e^{-jkR'}}{R'} [-E_2 \hat{\theta}' \pm H_1 \hat{\phi}'],$$

the selective power component due to the $\hat{\phi}'$ field can now be written as

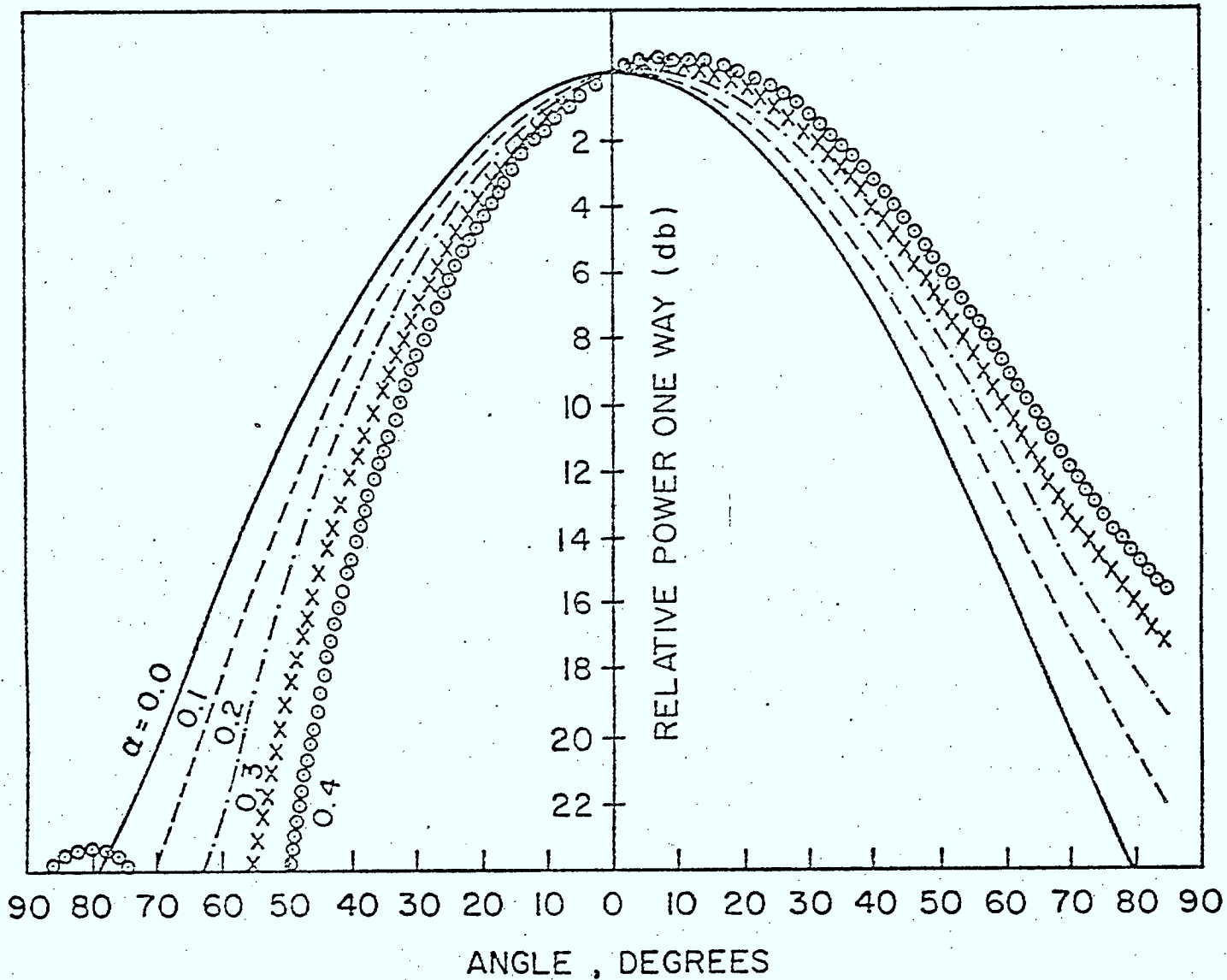


Fig. 6 Variation of $P(\theta') = 20 \log |E_1 \pm E_2|$ as a function of the polar angle θ' for different mixing ratios [$\alpha = .0, 0.1, 0.2, 0.3, \text{ and } 0.4$] of the compensating mode E_2 .

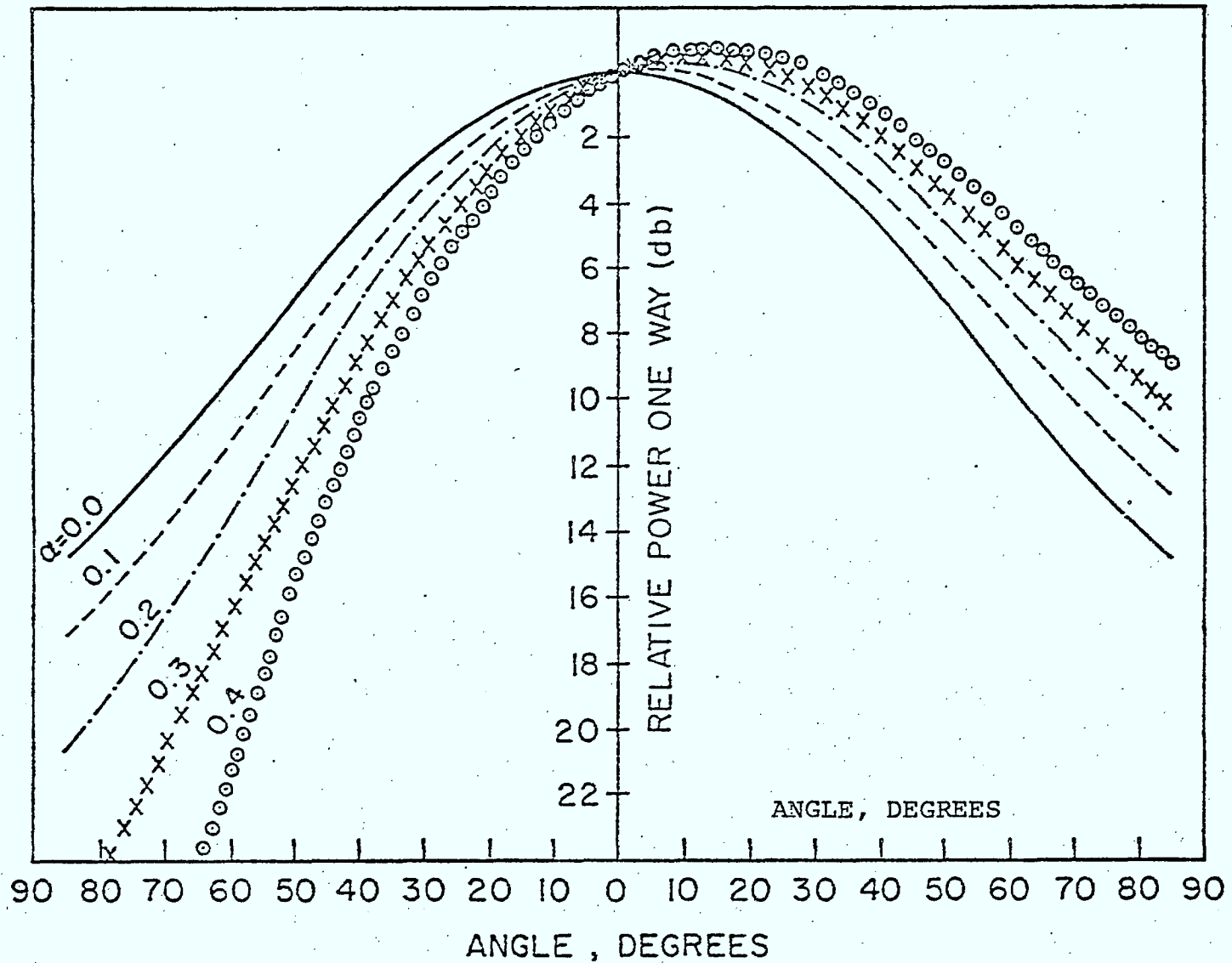


Fig. 7 Variation of $P(\theta') = 20 \log |H_1 \pm H_2|$ as a function of the polar angle θ' for different mixing ratio [$\alpha = .0, .1, .2, .3$, and $.4$] of the compensating mode H_2 .

$$(27) \quad P(\theta') = 20 \log |H_1| \text{ db}$$

For the case where the polarization of the electric field is perpendicular to the plane of symmetry, fig. 7 provides the needed display of the curves

$$(28) \quad P(\theta') = 20 \log |H_1 \pm H_2| \text{ db}$$

and again, the \pm signs are required because of the asymmetry in the radiation pattern according to

$$\underline{E}_f = \frac{e^{-jkR'}}{R'} [(E_1 \sin \phi' + E_2 \sin 2\phi') \hat{\theta}' + (H_1 \cos \phi' + H_2 \cos 2\phi') \hat{\phi}']$$

That is, the H-plane selective power component due to the $\hat{\theta}'$ -field becomes

$$(29) \quad P(\theta') = 20 \log |E_1| \text{ db}$$

The decision that has been taken, in here, is to test the validity of the matched-feed theory for the five cases mentioned above on an off-set system of $\theta_o = 50^\circ$ and $\theta_c = 45^\circ$. This decision is not at all arbitrary, although it can be so, but deliberate in order to test the feed close to its optimum operating conditions for the symmetrical illumination case. The final results of operating the program, with the polarization taken in the plane of symmetry, are shown in the tabulation following those of E_1 , H_1 , E_2 , and H_2 . Also shown, are the graphical display of the E- and H-plane radiation pattern of the antenna together with the cross-polarization in the H-plane. Note that the cross-polarization does not exist in the E-plane in this case (See equation (23)). The separate results for the five cases are combined together in fig. 8 to show the variation of the cross-polarization as a function of the mixing parameter ALFA of the compensating mode. A quick glance at those curves confirms that; for a crude estimate, the cross-polarization is depressed to a minimum in the neighbourhood of ALFA=0.3. No attempt, at this point,

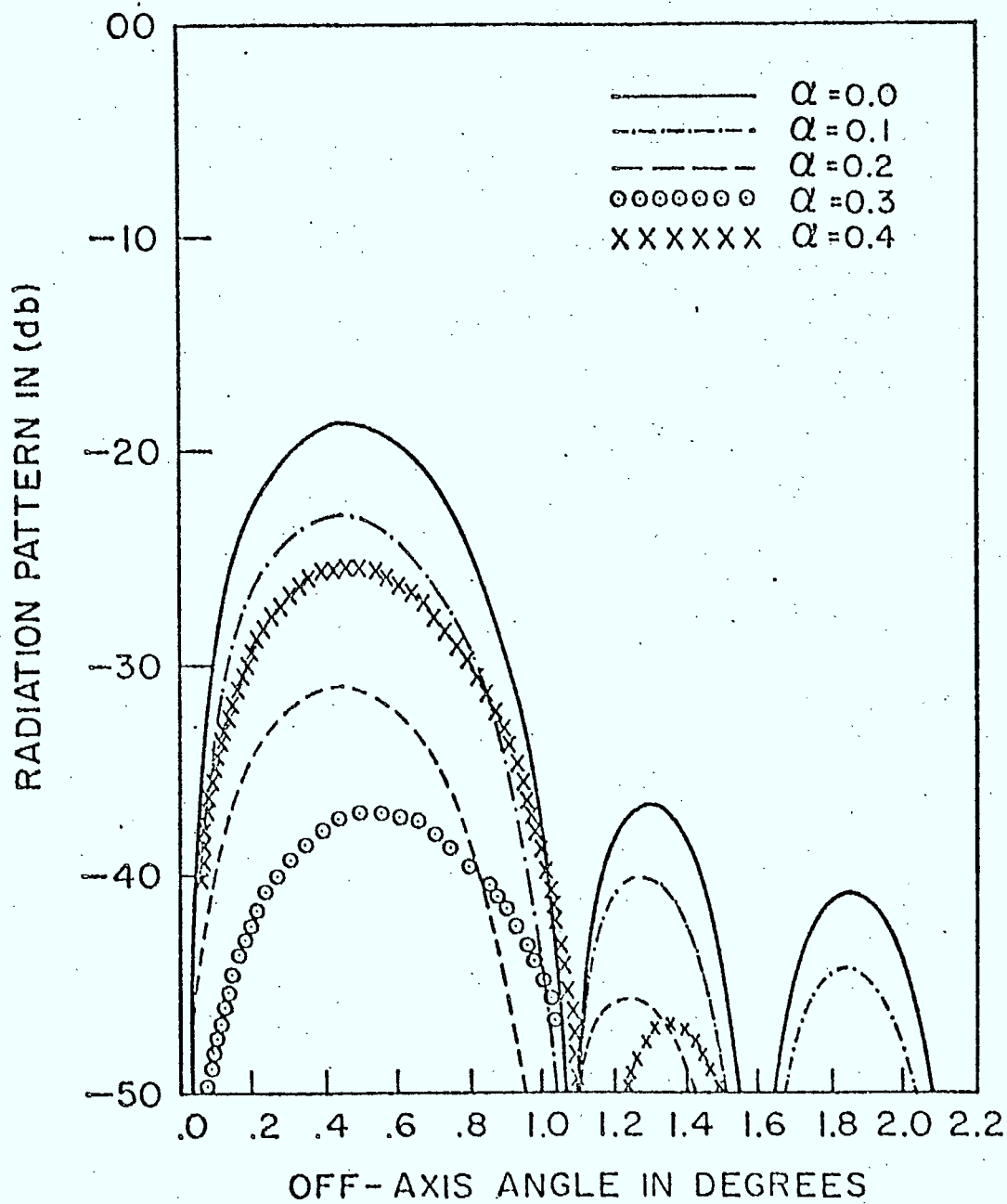


Fig. 8 Cross-polarization variation as a function of the mixing ratio (α) of the compensating mode.

is made to identify the absolute minimum for the operation of this feed. Instead, we have worked out the limiting case of $\theta_o = \theta_c = 50^\circ$ as our test case. The reason for that is clear for it is obvious from the results shown which gives output data within the constraints dictated by the contract goals. Also, it would be a wasted effort to refine ALFA for the absolute optimum and then find that achieving this value in practice, experimentally, is beyond our means. Therefore, the following section describes the experimental attempts that have been undertaken to obtain mixing of the compensating mode for values that correspond to ALFA in the neighbourhood of 0.3.

9. EXPERIMENTAL RESULTS

In the preceding sections, the characteristics of the matched primary feed radiation pattern required in an optimization of the overall antenna radiation performance have been established in terms of the relative amplitude and phase of the fundamental mode TE_{11} and the compensating TE_{21} mode. To summarize, it was shown that the two modes be nominally in phase quadrature at the feed's aperture and the relative amplitude of the compensating mode TE_{21} to that of the fundamental TE_{11} must be adjusted for the proper value depending upon the parameters of the off-set reflector to be fed. We have assumed in section (5) that the mode generating section starts at an obstruction that enhances the creation of the TE_{21} mode while has a diameter below the cut-off value of the next higher order mode. Note that we are also assuming, here, that the undesirable TM_{01} and the TM_{02} modes can be excluded or filtered by a suitable design of the generating mode section. Let us concentrate on the feed previously described by fig. 4 in section (5) where the dimension is suitable for an operational frequency of 10 GHz and the following

is the related experimental work and results. For the main electric field (TE_{11} mode) to be polarized in the symmetrical plane, say vertically, of the off-set antenna, then its component in the perpendicular direction becomes asymmetric with respect to both the x- and y-directions and does not affect any of the E- and H-plane radiation of the feed. For this particular polarization, a compensating mode that creates asymmetry in the E-plane radiation pattern of the feed is the desirable goal. This requirement can be physically justified on the basis it will compensate for the asymmetry in the aperture illumination created by the space attenuation factor $(\frac{1}{\rho^2})$ upon reflection from the paraboloidal surface of the off-set antenna. As a uniformly illuminated projected aperture yields a 100% aperture efficiency for the total radiation of the antenna, the above justification is self-explanatory in the sense that it compensates for the geometric asymmetry created by the off-set system the aperture illumination becomes closer to a uniform one than without the compensation. This physical picture should not confuse or contradict the main objective which is to lower the cross-polarization level of the antenna. To further explain, one must realize that the symmetrically fed case has no cross-polarization in any of the two main planes (E- and H-plane) and a reasonable unbalanced feed only yields a low level cross-polarization in the 45° and 135° planes while the same feed (even if it is absolutely balanced) would create a high level cross-polarization in the y-direction (H-plane) of the off-set system. To confirm this picture one should consult the numerical calculation shown before for the off-set system $\theta_o = 50^\circ$, $\theta_c = 45^\circ$ and ALFA = 0. That means, it is important to create the asymmetry in the E-plane radiation pattern of the matched feed that will lower the cross-polarization of the antenna in the y-direction (see

fig. 1) to a desirable level. Now to generate a compensating mode of the configuration shown in fig. 2-a relative to a vertically polarized fundamental we have attempted to drive a $\frac{3}{16}$ " diameter screw in the smaller diameter section of the feed (as shown in fig. 4) as close as possible to the transition that accomodates the propagation of both TE_{11} and TE_{21} modes. The feed is then mounted in a receiving mode for E-plane measurements in a microwave anechoic chamber operating in 10 GHz range. After the alignment of the transmitter and receiver has been adjusted, a measurement check on the feed without any protrusion in the guide is shown in fig. A. Besides the check mentioned, it is also useful to observe how close this radiation pattern compares with the thoeretical curve $20 \log E$, shown in fig. 6 for the case $ALFA = 0$. The measurements proceed after that with any arbitrary protrusion, using the screw in the E-plane and adding to it some nuts of different shapes and sizes to investigate the sensitivity of the radiation pattern according to the shape and size of the obstruction. Fig. B indicates a typical behaviour of one of the obstruction arrangements that accentuates the irregularities stemming from the presence of the undesirable modes previously assumed to have been filtered. The check that these irregularities are due to the propagation of the undesirable modes has been done by the use of different frequencies and observe the changes in the pattern which confirms our explanation. Success in partially eliminating the presence of those modes, has been done by trying flat obstructions with their flat surfaces parallel to the transition plane as shown in fig. C. Refining the flat obstruction with aluminum foil shows, for example, that a square area of 4 millimeter side and a thickness of about 1 millimeter gives the radiation pattern of fig. D. Aside from the wavy bump shown on the left part of

the radiation pattern surrounding the hypothetical dotted line, the radiation is almost clean from the undesirable modes as seen in the previous curves. We anticipate that rounding the corners of the square and having it correctly centred with respect to the main electric field in the guide a perfectly clean radiation pattern is assumed possible. The asymmetry in this radiation pattern, by comparison with fig. 6, gives a theoretical parameter ALFA in the neighbourhood of the value 0.2. Some other attempts, which are not documented here, has been made with a second screw at right-angle to this obstruction and the corresponding radiation was found insensitive to its presence. The functional dependence of the square planar obstruction on the frequency has also been measured in fig. E where the wavy bump size shows a slight dependence otherwise, the radiation pattern stays the same. Just for the sake of completing the data for this obstruction, the transmitter has been rotated by 90° and so is the feed, the corresponding H-plane measurement is shown in fig. F. The slight asymmetry involved in fig. F enhances our belief that the square obstruction is not exactly centred in the E-plane as it should be and that further refinement is definitely needed. Fig. G shows the effect of varying the frequency on the H-plane measurements of this obstruction. On the other hand, unfavourable results have been obtained when we tried to use the same obstruction perpendicularly to the main polarization where only a slight asymmetry has been noticed in the H-plane radiation measurements as shown in both fig. H and fig. I. That means that feed as described cannot be used to receive the dual polarization simultaneously which we would have hoped for. The understanding of this can be related to fig. 2-b where we need to generate the TE_{21} -mode in the configuration shown. The square obstruction, in this case, happened to be placed where both

the fundamental and the compensating modes are quite weak to be perturbed enough by the presence of the obstruction. With this logic in mind, two identical screws ($\frac{3}{16}$ " diameter) have been driven diagonally at -45° and -135° into the guide and made to protrude equal distances inside the structure at the two places where the compensating field is at its maximum and hence gets highly perturbed. Again, with the chamber lined up for H-plane measurements and the feed in a receiving mode, fig. A' gives the data of the radiation pattern without any protrusion. The result compares well with the theoretical curve $20 \log H_1$ shown in fig. 7 for the case of $ALFA = 0$. A slight protrusion of the two perpendicular screws, in their diagonal configuration with respect to a horizontally polarized field, yields the result shown in fig. B'. The asymmetry is already apparent in the radiation pattern which indicates quite a sensitivity for the two screws in this new position as shown. The effect of a gradual increase in the penetration of the two screws can be observed in the H-plane measurements of the feed's radiation pattern which is recorded in fig. B', fig. C', and fig. D'. When these curves are compared with the theoretical curves of fig. 7 it does confirm the ability to generate experimentally a mixing ratio of the compensating mode up to 0.35 to 0.4 for this type of main polarization. A selective case where the setting is adjusted to correspond to a mixing ratio of $ALFA$ in the neighbourhood of 0.25 and its recorded data for H-plane measurement of the radiation pattern is shown in fig. E'. On that setting a frequency measurement is recorded in fig. F' which leads to the obvious conclusion that the structure in this configuration is sensitive to the frequency. On the other hand, the use of the two perpendicular screws protruding diagonally with respect to a vertical polarization to replace the flat square

obstacle of the first part of the experiment becomes slightly discouraging in the sense that it does not yield the same corresponding mixing ratio for the horizontal polarization. This has been observed from fig. G' where the deepest penetration renders itself useless for applications while the other varied positions are recorded in fig. H', fig. I' and fig. J'. If we select the setting of fig. K' for the H-plane measurement and its corresponding E-plane radiation pattern, the results do compare with the case of flat square obstruction in the E-plane with mixing ratio in the neighbourhood of 0.25. This simple experimentation and data accumulation does help us to conclude, in this section, that the generation and the compensating TE_{21} -mode is feasible and can be accomplished with the two perpendicular screws in their diagonal configuration with respect to the field. At the same time, the setting of the obstructions that yield identical mixing ratios of the compensating mode for both polarization simultaneously is not an easy task by any means and further attempts to investigate it by experimental trials has not been done at the time of writing this report. Also, the records of the complete accumulated data are not listed here, for sake of brevity and space.

10. CONCLUSIONS

The principle task of the study undertaken in this report has been to establish the feasibility of the matched-feed devices for illuminating an off-set parabolic reflector in both principle polarization and to ensure that the design does satisfy a given set of technical specifications. The main conclusions drawn from the present study can be summarized as follows.

The modified stationary phase method for the far field computations has been successfully applied and extended to the special matched primary feed with its extra compensating mode and the yield is an efficient and economical computer program that is listed in the Appendix.

The use of the complex method of integration, residue theorem, is successful in analytically evaluating the ϕ' part of the double integration for the boresight gain of the antenna. This leads to the analytical conclusions that the seeming advantage of the off-set system over its symmetrical counter-part, by avoiding the aperture blockage, does not hold true for deep illumination, or small F/D ratio, of the reflector.

The capability of the matched primary-feed to match the off-set reflector focal-plane, in the receiving mode, is theoretically feasible and as a result of the matching does have the ability of suppressing the cross-polarization level of the antenna. That means when used in conjunction with off-set reflector surfaces, with moderate F/D ratio from 0.5 to 0.7, these devices can overcome a significant part of the depolarization and beam-squinting properties of the antenna. Also the use of the compensation in the matched primary-feed has an added advantage of improving the off-set antenna gain over the conventional feed beside the main reason of its use as the lowering agent of the depolarization level.

The overall picture is that a superior radiation performance can be achieved with the above mentioned range of F/D ratio as far as depolarization and the side lobes are concerned.

REFERENCES

- [1] J.S. Cook, E.M. Elam, and H.Zucker, "The open Cassegrain antenna: Part I-Electromagnetic design and analysis" Bell Syst. J., Vol. 44, pp. 1255-1300, Sept. 1965.
- [2] T.S. Chu and R.H. Turrin, "Depolarization properties of offset reflector antenna", IEEE Trans. Antennas Propagat, Vol. AP-21, pp. 339-345, May 1973.
- [3] A.W. Rudge, "Offset reflectors with offset feeds", IEE Electron Lett., Vol 9, pp. 611-613, Dec. 1973.
- [4] A.W. Rudge, "Mutriple-Beam Antenna: Offset reflectors with offset feeds", IEEE Trans. Antenna Propagat., Vol. AP-23, No. 3, pp. 317-322, May 1975.
- [5] L. Shafai, "Optimum Design of a low noise paraboloid Antenna", Research Contract DSS 01SU-36100-5-0313, Univ. of Manitoba, March 1976.
- [6] L. Shafai and O. Aboul-Atta, "A low Noise High Gain Antenna for Satellite Terminals", IEEE Canadian Communication and Power Conference, Montreal, 1975.
- [7] D.J. Bem, "Electric field distribution in the focal region of an offset paraboloid", Proc. IEE, Vol. 116, No. 5, pp. 579-684, 1969.
- [8] J. Dijk et al, "The polarization losses of offset paraboloid antennas", IEEE Trans. Antennas Propagat, Vol. AP22, pp. 513-520, July 1974.
- [9] P.D. Potter, "A new horn antenna with suppressed side lobes and equal band widths", Microwave J., Vol. 6, pp. 71-78, June 1963.
- [10] A.W. Rudge et al, "High Performance Offset-Reflector Spacecraft Antenna Development Study", ESA Contract No. 2654/76/NLSW, Report No. RFTS 121175, R.F. Technology Center, Cleeve Road Leatherhead Surry KT22 7SA England.
- [11] R.W. Rudge and N.A. Adatia, "New Class of Primary-feed Antennas for use with offset Parabolic-Reflector Antennas", Electronics Letters, Vol. 11, No. 24, pp. 597-599, Nov. 1975.
- [12] S. Silver, "Microwave Antenna Theory and Design", New York, McGraw-Hill, 1949.

- [13] R.E. Collin and F.J. Zucker, "Antenna Theory", Part I and II, New York, McGraw-Hill, 1969.
- [14] C. Dragone and D.C. Hogg, "The radiation pattern and impedance of offset and symmetrical near field Cassegrainian and Gregorian Antennas", IEEE Trans. AP-22, pp. 472-475, 1974.
- [15] A.W. Rudge, P.R. Foster, et al, "Study of the performance and limitations of multiple-beam antennas", ESTEC Contract 2277/74HP, ERA-IITRI RF Technology Center, 1975.
- [16] W.H. Terley and H. Zucker, "A stationary phase method for the computation of the far field of open Cassegrain Antennas", Bell Syst. Tech. J., pp-431-454, March 1970.
- [17] W.V.T. Rusch, "Antenna Notes, Vol. II", Electromagnetics Institute, Technical University Denmark, Lungby, NB 84b August 1974.
- [18] H.C. Minnet et al, "A method of synthesizing radiation patterns with axial symmetry", IRE Trans. Ant. Prop. AP-2, pp. 119-127, Sept. 1966.
- [19] A.R. Valentino and P.P. Toullos, "Fields in the focal region of offset Parabolic Antenna", IEEE Trans. Antennas propagate at. pp. 859-865. Nov., 1976.
- [20] S. Ramo and J.R. Whinnery, "Fields and Waves in Modern Radio", second addition, 1960, pp. 375, John Wiley & Sons, Inc. New York.

$\alpha = 0$

ANGLE	E1-PATTERN	H1-PATTERN	E2-PATTERN	H2-PATTERN
0.0	1.000000	1.000000	0.000000	0.000000
0.5	0.999987	0.999991	0.000000	0.000000
1.0	0.999747	0.999663	0.000000	0.000000
1.5	0.998881	0.999177	0.000000	0.000000
2.0	0.997388	0.998553	0.000000	0.000000
2.5	0.996669	0.997771	0.000000	0.000000
3.0	0.995225	0.996700	0.000000	0.000000
3.5	0.993322	0.995522	0.000000	0.000000
4.0	0.991354	0.994150	0.000000	0.000000
4.5	0.989331	0.992600	0.000000	0.000000
5.0	0.986632	0.990888	0.000000	0.000000
5.5	0.984008	0.988931	0.000000	0.000000
6.0	0.981008	0.986900	0.000000	0.000000
6.5	0.977884	0.984655	0.000000	0.000000
7.0	0.974335	0.982222	0.000000	0.000000
7.5	0.970551	0.979633	0.000000	0.000000
8.0	0.966554	0.976886	0.000000	0.000000
8.5	0.962342	0.973993	0.000000	0.000000
9.0	0.957998	0.970883	0.000000	0.000000
9.5	0.953330	0.967557	0.000000	0.000000
10.0	0.948440	0.964113	0.000000	0.000000
10.5	0.943227	0.960556	0.000000	0.000000
11.0	0.937993	0.956883	0.000000	0.000000
11.5	0.932337	0.952993	0.000000	0.000000
12.0	0.926667	0.948889	0.000000	0.000000
12.5	0.920664	0.944470	0.000000	0.000000
13.0	0.914447	0.940035	0.000000	0.000000
13.5	0.908110	0.935883	0.000000	0.000000
14.0	0.901555	0.931226	0.000000	0.000000
14.5	0.894831	0.926351	0.000000	0.000000
15.0	0.887889	0.921622	0.000000	0.000000
15.5	0.880830	0.916660	0.000000	0.000000
16.0	0.873354	0.911445	0.000000	0.000000
16.5	0.865511	0.906113	0.000000	0.000000
17.0	0.857353	0.900788	0.000000	0.000000
17.5	0.850330	0.895227	0.000000	0.000000
18.0	0.842292	0.889665	0.000000	0.000000
18.5	0.834490	0.883991	0.000000	0.000000
19.0	0.826675	0.878007	0.000000	0.000000
19.5	0.818847	0.872212	0.000000	0.000000
20.0	0.810007	0.866603	0.000000	0.000000
20.5	0.801555	0.860994	0.000000	0.000000
21.0	0.792992	0.855370	0.000000	0.000000
21.5	0.784118	0.849728	0.000000	0.000000
22.0	0.775335	0.844097	0.000000	0.000000

ANGLE	E1-PATTERN	H1-PATTERN	E2-PATTERN	H2-PATTERN
22.5	0.76643	0.83449	0.00000	0.00000
23.0	0.75742	0.82792	0.00000	C.C0000
23.5	0.74833	0.82129	0.00000	C.C0000
24.0	0.73916	0.81453	0.00000	C.C0000
24.5	0.72993	0.80781	0.00000	C.C0000
25.0	0.72063	0.80098	0.00000	C.C0000
25.5	0.71128	0.79409	0.00000	C.C0000
26.0	0.70188	0.78715	0.00000	C.C0000
26.5	0.69243	0.78015	0.00000	C.C0000
27.0	0.68295	0.77313	0.00000	C.C0000
27.5	0.67343	0.76607	0.00000	C.C0000
28.0	0.66388	0.75897	0.00000	C.C0000
28.5	0.65432	0.75186	0.00000	C.C0000
29.0	0.64473	0.74473	0.00000	C.C0000
29.5	0.63514	0.73762	0.00000	C.C0000
30.0	0.62554	0.73054	0.00000	C.C0000
30.5	0.61593	0.72357	0.00000	C.C0000
31.0	0.60634	0.71685	0.00000	C.C0000
31.5	0.59675	0.71003	0.00000	C.C0000
32.0	0.58718	0.71324	0.00000	C.C0000
32.5	0.57762	0.68461	0.00000	C.C0000
33.0	0.56809	0.68217	0.00000	C.C0000
33.5	0.55859	0.67597	0.00000	C.C0000
34.0	0.54912	0.66910	0.00000	C.C0000
34.5	0.53969	0.66202	0.00000	C.C0000
35.0	0.53030	0.65483	0.00000	C.C0000
35.5	0.52096	0.64759	0.00000	C.C0000
36.0	0.51166	0.64032	0.00000	C.C0000
36.5	0.50242	0.63305	0.00000	C.C0000
37.0	0.49324	0.62577	0.00000	C.C0000
37.5	0.48412	0.61850	0.00000	C.C0000
38.0	0.47506	0.61125	0.00000	C.C0000
38.5	0.46607	0.60401	0.00000	C.C0000
39.0	0.45715	0.59680	0.00000	C.C0000
39.5	0.44830	0.58961	0.00000	C.C0000
40.0	0.43954	0.58245	0.00000	C.C0000
40.5	0.43085	0.57532	0.00000	C.C0000
41.0	0.42224	0.56822	0.00000	C.C0000
41.5	0.41372	0.56116	0.00000	C.C0000
42.0	0.40529	0.55414	0.00000	C.C0000
42.5	0.39695	0.54715	0.00000	C.C0000
43.0	0.38870	0.54021	0.00000	C.C0000
43.5	0.38054	0.53332	0.00000	C.C0000
44.0	0.37248	0.52647	0.00000	C.C0000
44.5	0.36452	0.51967	0.00000	C.C0000

ANGLE	E1-PATTERN	H1-PATTERN	E2-PATTERN	H2-PATTERN
45.0	0.35666	0.31292	0.00000	0.00000
45.5	0.34890	0.50623	0.00000	C.C0000
46.0	0.34124	0.49953	0.00000	C.00000
46.5	0.33369	0.49293	0.00000	C.00000
47.0	0.32624	0.48645	0.00000	C.C0000
47.5	0.31890	0.47999	0.00000	C.C0000
48.0	0.31166	0.47357	0.00000	C.C0000
48.5	0.30434	0.46722	0.00000	0.00000
49.0	0.29752	0.46092	0.00000	0.00000
49.5	0.29062	0.45469	0.00000	C.C0000
50.0	0.28382	0.44853	0.00000	0.00000
50.5	0.27714	0.44242	0.00000	0.00000
51.0	0.27056	0.43633	0.00000	C.C0000
51.5	0.26410	0.43024	0.00000	C.C0000
52.0	0.25775	0.42415	0.00000	0.00000
52.5	0.25152	0.41806	0.00000	0.00000
53.0	0.24539	0.41197	0.00000	C.C0000
53.5	0.23938	0.40588	0.00000	C.C0000
54.0	0.23348	0.40157	0.00000	C.C0000
54.5	0.22769	0.39600	0.00000	0.00000
55.0	0.22202	0.39051	0.00000	C.C0000
55.5	0.21645	0.38509	0.00000	C.C0000
56.0	0.21100	0.37974	0.00000	C.C0000
56.5	0.20565	0.37446	0.00000	0.00000
57.0	0.20042	0.36923	0.00000	C.C0000
57.5	0.19530	0.36411	0.00000	C.C0000
58.0	0.19028	0.35903	0.00000	C.C0000
58.5	0.18537	0.35405	0.00000	C.C0000
59.0	0.18057	0.34913	0.00000	0.00000
59.5	0.17598	0.34429	0.00000	C.C0000
60.0	0.17129	0.33950	0.00000	C.00000
60.5	0.16681	0.33479	0.00000	0.00000
61.0	0.16245	0.33013	0.00000	0.00000
61.5	0.15815	0.32559	0.00000	C.C0000
62.0	0.15397	0.32109	0.00000	0.00000
62.5	0.14990	0.31666	0.00000	0.00000
63.0	0.14593	0.31231	0.00000	C.C0000
63.5	0.14205	0.30803	0.00000	C.C0000
64.0	0.13827	0.30381	0.00000	0.00000
64.5	0.13459	0.29965	0.00000	0.00000
65.0	0.13100	0.29553	0.00000	C.C0000
65.5	0.12751	0.29154	0.00000	C.C0000
66.0	0.12411	0.28764	0.00000	C.C0000
66.5	0.12080	0.28377	0.00000	0.00000
67.0	0.11758	0.27996	0.00000	C.C0000

ANGLE	E1-PATTERN	H1-PATTERN	E2-PATTERN	H2-PATTERN
67.5	0.11445	0.27622	0.00000	C.C0C00
68.0	0.11141	0.27255	0.00000	C.C0C00
68.5	0.10345	0.26894	0.00000	C.C0C00
69.0	0.10558	0.26540	0.00000	C.C0C00
69.5	0.10280	0.26192	0.00000	C.C0C00
70.0	0.10009	0.25850	0.00000	C.C0C00
70.5	0.09747	0.25515	0.00000	C.C0C00
71.0	0.09493	0.25195	0.00000	C.C0C00
71.5	0.09246	0.24886	0.00000	C.C0C00
72.0	0.09008	0.24587	0.00000	C.C0C00
72.5	0.08777	0.24296	0.00000	C.C0C00
73.0	0.08553	0.23932	0.00000	C.C0C00
73.5	0.08337	0.23633	0.00000	C.C0C00
74.0	0.08128	0.23340	0.00000	C.C0C00
74.5	0.07926	0.23053	0.00000	C.C0C00
75.0	0.07730	0.22777	0.00000	C.C0C00
75.5	0.07542	0.22495	0.00000	C.C0C00
76.0	0.07361	0.22225	0.00000	C.C0C00
76.5	0.07186	0.21960	0.00000	C.C0C00
77.0	0.07017	0.21701	0.00000	C.C0C00
77.5	0.06855	0.21447	0.00000	C.C0C00
78.0	0.06699	0.21193	0.00000	C.C0C00
78.5	0.06549	0.20954	0.00000	C.C0C00
79.0	0.06405	0.20716	0.00000	C.C0C00
79.5	0.06267	0.20482	0.00000	C.C0C00
80.0	0.06134	0.20253	0.00000	C.C0C00
80.5	0.06007	0.20029	0.00000	C.C0C00
81.0	0.05886	0.19810	0.00000	C.C0C00
81.5	0.05770	0.19596	0.00000	C.C0C00
82.0	0.05659	0.19386	0.00000	C.C0C00
82.5	0.05553	0.19181	0.00000	C.C0C00
83.0	0.05452	0.18980	0.00000	C.C0C00
83.5	0.05357	0.18784	0.00000	C.C0C00
84.0	0.05266	0.18592	0.00000	C.C0C00
84.5	0.05179	0.18404	0.00000	C.C0C00
85.0	0.05098	0.18220	0.00000	C.C0C00
85.5	0.05021	0.18041	0.00000	C.C0C00
86.0	0.04948	0.17865	0.00000	C.C0C00
86.5	0.04879	0.17693	0.00000	C.C0C00
87.0	0.04815	0.17525	0.00000	C.C0C00
87.5	0.04755	0.17361	0.00000	C.C0C00
88.0	0.04699	0.17201	0.00000	C.C0C00
88.5	0.04646	0.17044	0.00000	C.C0C00
89.0	0.04598	0.16891	0.00000	C.C0C00
89.5	0.04553	0.16741	0.00000	C.C0C00

$\alpha = 0.1$

ANGLE	H1-PATTERN	H1-PATTERN	H2-PATTERN	H2-PATTERN
0.0	1.00000	1.00000	0.00000	0.00000
0.5	0.99937	0.99991	0.00150	0.00151
1.0	0.99847	0.99961	0.00301	0.00302
1.5	0.99738	0.99917	0.00452	0.00452
2.0	0.99619	0.99853	0.00602	0.00602
2.5	0.99493	0.99771	0.00752	0.00752
3.0	0.99352	0.99670	0.00901	0.00902
3.5	0.99195	0.99552	0.01050	0.01051
4.0	0.98931	0.99413	0.01198	0.01200
4.5	0.98682	0.99260	0.01345	0.01348
5.0	0.98408	0.99089	0.01492	0.01495
5.5	0.98108	0.98893	0.01637	0.01642
6.0	0.97734	0.98690	0.01782	0.01787
6.5	0.97435	0.98463	0.01925	0.01932
7.0	0.97061	0.98222	0.02067	0.02076
7.5	0.96664	0.97963	0.02208	0.02219
8.0	0.96242	0.97683	0.02347	0.02360
8.5	0.95793	0.97393	0.02485	0.02501
9.0	0.95330	0.97083	0.02622	0.02640
9.5	0.94840	0.96757	0.02756	0.02778
10.0	0.94337	0.96415	0.02889	0.02914
10.5	0.93827	0.96056	0.03021	0.03050
11.0	0.93302	0.95683	0.03150	0.03183
11.5	0.92766	0.95293	0.03277	0.03315
12.0	0.92221	0.94883	0.03403	0.03446
12.5	0.91664	0.94470	0.03526	0.03574
13.0	0.91147	0.94035	0.03647	0.03701
13.5	0.90610	0.93583	0.03767	0.03826
14.0	0.90153	0.93125	0.03883	0.03950
14.5	0.89781	0.92651	0.03998	0.04071
15.0	0.89478	0.92162	0.04110	0.04191
15.5	0.89203	0.91660	0.04220	0.04308
16.0	0.88954	0.91145	0.04327	0.04424
16.5	0.88711	0.90613	0.04432	0.04537
17.0	0.88483	0.90073	0.04534	0.04649
17.5	0.88269	0.89527	0.04634	0.04758
18.0	0.88069	0.88965	0.04731	0.04865
18.5	0.87883	0.88391	0.04826	0.04970
19.0	0.87710	0.87807	0.04917	0.05073
19.5	0.87547	0.87212	0.05006	0.05173
20.0	0.87390	0.86608	0.05093	0.05271
20.5	0.87235	0.85994	0.05176	0.05367
21.0	0.87082	0.85370	0.05257	0.05461
21.5	0.86931	0.84733	0.05335	0.05552
22.0	0.86775	0.84097	0.05410	0.05640

ANGLE	E1-PATTERN	H1-PATTERN	E2-PATTERN	H2-PATTERN
22.5	0.76643	0.83449	0.05433	0.05727
23.0	0.75742	0.82792	0.05532	0.05811
23.5	0.74833	0.82129	0.05619	0.05892
24.0	0.73916	0.81453	0.05683	0.05971
24.5	0.72993	0.80781	0.05744	0.06048
25.0	0.72063	0.80103	0.05803	0.06122
25.5	0.71129	0.79409	0.05858	0.06194
26.0	0.70189	0.78715	0.05911	0.06263
26.5	0.69243	0.78013	0.05961	0.06330
27.0	0.68293	0.77313	0.06008	0.06394
27.5	0.67343	0.76607	0.06052	0.06456
28.0	0.66383	0.75897	0.06094	0.06516
28.5	0.65433	0.75186	0.06133	0.06573
29.0	0.64474	0.74473	0.06169	0.06627
29.5	0.63515	0.73762	0.06202	0.06679
30.0	0.62555	0.73051	0.06233	0.06729
30.5	0.61593	0.72337	0.06261	0.06777
31.0	0.60634	0.71623	0.06287	0.06822
31.5	0.59673	0.70903	0.06310	0.06864
32.0	0.58713	0.70184	0.06331	0.06905
32.5	0.57762	0.69461	0.06349	0.06943
33.0	0.56809	0.68741	0.06364	0.06979
33.5	0.55854	0.68017	0.06377	0.07012
34.0	0.54891	0.67290	0.06388	0.07043
34.5	0.53929	0.66562	0.06397	0.07072
35.0	0.52969	0.65833	0.06403	0.07099
35.5	0.52009	0.65104	0.06407	0.07124
36.0	0.51048	0.64375	0.06409	0.07146
36.5	0.50088	0.63646	0.06408	0.07166
37.0	0.49127	0.62917	0.06405	0.07185
37.5	0.48167	0.62187	0.06400	0.07201
38.0	0.47206	0.61458	0.06394	0.07215
38.5	0.46246	0.60729	0.06385	0.07227
39.0	0.45285	0.59999	0.06373	0.07237
39.5	0.44325	0.59270	0.06362	0.07246
40.0	0.43364	0.58541	0.06348	0.07252
40.5	0.42404	0.57812	0.06332	0.07257
41.0	0.41443	0.57083	0.06314	0.07260
41.5	0.40483	0.56354	0.06295	0.07261
42.0	0.39522	0.55625	0.06274	0.07260
42.5	0.38562	0.54896	0.06251	0.07257
43.0	0.37601	0.54167	0.06227	0.07253
43.5	0.36641	0.53438	0.06202	0.07248
44.0	0.35680	0.52709	0.06175	0.07240
44.5	0.34720	0.51980	0.06147	0.07231

ANGLE	E1-PATTERN	H1-PATTERN	E2-PATTERN	H2-PATTERN
45.0	0.35656	0.51293	0.06117	C.07221
45.5	0.34490	0.50623	0.06086	C.07209
46.0	0.33324	0.49953	0.06054	C.07196
46.5	0.32158	0.49283	0.06021	C.07181
47.0	0.31000	0.48613	0.05987	C.07165
47.5	0.29842	0.47943	0.05952	C.07143
48.0	0.28684	0.47273	0.05916	C.07130
48.5	0.27526	0.46603	0.05879	C.07110
49.0	0.26368	0.45933	0.05841	C.07089
49.5	0.25210	0.45263	0.05802	C.07067
50.0	0.24052	0.44593	0.05762	C.07044
50.5	0.22894	0.43923	0.05722	C.07019
51.0	0.21736	0.43253	0.05681	C.06994
51.5	0.20578	0.42583	0.05639	C.06968
52.0	0.19420	0.41913	0.05597	C.06941
52.5	0.18262	0.41243	0.05554	C.06912
53.0	0.17104	0.40573	0.05511	C.06883
53.5	0.15946	0.39903	0.05467	C.06854
54.0	0.14788	0.39233	0.05422	C.06823
54.5	0.13630	0.38563	0.05378	C.06792
55.0	0.12472	0.37893	0.05333	C.06760
55.5	0.11314	0.37223	0.05287	C.06727
56.0	0.10156	0.36553	0.05242	C.06694
56.5	0.09000	0.35883	0.05196	C.06660
57.0	0.07842	0.35213	0.05150	C.06626
57.5	0.06684	0.34543	0.05104	C.06591
58.0	0.05526	0.33873	0.05057	C.06556
58.5	0.04368	0.33203	0.05011	C.06521
59.0	0.03210	0.32533	0.04965	C.06486
59.5	0.02052	0.31863	0.04918	C.06452
60.0	0.00894	0.31193	0.04872	C.06418
60.5	0.00000	0.30523	0.04825	C.06387
61.0	0.00000	0.29853	0.04779	C.06363
61.5	0.00000	0.29183	0.04732	C.06364
62.0	0.00000	0.28513	0.04685	C.06375
62.5	0.00000	0.27843	0.04640	C.06367
63.0	0.00000	0.27173	0.04594	C.06399
63.5	0.00000	0.26503	0.04548	C.06378
64.0	0.00000	0.25833	0.04502	C.06348
64.5	0.00000	0.25163	0.04457	C.06313
65.0	0.00000	0.24493	0.04412	C.05975
65.5	0.00000	0.23823	0.04367	C.05937
66.0	0.00000	0.23153	0.04322	C.05897
66.5	0.00000	0.22483	0.04278	C.05857
67.0	0.00000	0.21813	0.04234	C.05817

ANGLE	H1-PATTERN	H1-PATTERN	H2-PATTERN	H2-PATTERN
67.5	0.11445	0.27622	0.04191	0.05776
68.0	0.11741	0.27255	0.04147	0.05735
68.5	0.10945	0.26894	0.04104	0.05694
69.0	0.10559	0.26540	0.04062	0.05652
69.5	0.10290	0.26192	0.04020	0.05611
70.0	0.10009	0.25850	0.03978	0.05570
70.5	0.09747	0.25515	0.03937	0.05528
71.0	0.09493	0.25186	0.03896	0.05487
71.5	0.09246	0.24863	0.03855	0.05445
72.0	0.09008	0.24547	0.03815	0.05404
72.5	0.08777	0.24236	0.03775	0.05363
73.0	0.08553	0.23930	0.03736	0.05321
73.5	0.08337	0.23630	0.03698	0.05280
74.0	0.08128	0.23334	0.03659	0.05239
74.5	0.07926	0.23053	0.03621	0.05198
75.0	0.07730	0.22777	0.03584	0.05157
75.5	0.07542	0.22509	0.03547	0.05116
76.0	0.07361	0.22245	0.03511	0.05076
76.5	0.07186	0.21986	0.03475	0.05035
77.0	0.07017	0.21731	0.03440	0.04995
77.5	0.06855	0.21481	0.03405	0.04955
78.0	0.06699	0.21234	0.03370	0.04915
78.5	0.06549	0.20991	0.03336	0.04875
79.0	0.06405	0.20751	0.03303	0.04835
79.5	0.06267	0.20514	0.03270	0.04796
80.0	0.06134	0.20280	0.03238	0.04756
80.5	0.06007	0.20049	0.03206	0.04717
81.0	0.05886	0.19821	0.03174	0.04678
81.5	0.05770	0.19595	0.03143	0.04639
82.0	0.05659	0.19371	0.03113	0.04600
82.5	0.05551	0.19150	0.03082	0.04563
83.0	0.05445	0.18930	0.03053	0.04525
83.5	0.05357	0.18712	0.03024	0.04487
84.0	0.05266	0.18495	0.02995	0.04449
84.5	0.05179	0.18280	0.02967	0.04412
85.0	0.05093	0.18067	0.02939	0.04374
85.5	0.05021	0.17856	0.02912	0.04337
86.0	0.04948	0.17646	0.02885	0.04300
86.5	0.04879	0.17438	0.02858	0.04264
87.0	0.04815	0.17231	0.02832	0.04228
87.5	0.04755	0.17026	0.02807	0.04191
88.0	0.04699	0.16821	0.02781	0.04155
88.5	0.04646	0.16618	0.02757	0.04120
89.0	0.04593	0.16416	0.02732	0.04084
89.5	0.04553	0.16214	0.02708	0.04049

$\alpha = 0.2$

ANGLE	E1-PATTERN	H1-PATTERN	E2-PATTERN	H2-PATTERN
0.0	1.00000	1.00000	0.00000	0.00000
0.5	0.99937	0.99991	0.00301	C.00302
1.0	0.99947	0.99963	0.00603	C.00603
1.5	0.99931	0.99917	C.00904	C.C0904
2.0	0.99788	0.99853	0.01204	C.C1205
2.5	0.99669	0.99771	0.01504	C.C1505
3.0	0.99523	0.99670	0.01802	C.C1804
3.5	0.99332	0.99552	0.02100	C.C2102
4.0	0.99154	0.99415	0.02396	C.C2399
4.5	0.98931	0.99260	0.02691	C.C2695
5.0	0.98692	0.99089	0.02993	C.C2990
5.5	0.98406	0.98898	0.03274	C.C3283
6.0	0.98103	0.98690	0.03553	C.C3575
6.5	0.97784	0.98463	0.03830	C.C3864
7.0	0.97435	0.98223	0.04134	C.C4152
7.5	0.97051	0.97963	0.04446	C.C4437
8.0	0.96654	0.97695	0.04694	C.C4721
8.5	0.96242	0.97393	0.04970	C.C5002
9.0	0.95793	0.97083	0.05242	C.C5280
9.5	0.95330	0.96757	0.05512	C.C5556
10.0	0.94840	0.96415	0.05779	C.C5829
10.5	0.94327	0.96055	0.06041	C.C6099
11.0	0.93793	0.95683	0.06300	C.C6366
11.5	0.93237	0.95293	0.06555	C.C6630
12.0	0.92661	0.94889	0.06806	C.C6891
12.5	0.92054	0.94470	C.07052	C.C7148
13.0	0.91417	0.94033	0.07293	C.C7402
13.5	0.90810	0.93583	0.07533	C.C7653
14.0	0.90135	0.93126	0.07767	C.C7900
14.5	0.89481	0.92651	0.07996	C.C8143
15.0	0.88789	0.92163	0.08220	C.C8382
15.5	0.88080	0.91663	0.08440	C.C8617
16.0	0.87334	0.91145	0.08654	C.C8848
16.5	0.86561	0.90613	0.08864	C.C9075
17.0	0.85733	0.90073	0.09069	C.C9298
17.5	0.84890	0.89527	0.09268	C.C9516
18.0	0.84022	0.88963	0.09462	C.C9730
18.5	0.83140	0.88391	0.09651	C.C9940
19.0	0.82267	0.87807	0.09835	C.10146
19.5	0.81384	0.87212	0.10013	C.10346
20.0	0.80497	0.86608	0.10185	C.10543
20.5	0.79595	0.85994	0.10353	C.10734
21.0	0.78679	0.85370	0.10514	C.10921
21.5	0.77748	0.84733	0.10670	C.11103
22.0	0.77535	0.84097	0.10821	C.11281

ANGLE	L1-PATTERN	H1-PATTERN	E2-PATTERN	H2-PATTERN
22.5	0.76643	0.33449	0.10966	C.11453
22.0	0.75742	0.32792	0.11123	C.11621
21.5	0.74833	0.32129	0.11238	C.11784
21.0	0.73911	0.31453	0.11366	C.11942
20.5	0.72993	0.30781	0.11489	C.12095
20.0	0.72063	0.30093	0.11605	C.12244
19.5	0.71122	0.29409	0.11716	C.12387
19.0	0.70171	0.28715	0.11822	C.12526
18.5	0.69224	0.28013	0.11922	C.12659
18.0	0.68273	0.27313	0.12016	C.12788
17.5	0.67313	0.26607	0.12105	C.12912
17.0	0.66333	0.25897	0.12188	C.13031
16.5	0.65344	0.25186	0.12266	C.13145
16.0	0.64344	0.24472	0.12339	C.13254
15.5	0.63351	0.23762	0.12405	C.13359
15.0	0.62353	0.23054	0.12466	C.13459
14.5	0.61359	0.22357	0.12523	C.13553
14.0	0.60363	0.21683	0.12577	C.13643
13.5	0.59367	0.21003	0.12628	C.13729
13.0	0.58371	0.20324	0.12676	C.13810
12.5	0.57378	0.19646	0.12721	C.13886
12.0	0.56383	0.18971	0.12762	C.13957
11.5	0.55385	0.18300	0.12800	C.14024
11.0	0.54389	0.17632	0.12835	C.14086
10.5	0.53391	0.16967	0.12867	C.14144
10.0	0.52393	0.16303	0.12896	C.14198
9.5	0.51396	0.15642	0.12922	C.14247
9.0	0.50398	0.14983	0.12945	C.14292
8.5	0.49399	0.14326	0.12965	C.14333
8.0	0.48399	0.13671	0.12982	C.14369
7.5	0.47399	0.13018	0.12996	C.14402
7.0	0.46399	0.12367	0.13007	C.14430
6.5	0.45399	0.11718	0.13015	C.14454
6.0	0.44399	0.11071	0.13020	C.14475
5.5	0.43399	0.10426	0.13023	C.14491
5.0	0.42399	0.09783	0.13024	C.14504
4.5	0.41399	0.09142	0.13023	C.14514
4.0	0.40399	0.08503	0.13020	C.14519
3.5	0.39399	0.07866	0.13015	C.14521
3.0	0.38399	0.07231	0.13007	C.14520
2.5	0.37399	0.06598	0.13003	C.14515
2.0	0.36399	0.05967	0.13003	C.14507
1.5	0.35399	0.05338	0.13003	C.14495
1.0	0.34399	0.04711	0.13003	C.14481
0.5	0.33399	0.04086	0.13003	C.14463

ANGLE	E1-PATTERN	H1-PATTERN	E2-PATTERN	H2-PATTERN
45.0	0.35666	0.51292	0.12234	0.14442
45.5	0.34890	0.50625	0.12173	C.14419
46.0	0.34124	0.49958	0.12109	C.14392
46.5	0.33358	0.49291	0.12043	C.14363
47.0	0.32624	0.48624	0.11974	C.14331
47.5	0.31890	0.47957	0.11904	C.14296
48.0	0.31166	0.47290	0.11833	C.14259
48.5	0.30432	0.46623	0.11762	C.14220
49.0	0.29698	0.45956	0.11691	C.14178
49.5	0.28964	0.45289	0.11620	C.14134
50.0	0.28230	0.44622	0.11549	C.14087
50.5	0.27496	0.43955	0.11478	C.14039
51.0	0.26762	0.43288	0.11407	C.13988
51.5	0.26028	0.42621	0.11336	C.13936
52.0	0.25294	0.41954	0.11265	C.13881
52.5	0.24560	0.41287	0.11194	C.13825
53.0	0.23826	0.40620	0.11123	C.13767
53.5	0.23092	0.39953	0.11052	C.13707
54.0	0.22358	0.39286	0.10981	C.13644
54.5	0.21624	0.38619	0.10910	C.13583
55.0	0.20890	0.37952	0.10839	C.13519
55.5	0.20156	0.37285	0.10768	C.13454
56.0	0.19422	0.36618	0.10697	C.13388
56.5	0.18688	0.35951	0.10626	C.13320
57.0	0.17954	0.35284	0.10555	C.13252
57.5	0.17220	0.34617	0.10484	C.13182
58.0	0.16486	0.33950	0.10413	C.13112
58.5	0.15752	0.33283	0.10342	C.13042
59.0	0.15018	0.32616	0.10271	C.12972
59.5	0.14284	0.31949	0.10200	C.12903
60.0	0.13550	0.31282	0.10129	C.12833
60.5	0.12816	0.30615	0.10058	C.12775
61.0	0.12082	0.29948	0.09987	C.12727
61.5	0.11348	0.29281	0.09916	C.12728
62.0	0.10614	0.28614	0.09845	C.13550
62.5	0.09880	0.27947	0.09774	C.12135
63.0	0.09146	0.27280	0.09703	C.12148
63.5	0.08412	0.26613	0.09632	C.12157
64.0	0.07678	0.25946	0.09561	C.12096
64.5	0.06944	0.25279	0.09490	C.12025
65.0	0.06210	0.24612	0.09419	C.11950
65.5	0.05476	0.23945	0.09348	C.11873
66.0	0.04742	0.23278	0.09277	C.11794
66.5	0.04008	0.22611	0.09206	C.11714
67.0	0.03274	0.21944	0.09135	C.11633

ANGLE	E1-PATTERN	H1-PATTERN	E2-PATTERN	H2-PATTERN
67.5	0.11445	0.27622	0.08381	0.11552
68.0	0.11141	0.27235	0.08295	C.11470
68.5	0.10845	0.26849	0.08209	C.11387
69.0	0.10558	0.26544	0.08124	C.11305
69.5	0.10280	0.26290	0.08039	C.11222
70.0	0.10009	0.26035	0.07956	C.11139
70.5	0.09747	0.25781	0.07873	C.11057
71.0	0.09493	0.25527	0.07791	C.10974
71.5	0.09246	0.25274	0.07710	C.10891
72.0	0.09008	0.25021	0.07630	C.10808
72.5	0.08777	0.24768	0.07551	0.10725
73.0	0.08553	0.24516	0.07472	C.10643
73.5	0.08337	0.24264	0.07395	C.10560
74.0	0.08128	0.24012	0.07319	C.10478
74.5	0.07926	0.23761	0.07243	C.10396
75.0	0.07730	0.23510	0.07168	C.10314
75.5	0.07542	0.23260	0.07095	C.10233
76.0	0.07361	0.23010	0.07022	C.10151
76.5	0.07186	0.22761	0.06950	C.10070
77.0	0.07017	0.22512	0.06879	C.09990
77.5	0.06855	0.22264	0.06810	C.09909
78.0	0.06699	0.22016	0.06741	C.09829
78.5	0.06549	0.21769	0.06673	C.09749
79.0	0.06405	0.21522	0.06606	C.09670
79.5	0.06267	0.21276	0.06540	C.09591
80.0	0.06134	0.21031	0.06475	C.09512
80.5	0.06007	0.20786	0.06411	C.09434
81.0	0.05886	0.20542	0.06348	C.09356
81.5	0.05770	0.20300	0.06286	C.09279
82.0	0.05659	0.20058	0.06225	C.09202
82.5	0.05553	0.19817	0.06165	C.09125
83.0	0.05452	0.19577	0.06106	C.09049
83.5	0.05357	0.19338	0.06047	C.08973
84.0	0.05266	0.19100	0.05990	C.08898
84.5	0.05179	0.18863	0.05934	C.08823
85.0	0.05098	0.18627	0.05878	C.08749
85.5	0.05021	0.18392	0.05823	C.08675
86.0	0.04948	0.18158	0.05770	C.08601
86.5	0.04879	0.17925	0.05717	C.08528
87.0	0.04815	0.17693	0.05665	C.08455
87.5	0.04755	0.17461	0.05613	C.08383
88.0	0.04699	0.17230	0.05563	C.08311
88.5	0.04646	0.17001	0.05513	C.08239
89.0	0.04598	0.16773	0.05465	C.08168
89.5	0.04555	0.16741	0.05417	C.08098

$\alpha = 0.3$

ANGLE	E1-PATTERN	H1-PATTERN	E2-PATTERN	H2-PATTERN
0.0	1.00000	1.00000	0.00000	C.00000
0.5	0.99987	0.99997	0.00451	C.00453
1.0	0.99947	0.99963	0.00904	C.00905
1.5	0.99881	0.99917	0.01356	C.01356
2.0	0.99788	0.99853	0.01806	C.01807
2.5	0.99669	0.99777	0.02255	C.02255
3.0	0.99523	0.99670	0.02703	C.02703
3.5	0.99352	0.99532	0.03150	C.03153
4.0	0.99154	0.99415	0.03594	C.03599
4.5	0.98931	0.99260	0.04036	C.04043
5.0	0.98682	0.99089	0.04475	C.04485
5.5	0.98403	0.98893	0.04912	C.04925
6.0	0.98103	0.98690	0.05345	C.05362
6.5	0.97784	0.98482	0.05775	C.05796
7.0	0.97435	0.98222	0.06201	C.06228
7.5	0.97067	0.97963	0.06623	C.06656
8.0	0.96664	0.97685	0.07042	C.07081
8.5	0.96242	0.97393	0.07453	C.07502
9.0	0.95793	0.97082	0.07855	C.07920
9.5	0.95330	0.96757	0.08269	C.08334
10.0	0.94940	0.96415	0.08653	C.08749
10.5	0.94537	0.96056	0.09062	C.09149
11.0	0.94117	0.95683	0.09450	C.09549
11.5	0.93683	0.95292	0.09832	C.09945
12.0	0.93261	0.94889	0.10208	C.10337
12.5	0.92864	0.94470	0.10579	C.10723
13.0	0.92447	0.94033	0.10942	C.11104
13.5	0.92081	0.93583	0.11300	C.11479
14.0	0.91755	0.93126	0.11650	C.11849
14.5	0.91431	0.92651	0.11994	C.12214
15.0	0.91108	0.92162	0.12330	C.12572
15.5	0.90789	0.91660	0.12659	C.12925
16.0	0.90465	0.91145	0.12981	C.13272
16.5	0.90131	0.90613	0.13295	C.13612
17.0	0.89783	0.90078	0.13603	C.13947
17.5	0.89420	0.89527	0.13902	C.14274
18.0	0.89042	0.88965	0.14193	C.14596
18.5	0.88649	0.88391	0.14477	C.14910
19.0	0.88267	0.87807	0.14752	C.15218
19.5	0.87875	0.87212	0.15019	C.15520
20.0	0.87477	0.86603	0.15278	C.15814
20.5	0.87075	0.85994	0.15529	C.16101
21.0	0.86669	0.85370	0.15771	C.16382
21.5	0.86251	0.84738	0.16005	C.16655
22.0	0.85823	0.84097	0.16231	C.16921

ANGLE	H1-PATTERN	H1-PATTERN	E2-PATTERN	H2-PATTERN
22.5	0.76643	0.33449	0.16449	0.17180
23.0	0.73742	0.32792	0.16657	0.17432
23.5	0.74333	0.82129	0.16858	0.17676
24.0	0.72916	0.61453	0.17055	0.17913
24.5	0.72992	0.80781	0.17233	0.18143
25.0	0.72200	0.80093	0.17408	0.18366
25.5	0.71138	0.79409	0.17575	0.18581
26.0	0.70071	0.78715	0.17733	0.18789
26.5	0.69243	0.78015	0.17882	0.18989
27.0	0.68295	0.77313	0.16024	0.19182
27.5	0.67343	0.76607	0.18157	0.19368
28.0	0.66538	0.75897	0.18282	0.19547
28.5	0.65543	0.75186	0.18393	0.19718
29.0	0.64473	0.74473	0.18507	0.19882
29.5	0.63354	0.73762	0.18607	0.20038
30.0	0.62235	0.73054	0.18700	0.20188
30.5	0.61159	0.72357	0.18784	0.20330
31.0	0.60063	0.71685	0.18881	0.20465
31.5	0.59675	0.71103	0.18930	0.20593
32.0	0.59871	0.71324	0.18992	0.20714
32.5	0.59776	0.68846	0.19046	0.20828
33.0	0.59809	0.68217	0.19093	0.20936
33.5	0.59859	0.67597	0.19132	0.21036
34.0	0.59491	0.66990	0.19164	0.21130
34.5	0.59296	0.66202	0.19190	0.21217
35.0	0.59303	0.65483	0.19208	0.21297
35.5	0.59209	0.64739	0.19220	0.21371
36.0	0.59116	0.64032	0.19223	0.21438
36.5	0.59024	0.63303	0.19223	0.21499
37.0	0.58932	0.62577	0.19221	0.21554
37.5	0.58841	0.61850	0.19201	0.21602
38.0	0.58750	0.61123	0.19181	0.21645
38.5	0.58660	0.60401	0.19155	0.21682
39.0	0.58571	0.59680	0.19124	0.21712
39.5	0.58483	0.58961	0.19086	0.21737
40.0	0.58393	0.58243	0.19044	0.21757
40.5	0.58303	0.57523	0.18996	0.21770
41.0	0.58222	0.56822	0.18943	0.21779
41.5	0.58137	0.56115	0.18884	0.21782
42.0	0.58052	0.55414	0.18821	0.21779
42.5	0.57969	0.54714	0.18754	0.21772
43.0	0.57887	0.54021	0.18682	0.21760
43.5	0.57805	0.53333	0.18605	0.21743
44.0	0.57724	0.52647	0.18525	0.21721
44.5	0.57644	0.51967	0.18440	0.21694

ANGLE	E1-PATTERN	H1-PATTERN	E2-PATTERN	H2-PATTERN
45.0	0.35665	0.51292	0.18351	C.21663
45.5	0.34890	0.50623	0.18259	C.21628
46.0	0.34124	0.49953	0.18163	C.21588
46.5	0.33359	0.49292	0.18064	C.21544
47.0	0.32624	0.48644	0.17961	C.21496
47.5	0.31890	0.47999	0.17856	C.21444
48.0	0.31166	0.47357	0.17747	C.21389
48.5	0.30454	0.46722	0.17636	C.21330
49.0	0.29752	0.46092	0.17522	C.21267
49.5	0.29062	0.45468	0.17406	C.21200
50.0	0.28382	0.44853	0.17287	C.21131
50.5	0.27714	0.44242	0.17166	C.21058
51.0	0.27056	0.43633	0.17042	C.20982
51.5	0.26410	0.43024	0.16917	C.20903
52.0	0.25775	0.42415	0.16790	C.20822
52.5	0.25152	0.41807	0.16662	C.20737
53.0	0.24539	0.41200	0.16532	C.20650
53.5	0.23938	0.40592	0.16400	C.20561
54.0	0.23338	0.40015	0.16267	C.20469
54.5	0.22739	0.39460	0.16133	C.20375
55.0	0.22142	0.38905	0.15998	C.20279
55.5	0.21545	0.38350	0.15862	C.20181
56.0	0.20950	0.37797	0.15726	C.20081
56.5	0.20355	0.37244	0.15588	C.19980
57.0	0.19762	0.36692	0.15450	C.19877
57.5	0.19170	0.36141	0.15311	C.19773
58.0	0.18583	0.35590	0.15172	C.19669
58.5	0.18000	0.35040	0.15033	C.19563
59.0	0.17423	0.34491	0.14894	C.19458
59.5	0.16851	0.33942	0.14754	C.19355
60.0	0.16281	0.33394	0.14615	C.19252
60.5	0.15715	0.32847	0.14475	C.19150
61.0	0.15151	0.32301	0.14336	C.19049
61.5	0.14589	0.31755	0.14197	C.18949
62.0	0.14030	0.31210	0.14058	C.18849
62.5	0.13473	0.30665	0.13919	C.18750
63.0	0.12919	0.30121	0.13781	C.18651
63.5	0.12367	0.29578	0.13644	C.18553
64.0	0.11817	0.29038	0.13507	C.18456
64.5	0.11269	0.28499	0.13371	C.18360
65.0	0.10723	0.27959	0.13236	C.18265
65.5	0.10179	0.27421	0.13101	C.18171
66.0	0.09637	0.26884	0.12967	C.18078
66.5	0.09097	0.26347	0.12835	C.17985
67.0	0.08558	0.25812	0.12703	C.17893

ANGLE	E1-PATTERN	H1-PATTERN	E2-PATTERN	H2-PATTERN
67.5	0.11445	0.27622	0.12572	C.17328
68.0	0.11141	0.27255	0.12442	C.17205
68.5	0.10845	0.26894	0.12313	C.17081
69.0	0.10558	0.26540	0.12186	C.16957
69.5	0.10280	0.26192	0.12059	C.16834
70.0	0.10009	0.25850	0.11934	C.16709
70.5	0.09747	0.25515	0.11810	C.16585
71.0	0.09493	0.25186	0.11687	C.16460
71.5	0.09246	0.24863	0.11565	C.16336
72.0	0.09008	0.24547	0.11445	C.16212
72.5	0.08777	0.24235	0.11326	C.16088
73.0	0.08553	0.23932	0.11209	C.15964
73.5	0.08337	0.23633	0.11093	C.15840
74.0	0.08128	0.23340	0.10978	C.15717
74.5	0.07925	0.23053	0.10864	C.15594
75.0	0.07720	0.22771	0.10752	C.15471
75.5	0.07522	0.22495	0.10642	C.15349
76.0	0.07331	0.22225	0.10533	C.15227
76.5	0.07136	0.21960	0.10425	C.15105
77.0	0.07017	0.21701	0.10319	C.14984
77.5	0.06835	0.21447	0.10214	C.14864
78.0	0.06669	0.21193	0.10111	C.14744
78.5	0.06519	0.20934	0.10009	C.14624
79.0	0.06405	0.20716	0.09909	C.14505
79.5	0.06267	0.20482	0.09810	C.14387
80.0	0.06134	0.20253	0.09713	C.14269
80.5	0.06007	0.20029	0.09617	C.14151
81.0	0.05886	0.19810	0.09522	C.14035
81.5	0.05770	0.19596	0.09429	C.13918
82.0	0.05659	0.19386	0.09338	C.13803
82.5	0.05553	0.19181	0.09247	C.13688
83.0	0.05452	0.18980	0.09159	C.13574
83.5	0.05357	0.18784	0.09071	C.13460
84.0	0.05266	0.18592	0.08985	C.13347
84.5	0.05179	0.18404	0.08900	C.13235
85.0	0.05098	0.18220	0.08817	C.13123
85.5	0.05021	0.18041	0.08735	C.13012
86.0	0.04948	0.17865	0.08654	C.12901
86.5	0.04879	0.17693	0.08575	C.12792
87.0	0.04815	0.17525	0.08497	C.12683
87.5	0.04755	0.17361	0.08420	C.12574
88.0	0.04699	0.17201	0.08344	C.12466
88.5	0.04646	0.17044	0.08270	C.12359
89.0	0.04598	0.16891	0.08197	C.12252
89.5	0.04553	0.16741	0.08125	C.12146

$\alpha = 0.4$

ANGLE	E1-PATTERN	H1-PATTERN	E2-PATTERN	H2-PATTERN
0.0	0.00000	1.00000	0.00000	C.00000
0.5	0.99987	0.99991	0.00602	C.00604
1.0	0.99747	0.99963	0.01205	C.01206
1.5	0.99381	0.99917	0.01807	C.01808
2.0	0.99000	0.99852	0.02408	C.02409
2.5	0.98609	0.99771	0.03007	C.03010
3.0	0.98213	0.99673	0.03605	C.03608
3.5	0.97812	0.99559	0.04200	C.04205
4.0	0.97407	0.99433	0.04792	C.04795
4.5	0.96998	0.99296	0.05381	C.05391
5.0	0.96585	0.99149	0.05967	C.05980
5.5	0.96168	0.98993	0.06549	C.06566
6.0	0.95747	0.98828	0.07127	C.07149
6.5	0.95322	0.98655	0.07700	C.07723
7.0	0.94893	0.98473	0.08268	C.08304
7.5	0.94460	0.98283	0.08831	C.08875
8.0	0.94023	0.98085	0.09389	C.09441
8.5	0.93582	0.97879	0.09941	C.10003
9.0	0.93137	0.97665	0.10486	C.10560
9.5	0.92688	0.97443	0.11025	C.11112
10.0	0.92235	0.97213	0.11557	C.11659
10.5	0.91778	0.96975	0.12082	C.12219
11.0	0.91317	0.96729	0.12600	C.12782
11.5	0.90852	0.96475	0.13109	C.13326
12.0	0.90383	0.96213	0.13611	C.13882
12.5	0.89910	0.95943	0.14105	C.14429
13.0	0.89433	0.95665	0.14590	C.14980
13.5	0.88952	0.95379	0.15066	C.15530
14.0	0.88467	0.95085	0.15533	C.16079
14.5	0.87978	0.94783	0.15991	C.16625
15.0	0.87485	0.94473	0.16440	C.17163
15.5	0.86988	0.94155	0.16879	C.17694
16.0	0.86487	0.93829	0.17309	C.18215
16.5	0.85982	0.93495	0.17728	C.18728
17.0	0.85473	0.93153	0.18137	C.19233
17.5	0.84960	0.92803	0.18536	C.19733
18.0	0.84443	0.92445	0.18924	C.20229
18.5	0.83922	0.92079	0.19302	C.20721
19.0	0.83397	0.91705	0.19669	C.21209
19.5	0.82868	0.91323	0.20025	C.21693
20.0	0.82335	0.90933	0.20371	C.22173
20.5	0.81798	0.90535	0.20705	C.22649
21.0	0.81257	0.90129	0.21028	C.23122
21.5	0.80712	0.89715	0.21341	C.23591
22.0	0.80163	0.89293	0.21642	C.24056

ANGLE	E1-PATTERN	H1-PATTERN	E2-PATTERN	H2-PATTERN
2.5	0.76643	0.83447	0.21931	C.22907
23.0	0.75742	0.82792	0.22210	C.23242
23.5	0.74833	0.82123	0.22477	C.23568
24.0	0.73916	0.81458	0.22733	C.23884
24.5	0.72993	0.80791	0.22977	C.24191
25.0	0.72063	0.80099	0.23211	C.24488
25.5	0.71128	0.79404	0.23433	C.24775
26.0	0.70188	0.78715	0.23644	C.25052
26.5	0.69243	0.78013	0.23843	C.25319
27.0	0.68293	0.77313	0.24032	C.25577
27.5	0.67343	0.76607	0.24209	C.25824
28.0	0.66388	0.75897	0.24376	C.26062
28.5	0.65432	0.75183	0.24531	C.26290
29.0	0.64473	0.74473	0.24676	C.26509
29.5	0.63514	0.73762	0.24810	C.26718
30.0	0.62554	0.73054	0.24933	C.26917
30.5	0.61593	0.72357	0.25046	C.27107
31.0	0.60634	0.71663	0.25148	C.27287
31.5	0.59673	0.70973	0.25241	C.27458
32.0	0.58716	0.70284	0.25323	C.27619
32.5	0.57755	0.69597	0.25395	C.27771
33.0	0.56799	0.68917	0.25457	C.27914
33.5	0.55844	0.68240	0.25510	C.28048
34.0	0.54891	0.67569	0.25553	C.28173
34.5	0.53934	0.66902	0.25596	C.28289
35.0	0.52980	0.66240	0.25636	C.28396
35.5	0.52029	0.65584	0.25671	C.28494
36.0	0.51081	0.64933	0.25703	C.28584
36.5	0.50134	0.64287	0.25731	C.28665
37.0	0.49191	0.63647	0.25756	C.28738
37.5	0.48251	0.63012	0.25779	C.28801
38.0	0.47314	0.62382	0.25799	C.28856
38.5	0.46381	0.61757	0.25816	C.28909
39.0	0.45451	0.61137	0.25831	C.28950
39.5	0.44524	0.60522	0.25844	C.28988
40.0	0.43601	0.59912	0.25854	C.29024
40.5	0.42681	0.59307	0.25861	C.29057
41.0	0.41764	0.58707	0.25866	C.29087
41.5	0.40851	0.58112	0.25869	C.29113
42.0	0.39941	0.57522	0.25870	C.29136
42.5	0.39034	0.56937	0.25869	C.29155
43.0	0.38131	0.56357	0.25866	C.29170
43.5	0.37231	0.55782	0.25861	C.29181
44.0	0.36334	0.55212	0.25854	C.29188
44.5	0.35441	0.54647	0.25844	C.29191
45.0	0.34551	0.54087	0.25831	C.29190

ANGLE	E1-PATTERN	H1-PATTERN	E2-PATTERN	H2-PATTERN
45.0	0.35686	0.51297	0.24468	C.28884
45.5	0.34890	0.50623	0.24345	C.28827
46.0	0.34124	0.49953	0.24218	C.28784
46.5	0.33369	0.49299	0.24085	C.28726
47.0	0.32624	0.48646	0.23949	C.28662
47.5	0.31890	0.47999	0.23808	C.28593
48.0	0.31166	0.47357	0.23663	C.28519
48.5	0.30454	0.46722	0.23515	C.28439
49.0	0.29752	0.46092	0.23363	C.28356
49.5	0.29062	0.45468	0.23207	C.28267
50.0	0.28383	0.44853	0.23049	C.28174
50.5	0.27714	0.44242	0.22887	C.28077
51.0	0.27056	0.43634	0.22723	C.27976
51.5	0.26410	0.43030	0.22557	C.27871
52.0	0.25775	0.42431	0.22387	C.27762
52.5	0.25152	0.41837	0.22216	C.27650
53.0	0.24539	0.41249	0.22042	C.27534
53.5	0.23938	0.40672	0.21867	C.27415
54.0	0.23348	0.40107	0.21690	C.27292
54.5	0.22769	0.39550	0.21511	C.27167
55.0	0.22202	0.39001	0.21331	C.27039
55.5	0.21645	0.38460	0.21150	C.26908
56.0	0.21098	0.37927	0.20967	C.26775
56.5	0.20561	0.37401	0.20784	C.26640
57.0	0.20034	0.36882	0.20600	C.26503
57.5	0.19517	0.36370	0.20415	C.26364
58.0	0.19010	0.35865	0.20230	C.26225
58.5	0.18513	0.35367	0.20044	C.26085
59.0	0.18026	0.34877	0.19858	C.25945
59.5	0.17549	0.34394	0.19672	C.25806
60.0	0.17082	0.33919	0.19486	C.25667
60.5	0.16625	0.33451	0.19300	C.25528
61.0	0.16178	0.32991	0.19114	C.25389
61.5	0.15741	0.32538	0.18929	C.25250
62.0	0.15314	0.32092	0.18744	C.25111
62.5	0.14897	0.31653	0.18559	C.24972
63.0	0.14490	0.31221	0.18375	C.24833
63.5	0.14093	0.30796	0.18192	C.24694
64.0	0.13706	0.30378	0.18010	C.24555
64.5	0.13329	0.29967	0.17828	C.24416
65.0	0.12962	0.29563	0.17648	C.24277
65.5	0.12605	0.29166	0.17468	C.24138
66.0	0.12258	0.28776	0.17290	C.23999
66.5	0.11921	0.28393	0.17113	C.23860
67.0	0.11594	0.28017	0.16937	C.23721

ANGLE	E1-PATTERN	H1-PATTERN	E2-PATTERN	H2-PATTERN
67.5	0.11445	0.27622	0.16762	C.23104
68.0	0.11141	0.27255	0.16589	C.22940
68.5	0.10845	0.26891	0.16418	C.22775
69.0	0.10558	0.26540	0.16247	C.22610
69.5	0.10280	0.26192	0.16077	C.22445
70.0	0.10009	0.25850	0.15912	C.22279
70.5	0.09747	0.25513	0.15746	C.22113
71.0	0.09493	0.25185	0.15583	C.21947
71.5	0.09246	0.24863	0.15420	C.21782
72.0	0.09008	0.24547	0.15260	C.21616
72.5	0.08777	0.24233	0.15102	C.21451
73.0	0.08553	0.23932	0.14945	C.21286
73.5	0.08337	0.23636	0.14790	C.21121
74.0	0.08129	0.23344	0.14637	C.20956
74.5	0.07926	0.23053	0.14486	C.20792
75.0	0.07730	0.22771	0.14337	C.20628
75.5	0.07542	0.22499	0.14189	C.20465
76.0	0.07361	0.22222	0.14044	C.20303
76.5	0.07196	0.21950	0.13900	C.20141
77.0	0.07035	0.21702	0.13759	C.19979
77.5	0.06885	0.21447	0.13619	C.19818
78.0	0.06699	0.21193	0.13482	C.19658
78.5	0.06519	0.20934	0.13346	C.19499
79.0	0.06340	0.20716	0.13222	C.19340
79.5	0.06175	0.20483	0.13080	C.19182
80.0	0.06007	0.20253	0.12950	C.19025
80.5	0.05836	0.20029	0.12822	C.18869
81.0	0.05670	0.19810	0.12696	C.18713
81.5	0.05509	0.19596	0.12572	C.18558
82.0	0.05352	0.19385	0.12450	C.18404
82.5	0.05200	0.19181	0.12330	C.18251
83.0	0.05052	0.18980	0.12211	C.18098
83.5	0.04907	0.18782	0.12095	C.17947
84.0	0.04766	0.18584	0.11980	C.17796
84.5	0.04629	0.18390	0.11867	C.17646
85.0	0.04498	0.18220	0.11756	C.17497
85.5	0.04371	0.18041	0.11647	C.17349
86.0	0.04248	0.17863	0.11539	C.17202
86.5	0.04130	0.17693	0.11433	C.17056
87.0	0.04015	0.17525	0.11329	C.16910
87.5	0.03903	0.17361	0.11227	C.16765
88.0	0.03794	0.17201	0.11126	C.16622
88.5	0.03688	0.17044	0.11027	C.16479
89.0	0.03585	0.16891	0.10929	C.16337
89.5	0.03485	0.16741	0.10833	C.16195

$$\alpha = 0.$$

 OFFSET REFLECTOR ANTENNA

INPUT DATA

LINEAR POLARIZATION IS IN THE PLANE OF SYMMETRY
 REFLECTOR DIAMETER IN WAVE LENGTH = 100.00 LAMDA
 THE FOCAL DISTANCE IN WAVE LENGTH = 47.73 LAMDA
 THE OFFSET ANGLE, THETA = 50.00 DEGREES
 THE HALF ANGLE OF ILLUMINATION = 45.00 DEGREES
 AZIMUTHAL ANGLE OF RADIATIONS = 0.00 DEGREES

OUTPUT DATA

ANTENNA GAIN IN DECIBELS = 47.945 DBS
 ANTENNA GAIN FACTOR = 0.631 RATIO
 THE SPILL OVER POWER IN PERCENT = 25.762 %
 THE APERTURE EFFICIENCY = 85.025 %
 THE TOTAL ANTENNA EFFICIENCY = 63.120 %

ANGLE	RAD. PATTERN	ANGLE	RAD. PATTERN	ANGLE	RAD. PATTERN
0.00	0.000	0.70	1.237	3.40	-37.301
0.05	-0.072	0.75	1.327	3.45	-38.989
0.10	-0.286	0.80	1.433	3.50	-41.412
0.15	-0.646	0.85	1.555	3.55	-44.294
0.20	-1.158	0.90	1.690	3.60	-47.544
0.25	-1.827	0.95	1.840	3.65	-49.617
0.30	-2.687	1.00	2.005	3.70	-49.180
0.35	-3.907	1.05	2.180	3.75	-39.421
0.40	-5.548	1.10	2.370	3.80	-28.377
0.45	-7.648	1.15	2.570	3.85	-13.954
0.50	-10.205	1.20	2.777	3.90	3.8105
0.55	-13.294	1.25	3.000	3.95	38.824
0.60	-16.844	1.30	3.246	4.00	40.160
0.65	-20.844	1.35	3.515	4.05	42.189
0.70	-25.432	1.40	3.805	4.10	44.892
0.75	-30.602	1.45	4.112	4.15	47.204
0.80	-36.364	1.50	4.437	4.20	46.551
0.85	-42.772	1.55	4.781	4.25	44.089
0.90	-49.855	1.60	5.141	4.30	41.999
0.95	-57.620	1.65	5.515	4.35	40.630
1.00	-66.095	1.70	5.905	4.40	39.917
1.05	-75.295	1.75	6.306	4.45	39.787
1.10	-85.247	1.80	6.726	4.50	40.224
1.15	-96.014	1.85	7.166	4.55	41.246
1.20	-107.679	1.90	7.628	4.60	42.924
1.25	-120.333	1.95	8.112	4.65	44.314
1.30	-134.088	2.00	8.619	4.70	48.019
1.35	-148.968	2.05	9.144	4.75	48.843
1.40	-165.083	2.10	9.686	4.80	46.800
1.45	-182.420	2.15	10.241	4.85	44.433
1.50	-200.950	2.20	10.807	4.90	42.729
1.55	-220.709	2.25	11.384	4.95	41.714
1.60	-241.743	2.30	11.971	5.00	41.307
1.65	-264.138	2.35	12.567	5.05	41.466

ANGLE	RAD. PATTERN	ANGLE	RAD. PATTERN	ANGLE	RAD. PATTERN
5.10	-42.190	6.80	-45.434	8.50	-48.197
5.15	-43.537	6.85	-46.401	8.55	-48.735
5.20	-45.585	6.90	-47.953	8.60	-49.873
5.25	-48.292	6.95	-50.203	8.65	-51.714
5.30	-50.424	7.00	-52.842	8.70	-54.320
5.35	-49.491	7.05	-53.993	8.75	-57.086
5.40	-46.958	7.10	-52.798	8.80	-57.143
5.45	-44.868	7.15	-49.791	8.85	-54.349
5.50	-42.249	7.20	-47.981	8.90	-52.097
5.55	-40.277	7.25	-46.850	8.95	-50.417
5.60	-43.634	7.30	-46.345	9.00	-49.431
5.65	-48.094	7.35	-48.398	9.05	-49.049
5.70	-47.053	7.40	-47.005	9.10	-49.224
5.75	-45.715	7.45	-48.219	9.15	-49.968
5.80	-48.115	7.50	-50.215	9.20	-51.334
5.85	-50.892	7.55	-52.683	9.25	-53.410
5.90	-51.828	7.60	-54.999	9.30	-56.125
5.95	-49.715	7.65	-54.497	9.35	-58.123
6.00	-47.247	7.70	-52.030	9.40	-59.602
6.05	-45.457	7.75	-49.840	9.45	-59.810
6.10	-44.281	7.80	-48.249	9.50	-59.200
6.15	-43.914	7.85	-47.316	9.55	-58.626
6.20	-44.011	7.90	-47.266	9.60	-58.094
6.25	-44.671	7.95	-47.376	9.65	-49.940
6.30	-45.934	8.00	-48.469	9.70	-50.324
6.35	-47.887	8.05	-50.009	9.75	-51.301
6.40	-50.513	8.10	-52.237	9.80	-52.506
6.45	-53.849	8.15	-53.134	9.85	-53.519
6.50	-52.260	8.20	-53.650	9.90	-53.729
6.55	-49.783	8.25	-54.427	9.95	-53.866
6.60	-47.609	8.30	-53.993	10.00	-53.330
6.65	-46.160	8.35	-53.049	10.05	-53.969
6.70	-45.361	8.40	-48.822	10.10	-52.231
6.75	-45.149	8.45	-48.226	10.15	-51.163

CORE USAGE OBJECT CODE = 29030 BYTES, ARRAY AREA = 25520 BYTES, TOTAL AREA AV
 DIAGNOSTICS NUMBER OF ERRORS = 0, NUMBER OF WARNINGS = 0, NUMBER C
 COMPILE TIME = 0.03 SEC, EXECUTION TIME = 20.37 SEC, 16.45.15 MONDAY
 CSSTOP

$\alpha = 0.$

OFFSET REFLECTOR ANTENNA

INPUT DATA

LINEAR POLARIZATION IS IN THE PLANE OF SYMMETRY		
REFLECTOR DIAMETER IN WAVE LENGTH	= 100.00	LAMDA
THE FOCAL DISTANCE IN WAVE LENGTH	= 47.73	LAMDA
THE OFFSET ANGLE, THETA	= 50.00	DEGREES
THE HALF-ANGLE OF ILLUMINATION	= 45.00	DEGREES
AZIMUTHAL ANGLE OF RADIATIONS	= 90.00	DEGREES

OUTPUT DATA

ANTENNA GAIN IN DECIBELS	= 47.945	DBS
ANTENNA GAIN FACTOR	= 0.631	RATIO
THE SPILL OVER POWER IN PERCENT	= 25.762	%
THE APERTURE EFFICIENCY	= 85.025	%
THE TOTAL ANTENNA EFFICIENCY	= 63.120	%

ANGLE

RAD. PATTERN

ANGLE

RAD. PATTERN

ANGLE

RAD. PATTERN

0.00
0.05
0.10
0.15
0.20
0.25
0.30
0.35
0.40
0.45
0.50
0.55
0.60
0.65
0.70
0.75
0.80
0.85
0.90
0.95
1.00

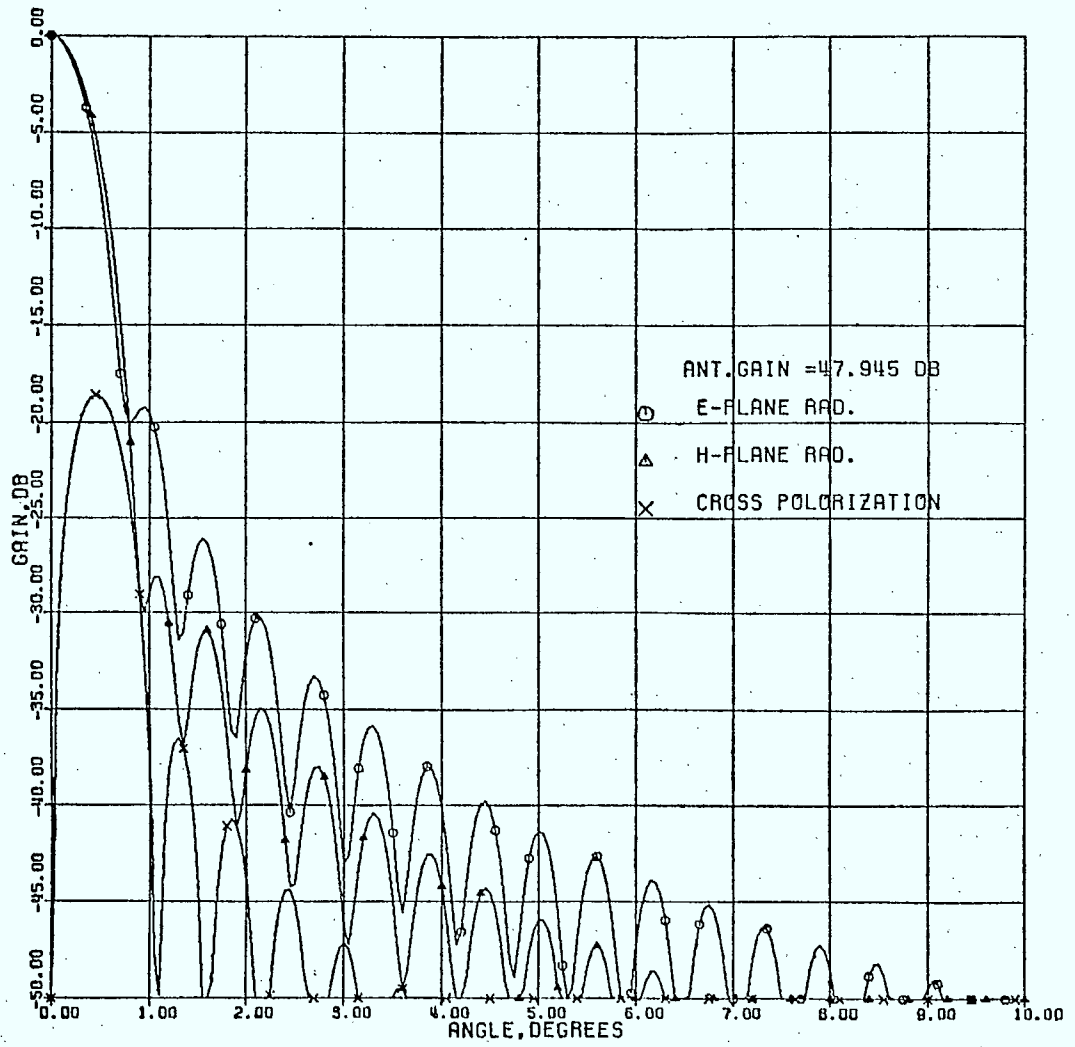
0.000
0.005
0.010
0.015
0.020
0.025
0.030
0.035
0.040
0.045
0.050
0.055
0.060
0.065
0.070
0.075
0.080
0.085
0.090
0.095
0.100

1.70
1.75
1.80
1.85
1.90
1.95
2.00
2.05
2.10
2.15
2.20
2.25
2.30
2.35
2.40
2.45
2.50
2.55
2.60
2.65
2.70

1.700
1.705
1.710
1.715
1.720
1.725
1.730
1.735
1.740
1.745
1.750
1.755
1.760
1.765
1.770
1.775
1.780
1.785
1.790
1.795
1.800

3.40
3.45
3.50
3.55
3.60
3.65
3.70
3.75
3.80
3.85
3.90
3.95
4.00
4.05
4.10
4.15
4.20
4.25
4.30
4.35
4.40

1.400
1.405
1.410
1.415
1.420
1.425
1.430
1.435
1.440
1.445
1.450
1.455
1.460
1.465
1.470
1.475
1.480
1.485
1.490
1.495
1.500



$\alpha = 0.1$

OFFSET REFLECTOR ANTENNA

INPUT DATA

LINEAR POLARIZATION IS IN THE PLANE OF SYMMETRY		
REFLECTOR DIAMETER IN WAVE LENGTH	= 100.00	LAMDA
THE FOCAL DISTANCE IN WAVE LENGTH	= 47.73	LAMDA
THE OFFSET ANGLE, THETA	= 50.00	DEGREES
THE HALF ANGLE OF ILLUMINATION	= 45.00	DEGREES
AZIMUTHAL ANGLE OF RADIATIONS	= 0.00	DEGREES

OUTPUT DATA

ANTENNA GAIN IN DECIBELS	= 48.078	DBS
ANTENNA GAIN FACTOR	= 0.631	RATIO
THE SPILL OVER POWER IN PERCENT	= 26.473	%
THE APERTURE EFFICIENCY	= 88.515	%
THE TOTAL ANTENNA EFFICIENCY	= 65.081	%

ANGLE	RAD. PATTERN	ANGLE	RAD. PATTERN	ANGLE	RAD. PATTERN
5.10	-43.699	6.80	-43.956	8.50	-48.606
5.15	-44.151	6.85	-44.245	8.55	-49.229
5.20	-44.603	6.90	-44.649	8.60	-50.448
5.25	-45.055	6.95	-45.272	8.65	-52.488
5.30	-45.507	7.00	-46.100	8.70	-55.611
5.35	-45.959	7.05	-47.272	8.75	-60.224
5.40	-46.411	7.10	-48.848	8.80	-66.713
5.45	-46.863	7.15	-50.944	8.85	-75.881
5.50	-47.315	7.20	-53.700	8.90	-88.998
5.55	-47.767	7.25	-57.255	8.95	-106.009
5.60	-48.219	7.30	-61.700	9.00	-128.936
5.65	-48.671	7.35	-67.150	9.05	-159.222
5.70	-49.123	7.40	-73.700	9.10	-199.496
5.75	-49.575	7.45	-81.450	9.15	-253.684
5.80	-50.027	7.50	-90.500	9.20	-326.884
5.85	-50.479	7.55	-101.000	9.25	-425.951
5.90	-50.931	7.60	-113.250	9.30	-557.888
5.95	-51.383	7.65	-127.500	9.35	-729.696
6.00	-51.835	7.70	-144.000	9.40	-950.400
6.05	-52.287	7.75	-163.000	9.45	-1230.000
6.10	-52.739	7.80	-184.750	9.50	-1578.500
6.15	-53.191	7.85	-209.500	9.55	-1996.000
6.20	-53.643	7.90	-237.500	9.60	-2483.500
6.25	-54.095	7.95	-269.000	9.65	-3051.000
6.30	-54.547	8.00	-304.500	9.70	-3708.500
6.35	-54.999	8.05	-344.500	9.75	-4466.000
6.40	-55.451	8.10	-389.500	9.80	-5333.500
6.45	-55.903	8.15	-439.500	9.85	-6321.000
6.50	-56.355	8.20	-494.500	9.90	-7438.500
6.55	-56.807	8.25	-554.500	9.95	-8686.000
6.60	-57.259	8.30	-619.500	10.00	-10063.500
6.65	-57.711	8.35	-689.500	10.05	-11581.000
6.70	-58.163	8.40	-764.500	10.10	-13248.500
6.75	-58.615	8.45	-844.500	10.15	-15066.000

CORE USAGE OBJECT CODE= 29120 BYTES, ARRAY AREA= 25520 BYTES, TOTAL ARE
 DIAGNOSTICS NUMBER OF ERRORS= 0, NUMBER OF WARNINGS= 0, NUMB
 COMPILE TIME= 0.64 SEC, EXECUTION TIME= 20.51 SEC, 16.00.43 TUESDA
 C\$STOP

$\alpha = 0.1$

OFFSET REFLECTOR ANTENNA

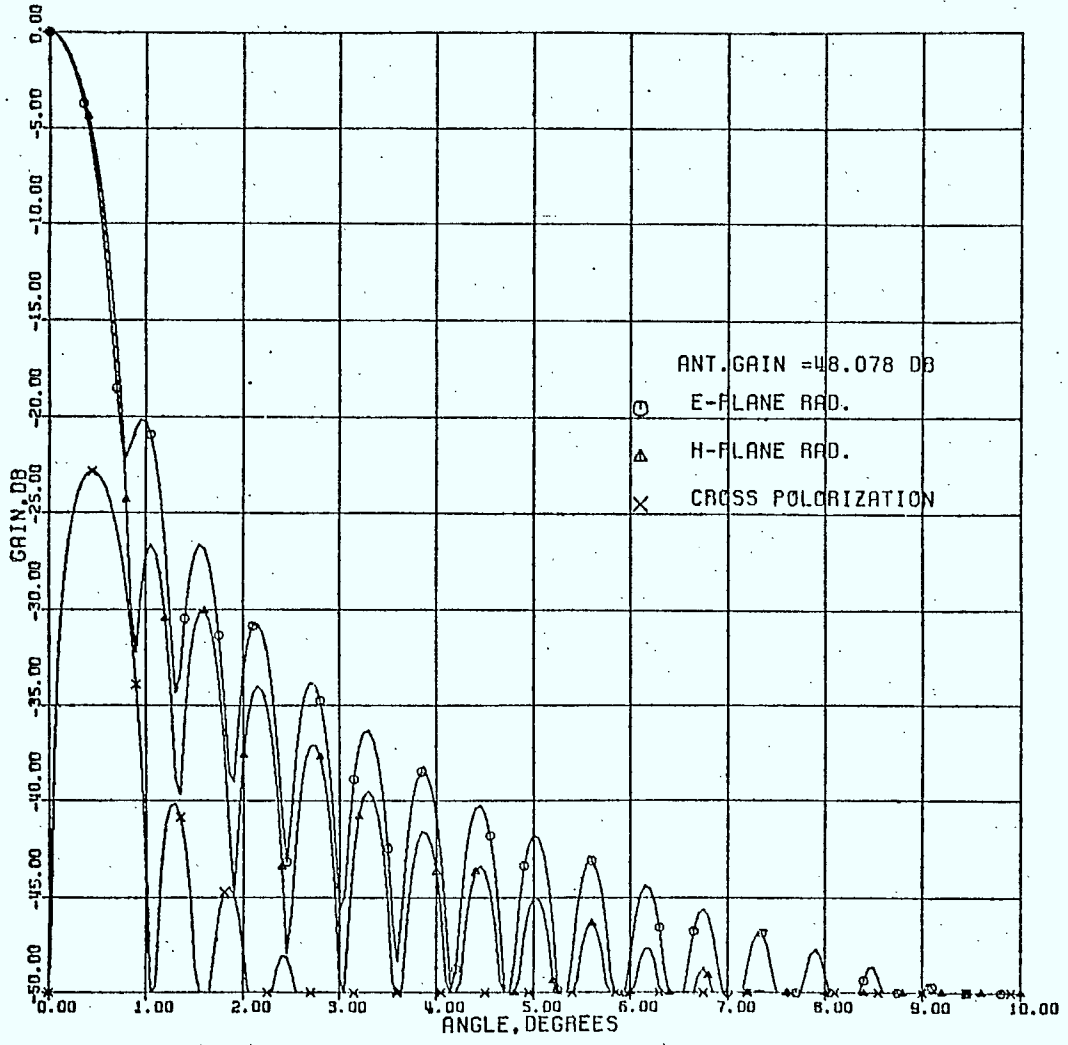
INPUT DATA

LINEAR POLARIZATION IS IN THE PLANE OF SYMMETRY		
REFLECTOR DIAMETER IN WAVE LENGTH	= 100.00	LAMDA
THE FOCAL DISTANCE IN WAVE LENGTH	= 47.73	LAMDA
THE OFFSET ANGLE, THETA	= 50.00	DEGREES
THE HALF ANGLE OF ILLUMINATION	= 45.00	DEGREES
AZIMUTHAL ANGLE OF RADIATIONS	= 90.00	DEGREES

OUTPUT DATA

ANTENNA GAIN IN DECIBELS	= 48.073	DBS
ANTENNA GAIN FACTOR	= 0.651	RATIO
THE SPILL OVER POWER IN PERCENT	= 26.475	%
THE APERTURE EFFICIENCY	= 88.515	%
THE TOTAL ANTENNA EFFICIENCY	= 65.081	%

ANGLE	RAD. PATTERN	ANGLE	RAD. PATTERN	ANGLE	RAD. PATTERN
10	-45.713	6.85	44.909	6.50	44.796
15	-47.093	6.85	44.909	6.55	44.812
20	-49.360	6.85	44.909	6.60	44.829
25	-52.926	6.85	44.909	6.65	44.847
30	-57.595	6.85	44.909	6.70	44.865
35	-63.630	6.85	44.909	6.75	44.884
40	-71.274	6.85	44.909	6.80	44.903
45	-80.633	6.85	44.909	6.85	44.923
50	-91.739	6.85	44.909	6.90	44.943
55	-104.620	6.85	44.909	6.95	44.964
60	-119.337	6.85	44.909	7.00	44.985
65	-135.936	6.85	44.909	7.05	45.007
70	-154.566	6.85	44.909	7.10	45.029
75	-175.277	6.85	44.909	7.15	45.052
80	-198.119	6.85	44.909	7.20	45.075
85	-223.143	6.85	44.909	7.25	45.099
90	-250.399	6.85	44.909	7.30	45.123
95	-279.830	6.85	44.909	7.35	45.148
100	-311.484	6.85	44.909	7.40	45.173
105	-345.409	6.85	44.909	7.45	45.198
110	-381.656	6.85	44.909	7.50	45.224
115	-420.277	6.85	44.909	7.55	45.250
120	-461.320	6.85	44.909	7.60	45.276
125	-504.836	6.85	44.909	7.65	45.303
130	-550.876	6.85	44.909	7.70	45.330
135	-600.491	6.85	44.909	7.75	45.357
140	-653.732	6.85	44.909	7.80	45.385
145	-710.750	6.85	44.909	7.85	45.413
150	-771.595	6.85	44.909	7.90	45.441
155	-836.317	6.85	44.909	7.95	45.470
160	-905.067	6.85	44.909	8.00	45.500
165	-978.000	6.85	44.909	8.05	45.530
170	-1055.277	6.85	44.909	8.10	45.560
175	-1137.067	6.85	44.909	8.15	45.590



$$\alpha = 0.2$$

 OFFSET REFLECTOR ANTENNA

 INPUT DATA

LINEAR POLARIZATION IS IN THE PLANE OF SYMMETRY
 REFLECTOR DIAMETER IN WAVE LENGTH = 100.00 LAMDA
 THE FOCAL DISTANCE IN WAVE LENGTH = 47.73 LAMDA
 THE OFFSET ANGLE, THETA = 50.00 DEGREES
 THE HALF ANGLE OF ILLUMINATION = 45.00 DEGREES
 AZIMUTHAL ANGLE OF RADIATIONS = 0.00 DEGREES
 OUTPUT DATA

 ANTENNA GAIN IN DECIBELS = 48.064 DBS
 ANTENNA GAIN FACTOR = 0.649 RATIO
 THE SPILL OVER POWER IN PERCENT = 28.473 %
 THE APERTURE EFFICIENCY = 90.698 %
 THE TOTAL ANTENNA EFFICIENCY = 64.874 %

ANGLE	RAD. PATTERN	ANGLE	RAD. PATTERN	ANGLE	RAD. PATTERN
6.10	-46.190	*****	0.820	*****	8.330
6.15	-44.728	*****	6.883	*****	8.335
6.20	-42.236	*****	6.900	*****	8.340
6.25	-39.737	*****	6.933	*****	8.345
6.30	-36.776	*****	7.000	*****	8.350
6.35	-33.807	*****	7.033	*****	8.355
6.40	-49.300	*****	7.100	*****	8.360
6.45	-46.300	*****	7.133	*****	8.365
6.50	-41.619	*****	7.200	*****	8.370
6.55	-42.750	*****	7.233	*****	8.375
6.60	-43.577	*****	7.300	*****	8.380
6.65	-44.700	*****	7.333	*****	8.385
6.70	-44.700	*****	7.400	*****	8.390
6.75	-44.300	*****	7.433	*****	8.395
6.80	-43.000	*****	7.500	*****	8.400
6.85	-40.233	*****	7.533	*****	8.405
6.90	-36.800	*****	7.600	*****	8.410
6.95	-32.800	*****	7.633	*****	8.415
6.00	-43.977	*****	7.700	*****	8.420
6.05	-46.700	*****	7.733	*****	8.425
6.10	-44.300	*****	7.800	*****	8.430
6.15	-44.300	*****	7.833	*****	8.435
6.20	-44.930	*****	7.900	*****	8.440
6.25	-45.669	*****	7.933	*****	8.445
6.30	-47.000	*****	8.000	*****	8.450
6.35	-49.497	*****	8.033	*****	8.455
6.40	-53.336	*****	8.100	*****	8.460
6.45	-57.000	*****	8.133	*****	8.465
6.50	-52.000	*****	8.200	*****	8.470
6.55	-49.121	*****	8.233	*****	8.475
6.60	-49.088	*****	8.300	*****	8.480
6.65	-47.297	*****	8.333	*****	8.485
6.70	-46.032	*****	8.400	*****	8.490
6.75	-46.032	*****	8.433	*****	8.495

CORE USAGE OBJECT CODE= 29120 BYTES, AREA= 25520 BYTES, TOTAL ARE
 DIAGNOSTICS NUMBER OF ERRORS= 0, NUMBER OF WARNINGS= 0, NUMB
 COMPILE TIME= 0.63 SEC, EXECUTION TIME= 20.42 SEC, 17.07.50 TUESDA
 CSSTOP

$\alpha = 0.2$

OFFSET REFLECTOR ANTENNA

INPUT DATA

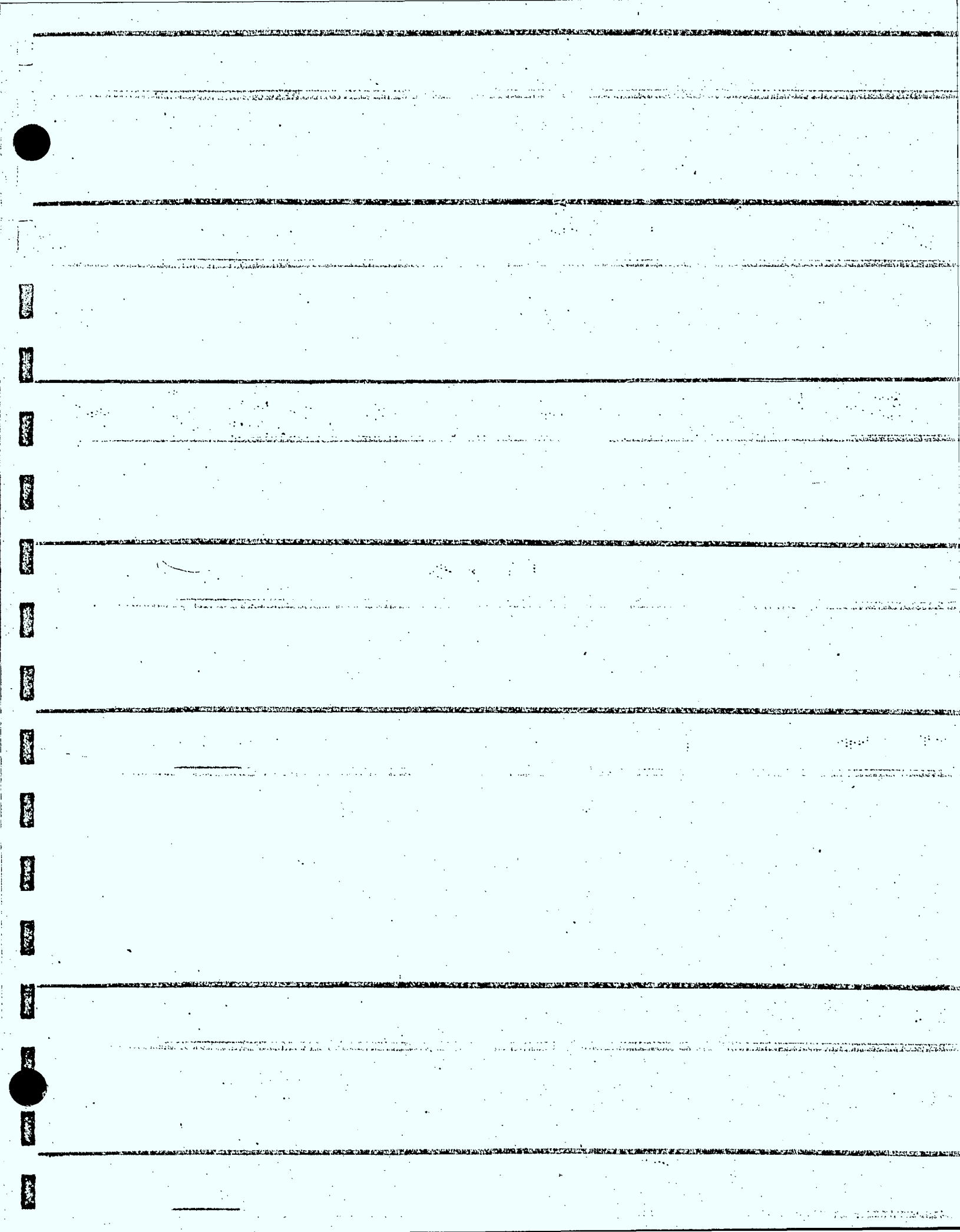
LINEAR POLARIZATION IS IN THE PLANE OF SYMMETRY
REFLECTOR DIAMETER IN WAVE LENGTH = 100.00 LAMDA
THE FOCAL DISTANCE IN WAVE LENGTH = 47.73 LAMDA
THE OFFSET ANGLE, THETA = 50.00 DEGREES
THE HALF ANGLE OF ILLUMINATION = 45.00 DEGREES
AZIMUTHAL ANGLE OF RADIATIONS = 90.00 DEGREES
OUTPUT DATA

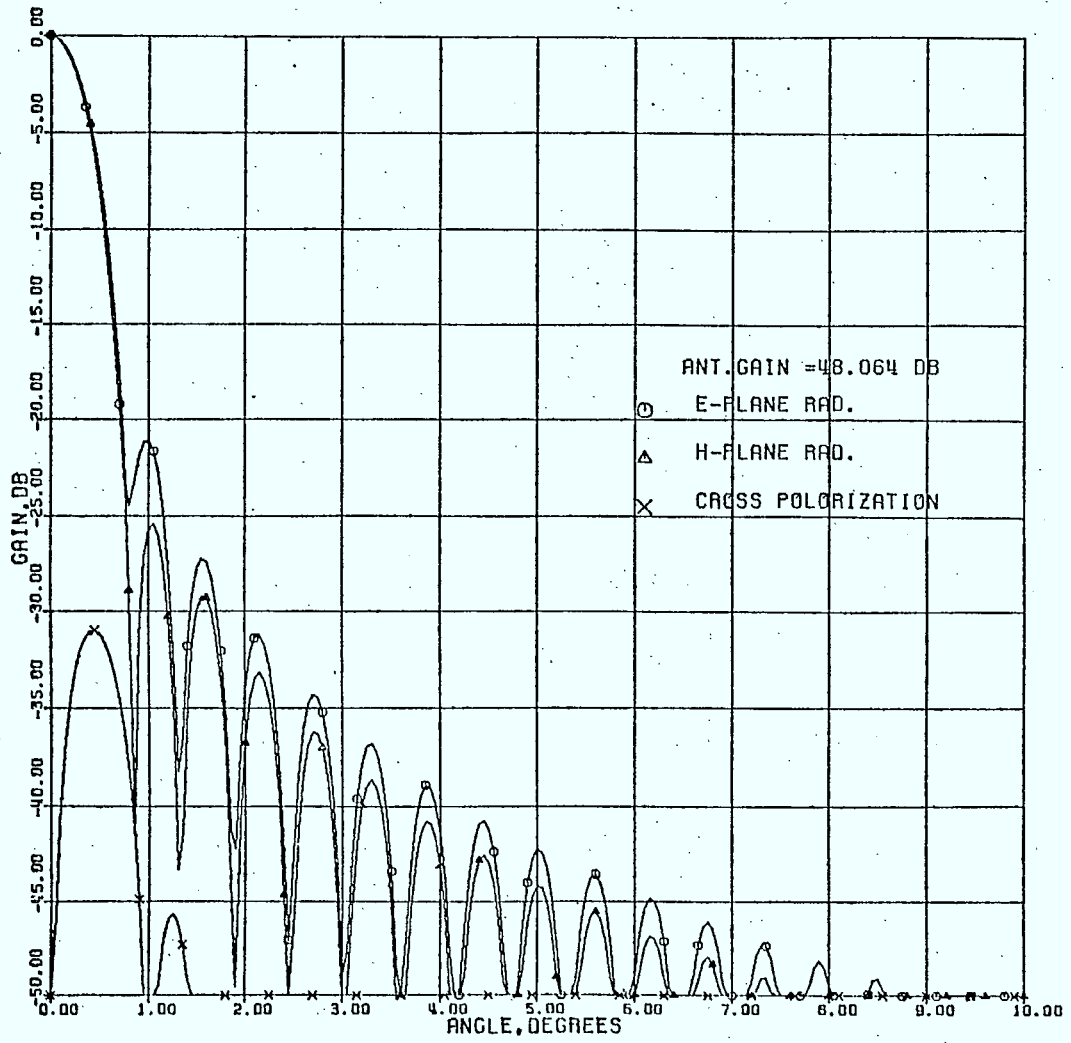
ANTENNA GAIN IN DECIBELS = 48.064 DBS
ANTENNA GAIN FACTOR = 0.649 RATIO
THE SPILL OVER POWER IN PERCENT = 28.473 %
THE APERTURE EFFICIENCY = 90.698 %
THE TOTAL ANTENNA EFFICIENCY = 64.874 %

ANGLE	RAD.	PATTERN
0.00	0.0000	*****
0.05	-0.0066	*****
0.10	-0.0133	*****
0.15	-0.0200	*****
0.20	-0.0266	*****
0.25	-0.0333	*****
0.30	-0.0400	*****
0.35	-0.0467	*****
0.40	-0.0533	*****
0.45	-0.0600	*****
0.50	-0.0667	*****
0.55	-0.0733	*****
0.60	-0.0800	*****
0.65	-0.0867	*****
0.70	-0.0933	*****
0.75	-0.1000	*****
0.80	-0.1067	*****
0.85	-0.1133	*****
0.90	-0.1200	*****
0.95	-0.1267	*****
1.00	-0.1333	*****
1.05	-0.1400	*****
1.10	-0.1467	*****
1.15	-0.1533	*****
1.20	-0.1600	*****
1.25	-0.1667	*****
1.30	-0.1733	*****
1.35	-0.1800	*****
1.40	-0.1867	*****
1.45	-0.1933	*****
1.50	-0.2000	*****
1.55	-0.2067	*****
1.60	-0.2133	*****
1.65	-0.2200	*****
1.70	-0.2267	*****
1.75	-0.2333	*****
1.80	-0.2400	*****
1.85	-0.2467	*****
1.90	-0.2533	*****
1.95	-0.2600	*****
2.00	-0.2667	*****
2.05	-0.2733	*****
2.10	-0.2800	*****
2.15	-0.2867	*****
2.20	-0.2933	*****
2.25	-0.3000	*****
2.30	-0.3067	*****
2.35	-0.3133	*****
2.40	-0.3200	*****
2.45	-0.3267	*****
2.50	-0.3333	*****
2.55	-0.3400	*****
2.60	-0.3467	*****
2.65	-0.3533	*****
2.70	-0.3600	*****
2.75	-0.3667	*****
2.80	-0.3733	*****
2.85	-0.3800	*****
2.90	-0.3867	*****
2.95	-0.3933	*****
3.00	-0.4000	*****

ANGLE	RAD.	PATTERN
0.70	0.7000	*****
0.75	0.7500	*****
0.80	0.8000	*****
0.85	0.8500	*****
0.90	0.9000	*****
0.95	0.9500	*****
1.00	1.0000	*****
1.05	1.0500	*****
1.10	1.1000	*****
1.15	1.1500	*****
1.20	1.2000	*****
1.25	1.2500	*****
1.30	1.3000	*****
1.35	1.3500	*****
1.40	1.4000	*****
1.45	1.4500	*****
1.50	1.5000	*****
1.55	1.5500	*****
1.60	1.6000	*****
1.65	1.6500	*****
1.70	1.7000	*****
1.75	1.7500	*****
1.80	1.8000	*****
1.85	1.8500	*****
1.90	1.9000	*****
1.95	1.9500	*****
2.00	2.0000	*****
2.05	2.0500	*****
2.10	2.1000	*****
2.15	2.1500	*****
2.20	2.2000	*****
2.25	2.2500	*****
2.30	2.3000	*****
2.35	2.3500	*****
2.40	2.4000	*****
2.45	2.4500	*****
2.50	2.5000	*****
2.55	2.5500	*****
2.60	2.6000	*****
2.65	2.6500	*****
2.70	2.7000	*****
2.75	2.7500	*****
2.80	2.8000	*****
2.85	2.8500	*****
2.90	2.9000	*****
2.95	2.9500	*****
3.00	3.0000	*****

ANGLE	RAD.	PATTERN
0.40	0.4000	*****
0.45	0.4500	*****
0.50	0.5000	*****
0.55	0.5500	*****
0.60	0.6000	*****
0.65	0.6500	*****
0.70	0.7000	*****
0.75	0.7500	*****
0.80	0.8000	*****
0.85	0.8500	*****
0.90	0.9000	*****
0.95	0.9500	*****
1.00	1.0000	*****
1.05	1.0500	*****
1.10	1.1000	*****
1.15	1.1500	*****
1.20	1.2000	*****
1.25	1.2500	*****
1.30	1.3000	*****
1.35	1.3500	*****
1.40	1.4000	*****
1.45	1.4500	*****
1.50	1.5000	*****
1.55	1.5500	*****
1.60	1.6000	*****
1.65	1.6500	*****
1.70	1.7000	*****
1.75	1.7500	*****
1.80	1.8000	*****
1.85	1.8500	*****
1.90	1.9000	*****
1.95	1.9500	*****
2.00	2.0000	*****
2.05	2.0500	*****
2.10	2.1000	*****
2.15	2.1500	*****
2.20	2.2000	*****
2.25	2.2500	*****
2.30	2.3000	*****
2.35	2.3500	*****
2.40	2.4000	*****
2.45	2.4500	*****
2.50	2.5000	*****
2.55	2.5500	*****
2.60	2.6000	*****
2.65	2.6500	*****
2.70	2.7000	*****
2.75	2.7500	*****
2.80	2.8000	*****
2.85	2.8500	*****
2.90	2.9000	*****
2.95	2.9500	*****
3.00	3.0000	*****





$\alpha = 0.3$

OFFSET REFLECTOR ANTENNA

INPUT DATA

LINEAR POLARIZATION IS IN THE PLANE OF SYMMETRY		
REFLECTOR DIAMETER IN WAVE LENGTH	= 100.00	LAMDA
THE FOCAL DISTANCE IN WAVE LENGTH	= 47.73	LAMDA
THE OFFSET ANGLE, THETA	= 50.00	DEGREES
THE HALF ANGLE OF ILLUMINATION	= 45.00	DEGREES
AZIMUTHAL ANGLE OF RADIATIONS	= 0.00	DEGREES

OUTPUT DATA

ANTENNA GAIN IN DECIBELS	= 47.923	DBS
ANTENNA GAIN FACTOR	= 0.628	RATIO
THE SPILL OVER POWER IN PERCENT	= 31.405	%
THE APERTURE EFFICIENCY	= 91.565	%
THE TOTAL ANTENNA EFFICIENCY	= 62.809	%

ANGLE RAD. PATTERN

ANGLE RAD. PATTERN

ANGLE RAD. PATTERN

ANGLE	RAD.	PATTERN
0.00	0.000	*****
0.05	0.070	*****
0.10	0.281	*****
0.15	0.636	*****
0.20	1.144	*****
0.25	2.000	*****
0.30	3.142	*****
0.35	4.712	*****
0.40	7.069	*****
0.45	11.071	*****
0.50	18.850	*****
0.55	32.071	*****
0.60	56.637	*****
0.65	100.999	*****
0.70	187.000	*****
0.75	357.777	*****
0.80	700.000	*****
0.85	1353.333	*****
0.90	2706.667	*****
0.95	5413.333	*****
1.00	10826.667	*****
1.05	21653.333	*****
1.10	43306.667	*****
1.15	86613.333	*****
1.20	173226.667	*****
1.25	346453.333	*****
1.30	692906.667	*****
1.35	1385813.333	*****
1.40	2771626.667	*****
1.45	5543253.333	*****
1.50	11086506.667	*****
1.55	22173013.333	*****
1.60	44346026.667	*****
1.65	88692053.333	*****
1.70	177384106.667	*****
1.75	354768213.333	*****
1.80	709536426.667	*****
1.85	1419072853.333	*****
1.90	2838145706.667	*****
1.95	5676291413.333	*****
2.00	11352582826.667	*****

ANGLE	RAD.	PATTERN
0.70	1.300	*****
0.75	1.322	*****
0.80	1.344	*****
0.85	1.366	*****
0.90	1.388	*****
0.95	1.410	*****
1.00	1.432	*****
1.05	1.454	*****
1.10	1.476	*****
1.15	1.498	*****
1.20	1.520	*****
1.25	1.542	*****
1.30	1.564	*****
1.35	1.586	*****
1.40	1.608	*****
1.45	1.630	*****
1.50	1.652	*****
1.55	1.674	*****
1.60	1.696	*****
1.65	1.718	*****
1.70	1.740	*****
1.75	1.762	*****
1.80	1.784	*****
1.85	1.806	*****
1.90	1.828	*****
1.95	1.850	*****
2.00	1.872	*****
2.05	1.894	*****
2.10	1.916	*****
2.15	1.938	*****
2.20	1.960	*****
2.25	1.982	*****
2.30	2.004	*****
2.35	2.026	*****
2.40	2.048	*****
2.45	2.070	*****
2.50	2.092	*****
2.55	2.114	*****
2.60	2.136	*****
2.65	2.158	*****
2.70	2.180	*****
2.75	2.202	*****
2.80	2.224	*****
2.85	2.246	*****
2.90	2.268	*****
2.95	2.290	*****
3.00	2.312	*****

ANGLE	RAD.	PATTERN
3.40	3.380	*****
3.45	3.402	*****
3.50	3.424	*****
3.55	3.446	*****
3.60	3.468	*****
3.65	3.490	*****
3.70	3.512	*****
3.75	3.534	*****
3.80	3.556	*****
3.85	3.578	*****
3.90	3.600	*****
3.95	3.622	*****
4.00	3.644	*****
4.05	3.666	*****
4.10	3.688	*****
4.15	3.710	*****
4.20	3.732	*****
4.25	3.754	*****
4.30	3.776	*****
4.35	3.798	*****
4.40	3.820	*****
4.45	3.842	*****
4.50	3.864	*****
4.55	3.886	*****
4.60	3.908	*****
4.65	3.930	*****
4.70	3.952	*****
4.75	3.974	*****
4.80	3.996	*****
4.85	4.018	*****
4.90	4.040	*****
4.95	4.062	*****
5.00	4.084	*****
5.05	4.106	*****
5.10	4.128	*****
5.15	4.150	*****
5.20	4.172	*****
5.25	4.194	*****
5.30	4.216	*****
5.35	4.238	*****
5.40	4.260	*****
5.45	4.282	*****
5.50	4.304	*****

ANGLE	RAD.	PATTERN
3.80	3.800	*****
3.85	3.822	*****
3.90	3.844	*****
3.95	3.866	*****
4.00	3.888	*****
4.05	3.910	*****
4.10	3.932	*****
4.15	3.954	*****
4.20	3.976	*****
4.25	3.998	*****
4.30	4.020	*****
4.35	4.042	*****
4.40	4.064	*****
4.45	4.086	*****
4.50	4.108	*****
4.55	4.130	*****
4.60	4.152	*****
4.65	4.174	*****
4.70	4.196	*****
4.75	4.218	*****
4.80	4.240	*****
4.85	4.262	*****
4.90	4.284	*****
4.95	4.306	*****
5.00	4.328	*****
5.05	4.350	*****
5.10	4.372	*****
5.15	4.394	*****
5.20	4.416	*****
5.25	4.438	*****
5.30	4.460	*****
5.35	4.482	*****
5.40	4.504	*****
5.45	4.526	*****
5.50	4.548	*****
5.55	4.570	*****
5.60	4.592	*****
5.65	4.614	*****
5.70	4.636	*****
5.75	4.658	*****
5.80	4.680	*****
5.85	4.702	*****
5.90	4.724	*****
5.95	4.746	*****
6.00	4.768	*****
6.05	4.790	*****
6.10	4.812	*****
6.15	4.834	*****
6.20	4.856	*****
6.25	4.878	*****
6.30	4.900	*****
6.35	4.922	*****
6.40	4.944	*****
6.45	4.966	*****
6.50	4.988	*****
6.55	5.010	*****
6.60	5.032	*****
6.65	5.054	*****
6.70	5.076	*****
6.75	5.098	*****
6.80	5.120	*****
6.85	5.142	*****
6.90	5.164	*****
6.95	5.186	*****
7.00	5.208	*****

ANGLE	RAD. PATTERN	ANGLE	RAD. PATTERN	ANGLE	RAD. PATTERN
0.10	-43.680	0.80	-46.921	8.50	-49.611
0.15	-43.257	0.85	-47.972	8.55	-50.195
0.20	-47.928	0.90	-49.871	8.60	-51.004
0.25	-52.612	0.95	-53.941	8.65	-51.794
0.30	-55.287	1.00	-56.911	8.70	-57.741
0.35	-55.111	1.05	-57.144	8.75	-66.051
0.40	-46.914	1.10	-52.462	8.80	-66.683
0.45	-43.158	1.15	-49.830	8.85	-55.813
0.50	-44.253	1.20	-48.433	8.90	-55.302
0.55	-44.044	1.25	-47.798	8.95	-55.122
0.60	-44.480	1.30	-47.317	9.00	-55.099
0.65	-44.356	1.35	-49.908	9.05	-55.009
0.70	-43.703	1.40	-52.333	9.10	-55.133
0.75	-43.511	1.45	-56.601	9.15	-55.939
0.80	-43.333	1.50	-58.222	9.20	-55.334
0.85	-43.184	1.55	-58.517	9.25	-57.008
0.90	-44.727	1.60	-59.000	9.30	-57.237
0.95	-44.777	1.65	-59.070	9.35	-57.237
0.00	-44.927	1.70	-59.000	9.40	-57.237
0.05	-44.955	1.75	-59.000	9.45	-57.237
0.10	-44.955	1.80	-59.000	9.50	-57.237
0.15	-44.955	1.85	-59.000	9.55	-57.237
0.20	-44.955	1.90	-59.000	9.60	-57.237
0.25	-44.955	1.95	-59.000	9.65	-57.237
0.30	-44.955	2.00	-59.000	9.70	-57.237
0.35	-44.955	2.05	-59.000	9.75	-57.237
0.40	-44.955	2.10	-59.000	9.80	-57.237
0.45	-44.955	2.15	-59.000	9.85	-57.237
0.50	-44.955	2.20	-59.000	9.90	-57.237
0.55	-44.955	2.25	-59.000	9.95	-57.237
0.60	-44.955	2.30	-59.000	10.00	-57.237
0.65	-44.955	2.35	-59.000	10.05	-57.237
0.70	-44.955	2.40	-59.000	10.10	-57.237
0.75	-44.955	2.45	-59.000	10.15	-57.237

CORE USAGE OBJECT CODE = 29120 BYTES, ARRAY AREA = 25520 BYTES, TOTAL ARE
 DIAGNOSTICS NUMBER OF ERRORS = 0, NUMBER OF WARNINGS = 0, NUMB
 COMPILE TIME = 0.63 SEC, EXECUTION TIME = 20.34 SEC, 17.38.C3 TUESDA

C&STOP

$\alpha = 0.3$

OFFSET REFLECTOR ANTENNA

INPUT DATA

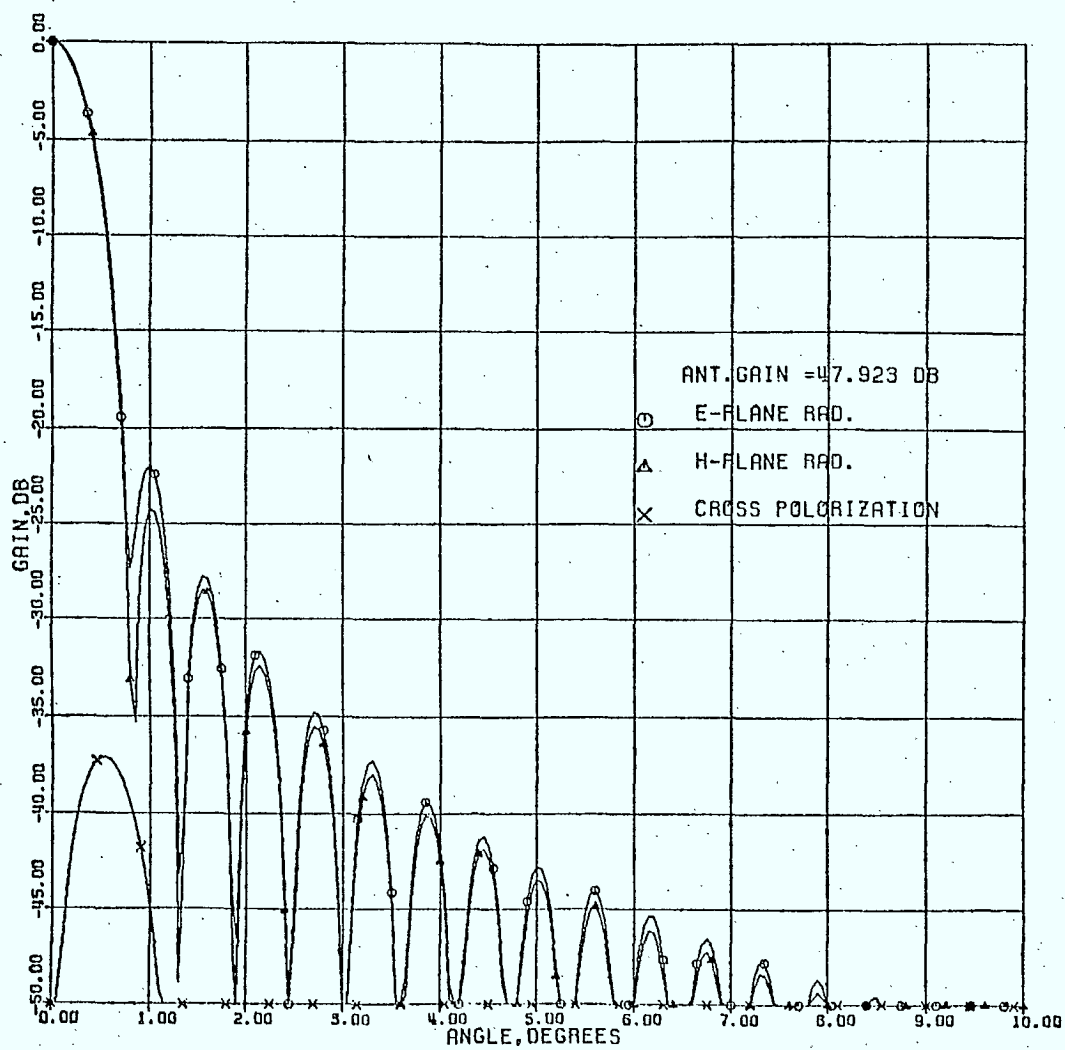
LINEAR POLARIZATION IS IN THE PLANE OF SYMMETRY		
REFLECTOR DIAMETER IN WAVE LENGTH	= 100.00	LAMDA
THE FOCAL DISTANCE IN WAVE LENGTH	= 47.73	LAMDA
THE OFFSET ANGLE, THETA	= 50.00	DEGREES
THE HALF ANGLE OF ILLUMINATION	= 45.00	DEGREES
AZIMUTHAL ANGLE OF RADIATIONS	= 90.00	DEGREES

OUTPUT DATA

ANTENNA GAIN IN DECIBELS	= 47.923	DBS
ANTENNA GAIN FACTOR	= 0.628	RATIO
THE SPILL OVER POWER IN PERCENT	= 31.405	%
THE APERTURE EFFICIENCY	= 91.565	%
THE TOTAL ANTENNA EFFICIENCY	= 62.809	%

ANGLE	RAD. PATTERN	ANGLE	RAD. PATTERN	ANGLE	RAD. PATTERN
0.00	0.000	*** **	0.000	3.40	0.000
0.05	0.067	*** **	0.067	3.45	0.067
0.10	0.134	*** **	0.134	3.50	0.134
0.15	0.201	*** **	0.201	3.55	0.201
0.20	0.268	*** **	0.268	3.60	0.268
0.25	0.335	*** **	0.335	3.65	0.335
0.30	0.402	*** **	0.402	3.70	0.402
0.35	0.469	*** **	0.469	3.75	0.469
0.40	0.536	*** **	0.536	3.80	0.536
0.45	0.603	*** **	0.603	3.85	0.603
0.50	0.670	*** **	0.670	3.90	0.670
0.55	0.737	*** **	0.737	3.95	0.737
0.60	0.804	*** **	0.804	4.00	0.804
0.65	0.871	*** **	0.871	4.05	0.871
0.70	0.938	*** **	0.938	4.10	0.938
0.75	1.005	*** **	1.005	4.15	1.005
0.80	1.072	*** **	1.072	4.20	1.072
0.85	1.139	*** **	1.139	4.25	1.139
0.90	1.206	*** **	1.206	4.30	1.206
0.95	1.273	*** **	1.273	4.35	1.273
1.00	1.340	*** **	1.340	4.40	1.340
1.05	1.407	*** **	1.407	4.45	1.407
1.10	1.474	*** **	1.474	4.50	1.474
1.15	1.541	*** **	1.541	4.55	1.541
1.20	1.608	*** **	1.608	4.60	1.608
1.25	1.675	*** **	1.675	4.65	1.675
1.30	1.742	*** **	1.742	4.70	1.742
1.35	1.809	*** **	1.809	4.75	1.809
1.40	1.876	*** **	1.876	4.80	1.876
1.45	1.943	*** **	1.943	4.85	1.943
1.50	2.010	*** **	2.010	4.90	2.010
1.55	2.077	*** **	2.077	4.95	2.077
1.60	2.144	*** **	2.144	5.00	2.144
1.65	2.211	*** **	2.211	5.05	2.211
1.70	2.278	*** **	2.278	5.10	2.278
1.75	2.345	*** **	2.345	5.15	2.345
1.80	2.412	*** **	2.412	5.20	2.412
1.85	2.479	*** **	2.479	5.25	2.479
1.90	2.546	*** **	2.546	5.30	2.546
1.95	2.613	*** **	2.613	5.35	2.613
2.00	2.680	*** **	2.680	5.40	2.680
2.05	2.747	*** **	2.747	5.45	2.747
2.10	2.814	*** **	2.814	5.50	2.814
2.15	2.881	*** **	2.881	5.55	2.881
2.20	2.948	*** **	2.948	5.60	2.948
2.25	3.015	*** **	3.015	5.65	3.015
2.30	3.082	*** **	3.082	5.70	3.082
2.35	3.149	*** **	3.149	5.75	3.149
2.40	3.216	*** **	3.216	5.80	3.216
2.45	3.283	*** **	3.283	5.85	3.283
2.50	3.350	*** **	3.350	5.90	3.350
2.55	3.417	*** **	3.417	5.95	3.417
2.60	3.484	*** **	3.484	6.00	3.484
2.65	3.551	*** **	3.551	6.05	3.551
2.70	3.618	*** **	3.618	6.10	3.618
2.75	3.685	*** **	3.685	6.15	3.685
2.80	3.752	*** **	3.752	6.20	3.752
2.85	3.819	*** **	3.819	6.25	3.819
2.90	3.886	*** **	3.886	6.30	3.886
2.95	3.953	*** **	3.953	6.35	3.953
3.00	4.020	*** **	4.020	6.40	4.020

<u>ANGLE</u>	<u>RAD.</u>	<u>PATTERN</u>	<u>ANGLE</u>	<u>RAD.</u>	<u>PATTERN</u>	<u>ANGLE</u>	<u>RAD.</u>	<u>PATTERN</u>
50	1.47	330	6.80	1.47	8.30	50	1.47	330
55	1.49	302	6.83	1.48	8.53	55	1.50	310
60	1.53	255	6.90	1.52	8.70	60	1.54	220
65	1.53	208	6.95	1.54	8.88	65	1.54	170
70	1.55	162	7.00	1.56	9.06	70	1.56	120
75	1.57	117	7.05	1.57	9.24	75	1.58	70
80	1.57	72	7.10	1.58	9.41	80	1.58	20
85	1.59	28	7.15	1.59	9.58	85	1.59	330
90	1.57	0	7.20	1.60	9.75	90	1.57	300
95	1.55	338	7.25	1.59	9.91	95	1.55	270
100	1.50	293	7.30	1.58	10.07	100	1.50	240
105	1.44	248	7.35	1.57	10.23	105	1.44	210
110	1.37	203	7.40	1.56	10.38	110	1.37	180
115	1.29	158	7.45	1.55	10.53	115	1.29	150
120	1.20	113	7.50	1.53	10.67	120	1.20	120
125	1.11	68	7.55	1.52	10.81	125	1.11	90
130	1.02	23	7.60	1.50	10.95	130	1.02	60
135	0.92	-22	7.65	1.49	11.09	135	0.92	30
140	0.83	-77	7.70	1.48	11.23	140	0.83	0
145	0.73	-132	7.75	1.46	11.37	145	0.73	330
150	0.64	-187	7.80	1.45	11.51	150	0.64	300
155	0.54	-242	7.85	1.44	11.65	155	0.54	270
160	0.45	-297	7.90	1.42	11.79	160	0.45	240
165	0.35	-352	7.95	1.41	11.93	165	0.35	210
170	0.26	-407	8.00	1.40	12.07	170	0.26	180
175	0.16	-462	8.05	1.38	12.21	175	0.16	150
180	0.07	-517	8.10	1.37	12.35	180	0.07	120
185	0.02	-572	8.15	1.36	12.49	185	0.02	90
190	0.00	-627	8.20	1.35	12.63	190	0.00	60
195	0.00	-682	8.25	1.34	12.77	195	0.00	30
200	0.00	-737	8.30	1.33	12.91	200	0.00	0
205	0.00	-792	8.35	1.32	13.05	205	0.00	330
210	0.00	-847	8.40	1.31	13.19	210	0.00	300
215	0.00	-902	8.45	1.30	13.33	215	0.00	270
220	0.00	-957	8.50	1.29	13.47	220	0.00	240
225	0.00	-1012	8.55	1.28	13.61	225	0.00	210
230	0.00	-1067	8.60	1.27	13.75	230	0.00	180
235	0.00	-1122	8.65	1.26	13.89	235	0.00	150
240	0.00	-1177	8.70	1.25	14.03	240	0.00	120
245	0.00	-1232	8.75	1.24	14.17	245	0.00	90
250	0.00	-1287	8.80	1.23	14.31	250	0.00	60
255	0.00	-1342	8.85	1.22	14.45	255	0.00	30
260	0.00	-1397	8.90	1.21	14.59	260	0.00	0
265	0.00	-1452	8.95	1.20	14.73	265	0.00	330
270	0.00	-1507	9.00	1.19	14.87	270	0.00	300
275	0.00	-1562	9.05	1.18	15.01	275	0.00	270
280	0.00	-1617	9.10	1.17	15.15	280	0.00	240
285	0.00	-1672	9.15	1.16	15.29	285	0.00	210
290	0.00	-1727	9.20	1.15	15.43	290	0.00	180
295	0.00	-1782	9.25	1.14	15.57	295	0.00	150
300	0.00	-1837	9.30	1.13	15.71	300	0.00	120
305	0.00	-1892	9.35	1.12	15.85	305	0.00	90
310	0.00	-1947	9.40	1.11	15.99	310	0.00	60
315	0.00	-2002	9.45	1.10	16.13	315	0.00	30
320	0.00	-2057	9.50	1.09	16.27	320	0.00	0
325	0.00	-2112	9.55	1.08	16.41	325	0.00	330
330	0.00	-2167	9.60	1.07	16.55	330	0.00	300
335	0.00	-2222	9.65	1.06	16.69	335	0.00	270
340	0.00	-2277	9.70	1.05	16.83	340	0.00	240
345	0.00	-2332	9.75	1.04	16.97	345	0.00	210
350	0.00	-2387	9.80	1.03	17.11	350	0.00	180
355	0.00	-2442	9.85	1.02	17.25	355	0.00	150
360	0.00	-2497	9.90	1.01	17.39	360	0.00	120



$$\alpha = 0.4$$

 OFFSET REFLECTOR ANTENNA

 INPUT DATA

LINEAR POLARIZATION IS IN THE PLANE OF SYMMETRY
 REFLECTOR DIAMETER IN WAVE LENGTH = 100.00 LAMDA
 THE FOCAL DISTANCE IN WAVE LENGTH = 47.73 LAMDA
 THE OFFSET ANGLE, THETA = 50.00 DEGREES
 THE HALF ANGLE OF ILLUMINATION = 45.00 DEGREES
 AZIMUTHAL ANGLE OF RADIATIONS = 0.00 DEGREES

 OUTPUT DATA

 ANTENNA GAIN IN DECIBELS = 47.633 DBS
 ANTENNA GAIN FACTOR = 0.594 RATIO
 THE SPILL OVER POWER IN PERCENT = 34.840 %
 THE APERTURE EFFICIENCY = 91.212 %
 THE TOTAL ANTENNA EFFICIENCY = 59.434 %

ANGLE RAD. PATTERN

0.00	0.000	*****
0.05	0.009	*****
0.10	0.018	*****
0.15	0.027	*****
0.20	0.036	*****
0.25	0.045	*****
0.30	0.054	*****
0.35	0.063	*****
0.40	0.072	*****
0.45	0.081	*****
0.50	0.090	*****
0.55	0.099	*****
0.60	0.108	*****
0.65	0.117	*****
0.70	0.126	*****
0.75	0.135	*****
0.80	0.144	*****
0.85	0.153	*****
0.90	0.162	*****
0.95	0.171	*****
1.00	0.180	*****
1.05	0.189	*****
1.10	0.198	*****
1.15	0.207	*****
1.20	0.216	*****
1.25	0.225	*****
1.30	0.234	*****
1.35	0.243	*****
1.40	0.252	*****
1.45	0.261	*****
1.50	0.270	*****
1.55	0.279	*****
1.60	0.288	*****
1.65	0.297	*****
1.70	0.306	*****
1.75	0.315	*****
1.80	0.324	*****
1.85	0.333	*****
1.90	0.342	*****
1.95	0.351	*****
2.00	0.360	*****

0.70	0.000	*****
0.75	0.009	*****
0.80	0.018	*****
0.85	0.027	*****
0.90	0.036	*****
0.95	0.045	*****
1.00	0.054	*****
1.05	0.063	*****
1.10	0.072	*****
1.15	0.081	*****
1.20	0.090	*****
1.25	0.099	*****
1.30	0.108	*****
1.35	0.117	*****
1.40	0.126	*****
1.45	0.135	*****
1.50	0.144	*****
1.55	0.153	*****
1.60	0.162	*****
1.65	0.171	*****
1.70	0.180	*****
1.75	0.189	*****
1.80	0.198	*****
1.85	0.207	*****
1.90	0.216	*****
1.95	0.225	*****
2.00	0.234	*****

ANGLE RAD. PATTERN

0.63	0.000	*****
0.68	0.009	*****
0.73	0.018	*****
0.78	0.027	*****
0.83	0.036	*****
0.88	0.045	*****
0.93	0.054	*****
0.98	0.063	*****
1.03	0.072	*****
1.08	0.081	*****
1.13	0.090	*****
1.18	0.099	*****
1.23	0.108	*****
1.28	0.117	*****
1.33	0.126	*****
1.38	0.135	*****
1.43	0.144	*****
1.48	0.153	*****
1.53	0.162	*****
1.58	0.171	*****
1.63	0.180	*****
1.68	0.189	*****
1.73	0.198	*****
1.78	0.207	*****
1.83	0.216	*****
1.88	0.225	*****
1.93	0.234	*****
1.98	0.243	*****
2.03	0.252	*****

0.40	0.000	*****
0.45	0.009	*****
0.50	0.018	*****
0.55	0.027	*****
0.60	0.036	*****
0.65	0.045	*****
0.70	0.054	*****
0.75	0.063	*****
0.80	0.072	*****
0.85	0.081	*****
0.90	0.090	*****
0.95	0.099	*****
1.00	0.108	*****
1.05	0.117	*****
1.10	0.126	*****
1.15	0.135	*****
1.20	0.144	*****
1.25	0.153	*****
1.30	0.162	*****
1.35	0.171	*****
1.40	0.180	*****
1.45	0.189	*****
1.50	0.198	*****
1.55	0.207	*****
1.60	0.216	*****
1.65	0.225	*****
1.70	0.234	*****
1.75	0.243	*****
1.80	0.252	*****
1.85	0.261	*****
1.90	0.270	*****
1.95	0.279	*****
2.00	0.288	*****

ANGLE RAD. PATTERN

0.39	0.286	*****
0.41	0.274	*****
0.44	0.261	*****
0.47	0.249	*****
0.51	0.237	*****
0.54	0.225	*****
0.57	0.213	*****
0.60	0.201	*****
0.63	0.189	*****
0.66	0.177	*****
0.69	0.165	*****
0.72	0.153	*****
0.75	0.141	*****
0.78	0.129	*****
0.81	0.117	*****
0.84	0.105	*****
0.87	0.093	*****
0.90	0.081	*****
0.93	0.069	*****
0.96	0.057	*****
0.99	0.045	*****
1.02	0.033	*****
1.05	0.021	*****
1.08	0.009	*****
1.11	0.000	*****
1.14	0.000	*****
1.17	0.000	*****
1.20	0.000	*****
1.23	0.000	*****
1.26	0.000	*****
1.29	0.000	*****
1.32	0.000	*****
1.35	0.000	*****
1.38	0.000	*****
1.41	0.000	*****
1.44	0.000	*****
1.47	0.000	*****
1.50	0.000	*****
1.53	0.000	*****
1.56	0.000	*****
1.59	0.000	*****
1.62	0.000	*****
1.65	0.000	*****
1.68	0.000	*****
1.71	0.000	*****
1.74	0.000	*****
1.77	0.000	*****
1.80	0.000	*****
1.83	0.000	*****
1.86	0.000	*****
1.89	0.000	*****
1.92	0.000	*****
1.95	0.000	*****
1.98	0.000	*****
2.01	0.000	*****

ANGLE	RAD. PATTERN	ANGLE	RAD. PATTERN	ANGLE	RAD. PATTERN
5.0	-4.197	6.80	-47.393	8.50	-50.687
5.1	-4.197	6.80	-47.393	8.60	-50.687
5.2	-4.197	6.80	-47.393	8.70	-50.687
5.3	-4.197	6.80	-47.393	8.80	-50.687
5.4	-4.197	6.80	-47.393	8.90	-50.687
5.5	-4.197	6.80	-47.393	9.00	-50.687
5.6	-4.197	6.80	-47.393	9.10	-50.687
5.7	-4.197	6.80	-47.393	9.20	-50.687
5.8	-4.197	6.80	-47.393	9.30	-50.687
5.9	-4.197	6.80	-47.393	9.40	-50.687
6.0	-4.197	6.80	-47.393	9.50	-50.687
6.1	-4.197	6.80	-47.393	9.60	-50.687
6.2	-4.197	6.80	-47.393	9.70	-50.687
6.3	-4.197	6.80	-47.393	9.80	-50.687
6.4	-4.197	6.80	-47.393	9.90	-50.687
6.5	-4.197	6.80	-47.393	10.00	-50.687
6.6	-4.197	6.80	-47.393	10.10	-50.687
6.7	-4.197	6.80	-47.393	10.20	-50.687
6.8	-4.197	6.80	-47.393	10.30	-50.687
6.9	-4.197	6.80	-47.393	10.40	-50.687
7.0	-4.197	6.80	-47.393	10.50	-50.687
7.1	-4.197	6.80	-47.393	10.60	-50.687
7.2	-4.197	6.80	-47.393	10.70	-50.687
7.3	-4.197	6.80	-47.393	10.80	-50.687
7.4	-4.197	6.80	-47.393	10.90	-50.687
7.5	-4.197	6.80	-47.393	11.00	-50.687

COPY USAGE CPU-FCT CODE = 29672 BYTES, AREA = 25520 BYTES, TOTAL A

DIAGNOSTICS NUMBER OF ERRORS = 0, NUMBER OF WARNINGS = 0, NU

COMPILE TIME = 0.65 SEC, EXECUTION TIME = 20.39 SEC, 10.34.18 WEDN

CASOP

$\alpha = 0.4$

OFFSET REFLECTOR ANTENNA

INPUT DATA

LINEAR POLARIZATION IS IN THE PLANE OF SYMMETRY		
REFLECTOR DIAMETER IN WAVE LENGTH	= 100.00	LAMDA
THE FOCAL DISTANCE IN WAVE LENGTH	= 47.73	LAMDA
THE OFFSET ANGLE, THETA	= 50.00	DEGREES
THE HALF ANGLE OF ILLUMINATION	= 45.00	DEGREES
AZIMUTHAL ANGLE OF RADIATIONS	= 90.00	DEGREES

OUTPUT DATA

ANTENNA GAIN IN DECIBELS	= 47.683	DBS
ANTENNA GAIN FACTOR	= 0.594	RATIO
THE SPILL OVER POWER IN PERCENT	= 34.840	%
THE APERTURE EFFICIENCY	= 91.212	%
THE TOTAL ANTENNA EFFICIENCY	= 59.434	%

ANGLE	RAD.	PATTERN	ANGLE	RAD.	PATTERN	ANGLE	RAD.	PATTERN
0.10	1.49	.759	6.80	1.47	.051	8.50	1.49	.695
0.20	1.43	.933	6.90	1.44	.129	8.55	1.43	.263
0.30	1.47	.928	7.00	1.40	.209	8.60	1.40	.604
0.40	1.51	.907	7.10	1.36	.291	8.65	1.37	.862
0.50	1.55	.871	7.20	1.32	.376	8.70	1.34	.014
0.60	1.59	.821	7.30	1.28	.464	8.75	1.31	.099
0.70	1.63	.758	7.40	1.24	.556	8.80	1.28	.090
0.80	1.67	.683	7.50	1.20	.653	8.85	1.25	.277
0.90	1.71	.597	7.60	1.16	.756	8.90	1.22	.299
1.00	1.75	.501	7.70	1.12	.866	8.95	1.19	.157
1.10	1.79	.396	7.80	1.08	.984	9.00	1.16	.574
1.20	1.83	.283	7.90	1.04	1.110	9.05	1.13	.716
1.30	1.87	.163	8.00	1.00	1.246	9.10	1.10	.880
1.40	1.91	.037	8.10	.96	1.393	9.15	1.07	.247
1.50	1.95	.096	8.20	.92	1.552	9.20	1.04	.082
1.60	1.99	.151	8.30	.88	1.724	9.25	1.01	.192
1.70	2.03	.203	8.40	.84	1.909	9.30	.98	.577
1.80	2.07	.252	8.50	.80	2.108	9.35	.95	.840
1.90	2.11	.299	8.60	.76	2.321	9.40	.92	.097
2.00	2.15	.344	8.70	.72	2.549	9.45	.89	.008
2.10	2.19	.387	8.80	.68	2.793	9.50	.86	.097
2.20	2.23	.429	8.90	.64	3.054	9.55	.83	.250
2.30	2.27	.469	9.00	.60	3.333	9.60	.80	.511
2.40	2.31	.508	9.10	.56	3.631	9.65	.77	.769
2.50	2.35	.546	9.20	.52	3.949	9.70	.74	.915
2.60	2.39	.583	9.30	.48	4.288	9.75	.71	.961
2.70	2.43	.619	9.40	.44	4.649	9.80	.68	.992
2.80	2.47	.654	9.50	.40	5.033	9.85	.65	.990
2.90	2.51	.689	9.60	.36	5.441	9.90	.62	.936
3.00	2.55	.724	9.70	.32	5.874	9.95	.59	.825
3.10	2.59	.759	9.80	.28	6.333	10.00	.56	.640
3.20	2.63	.794	9.90	.24	6.819	10.05	.53	.381
3.30	2.67	.829	10.00	.20	7.334	10.10	.50	.140
3.40	2.71	.864		.16	7.879	10.15	.47	.001
3.50	2.75	.899		.12	8.456	10.20	.44	.731
3.60	2.79	.934		.08	9.067			
3.70	2.83	.969		.04	9.714			
3.80	2.87	.100		.00	10.399			
3.90	2.91	.131			11.124			
4.00	2.95	.162			11.891			
4.10	2.99	.193			12.704			
4.20	3.03	.224			13.567			
4.30	3.07	.255			14.484			
4.40	3.11	.286			15.460			
4.50	3.15	.317			16.499			
4.60	3.19	.348			17.607			
4.70	3.23	.379			18.790			
4.80	3.27	.410			20.044			
4.90	3.31	.441			21.376			
5.00	3.35	.472			22.793			

ANGLE	X-POLARIZATION	ANGLE	X-POLARIZATION	ANGLE	X-POLARIZATION
5.50	-74.515	6.80	-82.585	8.50	-100.000
5.55	-69.519	6.85	-75.273	8.55	-91.881
5.60	-67.010	6.90	-71.317	8.60	-76.660
5.65	-55.602	6.95	-66.910	8.65	-73.991
5.70	-63.000	7.00	-68.959	8.70	-72.173
5.75	-53.071	7.05	-61.043	8.75	-71.649
5.80	-63.813	7.10	-69.080	8.80	-71.159
5.85	-67.131	7.15	-70.159	8.85	-72.129
5.90	-59.936	7.20	-72.151	8.90	-73.229
5.95	-74.509	7.25	-75.352	8.95	-73.556
6.00	-80.022	7.30	-82.353	9.00	-79.954
6.05	-80.022	7.35	-79.242	9.05	-89.447
6.10	-72.895	7.40	-71.109	9.10	-80.438
6.15	-59.423	7.45	-71.833	9.15	-76.028
6.20	-67.147	7.50	-70.106	9.20	-74.028
6.25	-60.325	7.55	-69.774	9.25	-72.844
6.30	-56.730	7.60	-66.311	9.30	-72.599
6.35	-67.384	7.65	-70.309	9.35	-72.603
6.40	-59.475	7.70	-71.477	9.40	-73.371
6.45	-73.228	7.75	-74.503	9.45	-75.116
6.50	-80.090	7.80	-79.011	9.50	-76.031
6.55	-73.024	7.85	-85.232	9.55	-100.000
6.60	-59.410	7.90	-77.539	9.60	-85.179
6.65	-68.211	7.95	-71.007	9.65	-79.079
6.70	-67.713	8.00	-72.024	9.70	-76.008
6.75	-57.683	8.05	-70.930	9.75	-74.008
6.80	-63.423	8.10	-70.632	9.80	-73.398
6.85	-69.944	8.15	-70.174	9.85	-73.208
6.90	-72.537	8.20	-71.934	9.90	-73.660
6.95	-77.226	8.25	-71.357	10.00	-74.816
7.00	-89.997	8.30	-77.064	10.05	-76.894
7.05	-89.997	8.35	-82.287	10.10	-80.474

CORE USAGE SUBJECT CODE= 29672 BYTES, ARRAY AREA= 25520 BYTES, TOTAL AREA
 DIAGNOSTICS NUMBER OF ERRORS= 0, NUMBER OF WARNINGS= 0, NUMBE
 COMPILE TIME= 0.66 SEC, EXECUTION TIME= 38.45 SEC, 10.42.33 WEDNESD

C\$STOP

TEST CASE 1

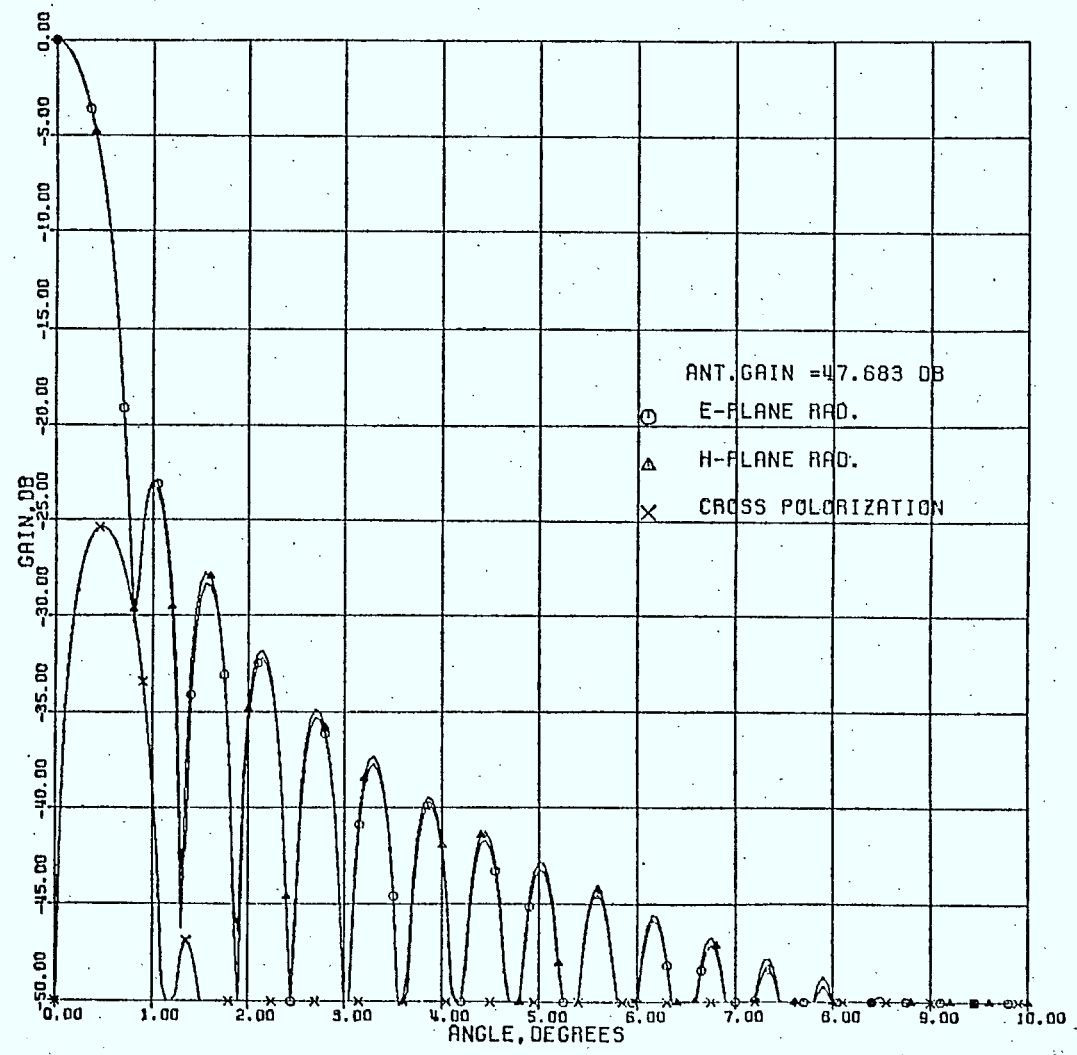
$$\alpha = 0.3$$

$$D = 100 \lambda$$

$$f = 41.95 \lambda$$

$$\theta_0 = 50^\circ$$

$$\theta_c = 50^\circ$$



$\alpha = 0.3$

OFFSET REFLECTOR ANTENNA

INPUT DATA

LINEAR POLARIZATION IS IN THE PLANE OF SYMMETRY
REFLECTOR DIAMETER IN WAVE LENGTH = 100.00 LAMDA
THE FOCAL DISTANCE IN WAVE LENGTH = 42.95 LAMDA
THE OFFSET ANGLE, THETA = 50.00 DEGREES
THE HALF ANGLE OF ILLUMINATION = 50.00 DEGREES
AZIMUTHAL ANGLE OF RADIATIONS = 0.00 DEGREES

OUTPUT DATA

ANTENNA GAIN IN DECIBELS = 43.112 DBS
ANTENNA GAIN FACTOR = 0.636 RATIO
THE SPILL OVER POWER IN PERCENT = 25.43 %
THE APERTURE EFFICIENCY = 87.971 %
THE TOTAL ANTENNA EFFICIENCY = 65.597 %

ANGLE

RAD. PATTERN

ANGLE

RAD. PATTERN

ANGLE

RAD. PATTERN

0.000000	4.712389	*****	6.800000
0.000000	4.536461	*****	6.900000
0.000000	4.360533	*****	7.000000
0.000000	4.184605	*****	7.100000
0.000000	4.008677	*****	7.200000
0.000000	3.832749	*****	7.300000
0.000000	3.656821	*****	7.400000
0.000000	3.480893	*****	7.500000
0.000000	3.304965	*****	7.600000
0.000000	3.129037	*****	7.700000
0.000000	2.953109	*****	7.800000
0.000000	2.777181	*****	7.900000
0.000000	2.601253	*****	8.000000
0.000000	2.425325	*****	8.100000
0.000000	2.249397	*****	8.200000
0.000000	2.073469	*****	8.300000
0.000000	1.897541	*****	8.400000
0.000000	1.721613	*****	8.500000
0.000000	1.545685	*****	8.600000
0.000000	1.369757	*****	8.700000
0.000000	1.193829	*****	8.800000
0.000000	1.017901	*****	8.900000
0.000000	0.841973	*****	9.000000

4.712389	5.651000	*****	8.500000
4.536461	5.500000	*****	8.600000
4.360533	5.348000	*****	8.700000
4.184605	5.196000	*****	8.800000
4.008677	5.044000	*****	8.900000
3.832749	4.892000	*****	9.000000
3.656821	4.740000	*****	9.100000
3.480893	4.588000	*****	9.200000
3.304965	4.436000	*****	9.300000
3.129037	4.284000	*****	9.400000
2.953109	4.132000	*****	9.500000
2.777181	3.980000	*****	9.600000
2.601253	3.828000	*****	9.700000
2.425325	3.676000	*****	9.800000
2.249397	3.524000	*****	9.900000
2.073469	3.372000	*****	10.000000
1.897541	3.220000	*****	10.100000
1.721613	3.068000	*****	10.200000
1.545685	2.916000	*****	10.300000
1.369757	2.764000	*****	10.400000
1.193829	2.612000	*****	10.500000

3.016667	2.166667	*****	8.500000
3.000000	2.750000	*****	8.600000
3.000000	3.333333	*****	8.700000
3.000000	3.916667	*****	8.800000
3.000000	4.500000	*****	8.900000
3.000000	5.083333	*****	9.000000
3.000000	5.666667	*****	9.100000
3.000000	6.250000	*****	9.200000
3.000000	6.833333	*****	9.300000
3.000000	7.416667	*****	9.400000
3.000000	8.000000	*****	9.500000
3.000000	8.583333	*****	9.600000
3.000000	9.166667	*****	9.700000
3.000000	9.750000	*****	9.800000
3.000000	10.333333	*****	9.900000
3.000000	10.916667	*****	10.000000
3.000000	11.500000	*****	10.100000
3.000000	12.083333	*****	10.200000
3.000000	12.666667	*****	10.300000
3.000000	13.250000	*****	10.400000
3.000000	13.833333	*****	10.500000

CORE USAGE OBJECT CODE = 29672 BYTES, AREA = 25520 BYTES, TOTAL AREA =
 DIAGNOSTICS NUMBER OF ERRORS = 0, NUMBER OF WARNINGS = 0, NUMBER
 COMPILE TIME = 0.65 SEC, EXECUTION TIME = 20.49 SEC, 14.28.45 WEDNESDAY

C3STOP

$$\alpha = 0.3$$

 OFFSET REFLECTOR ANTENNA

 INPUT DATA

LINEAR POLARIZATION IS IN THE PLANE OF SYMMETRY
 REFLECTOR DIAMETER IN WAVE LENGTH = 100.00 LAMDA
 THE FOCAL DISTANCE IN WAVE LENGTH = 41.95 LAMDA
 THE OFFSET ANGLE, THETA = 50.00 DEGREES
 THE HALF ANGLE OF ILLUMINATION = 50.00 DEGREES
 AZIMUTHAL ANGLE OF RADIATIONS = 90.00 DEGREES

 OUTPUT DATA

ANTENNA GAIN IN DECIBELS = 49.112 DBS
 ANTENNA GAIN FACTOR = 0.656 PATIO
 THE SPILL OVER POWER IN PERCENT = 25.434 %
 THE APERTURE EFFICIENCY = 87.971 %
 THE TOTAL ANTENNA EFFICIENCY = 65.597 %

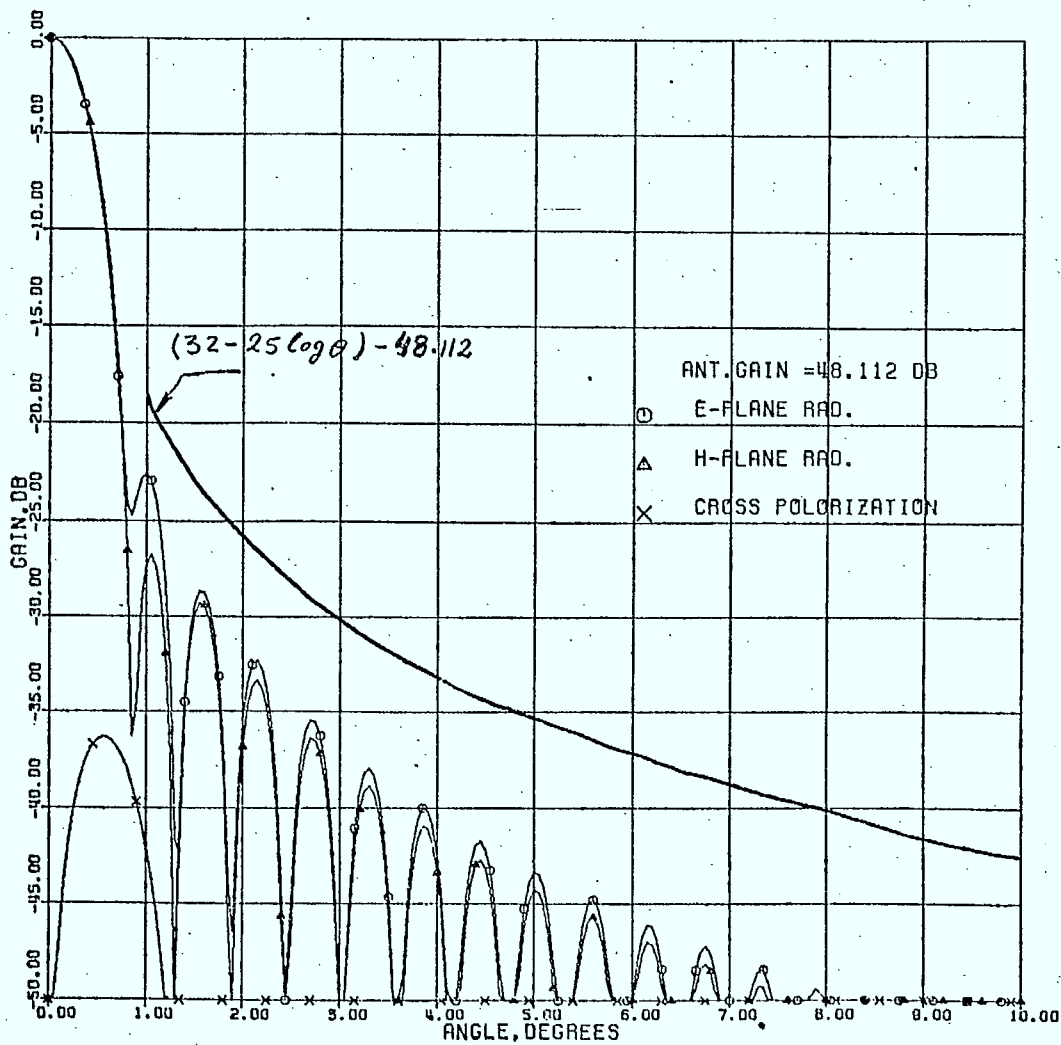
ANGLE	RAD.	PATTERN	ANGLE	RAD.	PATTERN	ANGLE	RAD.	PATTERN
0.00	0.000	*****	4.70	1.603	*****	4.40	1.403	54
0.05	0.063	*****	4.75	1.934	*****	4.45	1.433	33
0.10	0.201	*****	4.80	1.896	*****	4.50	1.453	62
0.15	0.591	*****	4.85	1.777	*****	4.55	1.522	7
0.20	1.058	*****	4.90	1.947	*****	4.60	1.700	162
0.25	1.668	*****	4.95	1.912	*****	4.65	1.500	617
0.30	2.429	*****	5.00	1.833	*****	4.70	1.433	560
0.35	3.352	*****	5.05	1.633	*****	4.75	1.422	951
0.40	4.439	*****	5.10	1.524	*****	4.80	1.401	144
0.45	5.789	*****	5.15	1.407	*****	4.85	1.400	554
0.50	7.271	*****	5.20	1.283	*****	4.90	1.411	645
0.55	8.908	*****	5.25	1.153	*****	4.95	1.441	802
0.60	1.070	*****	5.30	1.017	*****	5.00	1.455	929
0.65	1.612	*****	5.35	0.863	*****	5.05	1.450	1035
0.70	2.031	*****	5.40	0.969	*****	5.10	1.422	1177
0.75	2.336	*****	5.45	0.919	*****	5.15	1.376	1309
0.80	2.526	*****	5.50	0.808	*****	5.20	1.310	1475
0.85	2.646	*****	5.55	0.718	*****	5.25	1.224	1604
0.90	2.780	*****	5.60	0.657	*****	5.30	1.123	1702
0.95	2.880	*****	5.65	0.608	*****	5.35	1.009	1775
1.00	2.917	*****	5.70	0.548	*****	5.40	0.922	1829
1.05	2.922	*****	5.75	0.481	*****	5.45	0.833	1860
1.10	2.901	*****	5.80	0.409	*****	5.50	0.744	1877
1.15	2.956	*****	5.85	0.322	*****	5.55	0.666	1880
1.20	3.091	*****	5.90	0.229	*****	5.60	0.595	1875
1.25	3.224	*****	5.95	0.133	*****	5.65	0.525	1855
1.30	3.350	*****	6.00	0.034	*****	5.70	0.456	1823
1.35	3.472	*****	6.05	0.025	*****	5.75	0.388	1771
1.40	3.599	*****	6.10	0.017	*****	5.80	0.323	1704
1.45	3.717	*****	6.15	0.009	*****	5.85	0.260	1625
1.50	3.827	*****	6.20	0.003	*****	5.90	0.200	1534
1.55	3.930	*****	6.25	0.000	*****	5.95	0.144	1438
1.60	4.027	*****	6.30	0.000	*****	6.00	0.091	1337
1.65	4.119	*****	6.35	0.000	*****	6.05	0.040	1232
1.70	4.207	*****	6.40	0.000	*****	6.10	0.000	1115

ANGLE	RAD.	PATTERN	ANGLE	RAD.	PATTERN	ANGLE	RAD.	PATTERN
5.00	1.57	*****	6.80	1.18	*****	8.50	1.43	*****
5.10	1.62	*****	6.85	1.20	*****	8.55	1.45	*****
5.20	1.67	*****	6.90	1.22	*****	8.60	1.47	*****
5.30	1.72	*****	6.95	1.24	*****	8.65	1.49	*****
5.40	1.77	*****	7.00	1.26	*****	8.70	1.51	*****
5.50	1.82	*****	7.05	1.28	*****	8.75	1.53	*****
5.60	1.87	*****	7.10	1.30	*****	8.80	1.55	*****
5.70	1.92	*****	7.15	1.32	*****	8.85	1.57	*****
5.80	1.97	*****	7.20	1.34	*****	8.90	1.59	*****
5.90	2.02	*****	7.25	1.36	*****	8.95	1.61	*****
6.00	2.07	*****	7.30	1.38	*****	9.00	1.63	*****
6.10	2.12	*****	7.35	1.40	*****	9.05	1.65	*****
6.20	2.17	*****	7.40	1.42	*****	9.10	1.67	*****
6.30	2.22	*****	7.45	1.44	*****	9.15	1.69	*****
6.40	2.27	*****	7.50	1.46	*****	9.20	1.71	*****
6.50	2.32	*****	7.55	1.48	*****	9.25	1.73	*****
6.60	2.37	*****	7.60	1.50	*****	9.30	1.75	*****
6.70	2.42	*****	7.65	1.52	*****	9.35	1.77	*****
6.80	2.47	*****	7.70	1.54	*****	9.40	1.79	*****
6.90	2.52	*****	7.75	1.56	*****	9.45	1.81	*****
7.00	2.57	*****	7.80	1.58	*****	9.50	1.83	*****
7.10	2.62	*****	7.85	1.60	*****	9.55	1.85	*****
7.20	2.67	*****	7.90	1.62	*****	9.60	1.87	*****
7.30	2.72	*****	7.95	1.64	*****	9.65	1.89	*****
7.40	2.77	*****	8.00	1.66	*****	9.70	1.91	*****
7.50	2.82	*****	8.05	1.68	*****	9.75	1.93	*****
7.60	2.87	*****	8.10	1.70	*****	9.80	1.95	*****
7.70	2.92	*****	8.15	1.72	*****	9.85	1.97	*****
7.80	2.97	*****	8.20	1.74	*****	9.90	1.99	*****
7.90	3.02	*****	8.25	1.76	*****	9.95	2.01	*****
8.00	3.07	*****	8.30	1.78	*****	10.00	2.03	*****
8.10	3.12	*****	8.35	1.80	*****	10.05	2.05	*****
8.20	3.17	*****	8.40	1.82	*****	10.10	2.07	*****
8.30	3.22	*****	8.45	1.84	*****	10.15	2.09	*****
8.40	3.27	*****	8.50	1.86	*****	10.20	2.11	*****
8.50	3.32	*****	8.55	1.88	*****	10.25	2.13	*****
8.60	3.37	*****	8.60	1.90	*****	10.30	2.15	*****
8.70	3.42	*****	8.65	1.92	*****	10.35	2.17	*****
8.80	3.47	*****	8.70	1.94	*****	10.40	2.19	*****
8.90	3.52	*****	8.75	1.96	*****	10.45	2.21	*****
9.00	3.57	*****	8.80	1.98	*****	10.50	2.23	*****
9.10	3.62	*****	8.85	2.00	*****	10.55	2.25	*****
9.20	3.67	*****	8.90	2.02	*****	10.60	2.27	*****
9.30	3.72	*****	8.95	2.04	*****	10.65	2.29	*****
9.40	3.77	*****	9.00	2.06	*****	10.70	2.31	*****
9.50	3.82	*****	9.05	2.08	*****	10.75	2.33	*****
9.60	3.87	*****	9.10	2.10	*****	10.80	2.35	*****
9.70	3.92	*****	9.15	2.12	*****	10.85	2.37	*****
9.80	3.97	*****	9.20	2.14	*****	10.90	2.39	*****
9.90	4.02	*****	9.25	2.16	*****	10.95	2.41	*****
10.00	4.07	*****	9.30	2.18	*****	11.00	2.43	*****

ANGLE	X-POLARIZATION		ANGLE	X-POLARIZATION		ANGLE	X-POLARIZATION
0.00	-100.000	*****	1.70	-62.122	*****	3.40	-74.817
0.05	-93.223	*****	1.75	-63.627	*****	3.45	-75.C36
0.10	-87.280	*****	1.80	-66.049	*****	3.50	-75.887
0.15	-82.916	*****	1.85	-69.919	*****	3.55	-77.466
0.20	-79.640	*****	1.90	-77.216	*****	3.60	-80.C52
0.25	-77.989	*****	1.95	-88.210	*****	3.65	-84.445
0.30	-78.759	*****	2.00	-74.273	*****	3.70	-84.674
0.35	-77.822	*****	2.05	-69.938	*****	3.75	-92.115
0.40	-77.717	*****	2.10	-67.769	*****	3.80	-94.589
0.45	-77.500	*****	2.15	-65.951	*****	3.85	-98.925
0.50	-77.144	*****	2.20	-66.283	*****	3.90	-78.520
0.55	-76.666	*****	2.25	-66.531	*****	3.95	-77.521
0.60	-76.066	*****	2.30	-67.269	*****	4.00	-77.617
0.65	-75.354	*****	2.35	-68.859	*****	4.05	-77.946
0.70	-74.578	*****	2.40	-71.194	*****	4.10	-76.926
0.75	-73.750	*****	2.45	-74.388	*****	4.15	-80.692
0.80	-72.907	*****	2.50	-81.807	*****	4.20	-83.608
0.85	-72.060	*****	2.55	-90.907	*****	4.25	-88.828
0.90	-71.250	*****	2.60	-79.948	*****	4.30	-100.C00
0.95	-70.478	*****	2.65	-75.246	*****	4.35	-92.C45
1.00	-70.043	*****	2.70	-72.860	*****	4.40	-95.661
1.05	-70.000	*****	2.75	-71.150	*****	4.45	-82.557
1.10	-70.000	*****	2.80	-71.150	*****	4.50	-80.840
1.15	-70.000	*****	2.85	-71.335	*****	4.55	-79.992
1.20	-70.000	*****	2.90	-72.122	*****	4.60	-79.824
1.25	-70.000	*****	2.95	-73.534	*****	4.65	-80.280
1.30	-70.000	*****	3.00	-75.970	*****	4.70	-81.407
1.35	-70.000	*****	3.05	-79.852	*****	4.75	-83.378
1.40	-70.000	*****	3.10	-87.651	*****	4.80	-86.661
1.45	-70.000	*****	3.15	-95.115	*****	4.85	-92.892
1.50	-70.000	*****	3.20	-82.928	*****	4.90	-100.C00
1.55	-70.000	*****	3.25	-78.052	*****	4.95	-91.544
1.60	-70.000	*****	3.30	-76.408	*****	5.00	-86.720
1.65	-70.000	*****	3.35	-75.230	*****	5.05	-84.C11

ANGLE	X-POLARIZATION	*****	ANGLE	X-POLARIZATION	*****	ANGLE	X-POLARIZATION
5.10	-82.510	*****	6.80	-39.060	*****	8.50	-95.550
5.15	-81.834	*****	6.85	-87.435	*****	8.55	-92.486
5.20	-81.176	*****	6.90	-86.618	*****	8.60	-90.760
5.25	-80.508	*****	6.95	-86.537	*****	8.65	-88.887
5.30	-80.847	*****	7.00	-87.069	*****	8.70	-86.693
5.35	-81.183	*****	7.05	-86.512	*****	8.75	-90.132
5.40	-81.533	*****	7.10	-90.494	*****	8.80	-91.261
5.45	-81.777	*****	7.15	-91.249	*****	8.85	-93.270
5.50	-82.000	*****	7.20	-90.000	*****	8.90	-96.698
5.55	-82.197	*****	7.25	-90.000	*****	8.95	-100.000
5.60	-82.776	*****	7.30	-96.121	*****	9.00	-100.000
5.65	-83.398	*****	7.35	-91.800	*****	9.05	-100.000
5.70	-83.911	*****	7.40	-89.443	*****	9.10	-95.527
5.75	-84.410	*****	7.45	-88.138	*****	9.15	-92.947
5.80	-84.903	*****	7.50	-87.586	*****	9.20	-91.509
5.85	-85.427	*****	7.55	-87.680	*****	9.25	-90.856
5.90	-85.922	*****	7.60	-88.411	*****	9.30	-90.861
5.95	-86.449	*****	7.65	-89.918	*****	9.35	-91.514
6.00	-87.051	*****	7.70	-92.465	*****	9.40	-92.910
6.05	-87.000	*****	7.75	-96.930	*****	9.45	-95.327
6.10	-87.000	*****	7.80	-100.000	*****	9.50	-99.575
6.15	-87.232	*****	7.85	-100.000	*****	9.55	-100.000
6.20	-87.589	*****	7.90	-95.561	*****	9.60	-100.000
6.25	-87.977	*****	7.95	-91.997	*****	9.65	-99.109
6.30	-88.322	*****	8.00	-89.993	*****	9.70	-93.999
6.35	-88.633	*****	8.05	-88.923	*****	9.75	-93.220
6.40	-88.922	*****	8.10	-88.558	*****	9.80	-92.078
6.45	-89.292	*****	8.15	-88.822	*****	9.85	-91.658
6.50	-89.647	*****	8.20	-89.744	*****	9.90	-91.881
6.55	-90.120	*****	8.25	-91.468	*****	9.95	-92.768
6.60	-90.034	*****	8.30	-94.288	*****	10.00	-94.472
6.65	-90.000	*****	8.35	-99.764	*****	10.05	-97.387
6.70	-91.666	*****	8.40	-100.000	*****	10.10	-100.000
6.75	-91.967	*****	8.45	-100.000	*****	10.15	-100.000

CORE USAGE OBJECT CODE= 29672 BYTES, ARRAY AREA= 25520 BYTES, TOTAL AR
 DIAGNOSTICS NUMBER OF ERRORS= 0, NUMBER OF WARNINGS= 0, NUM
 COMPILE TIME= 0.66 SEC, EXECUTION TIME= 38.20 SEC, 14.30.14 WEDNE
 C\$STOP



TEST CASE 2

$$\alpha = 0.07$$

$$D = 120 \lambda$$

$$f = 103.92 \lambda$$

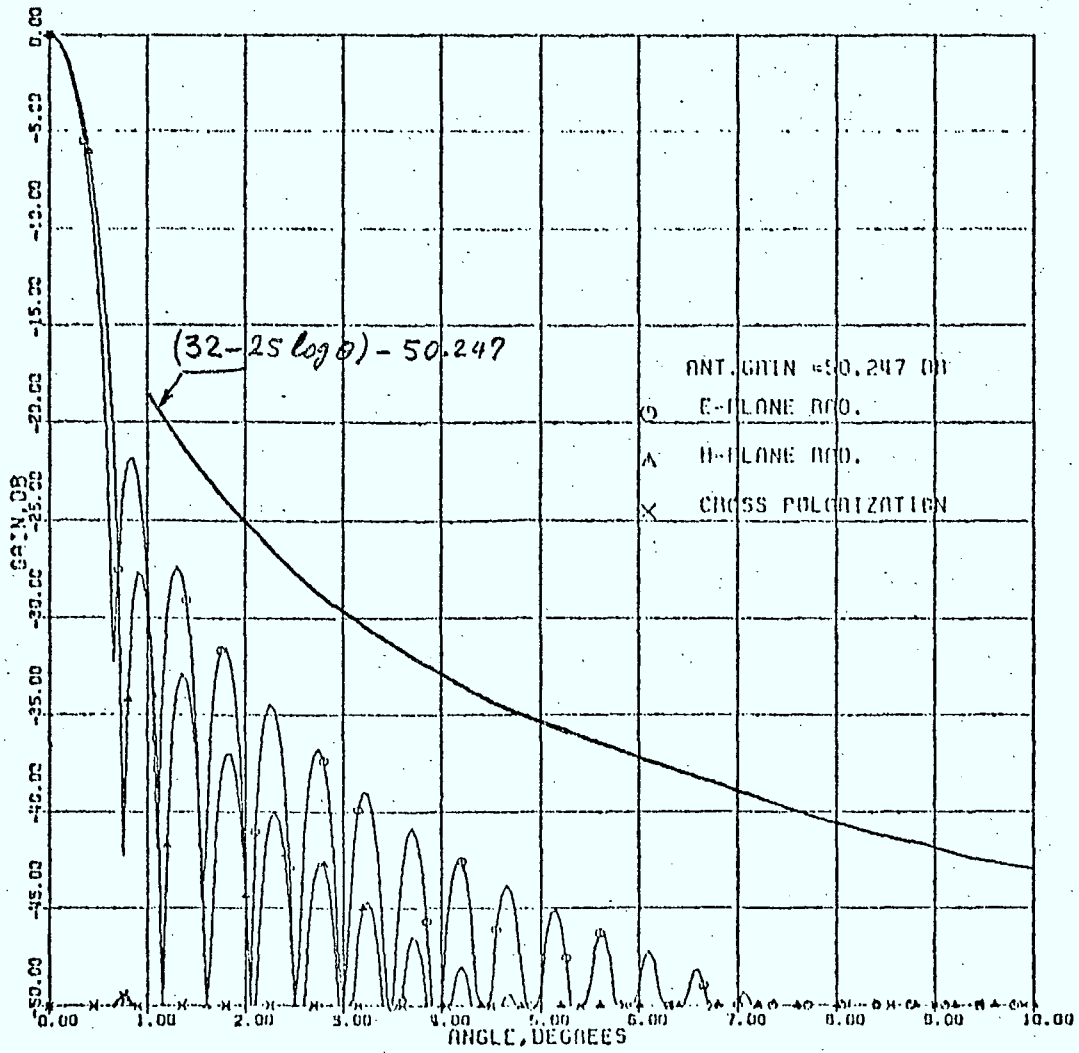
$$\theta_0 = 30^\circ$$

$$\theta_c = 30^\circ$$

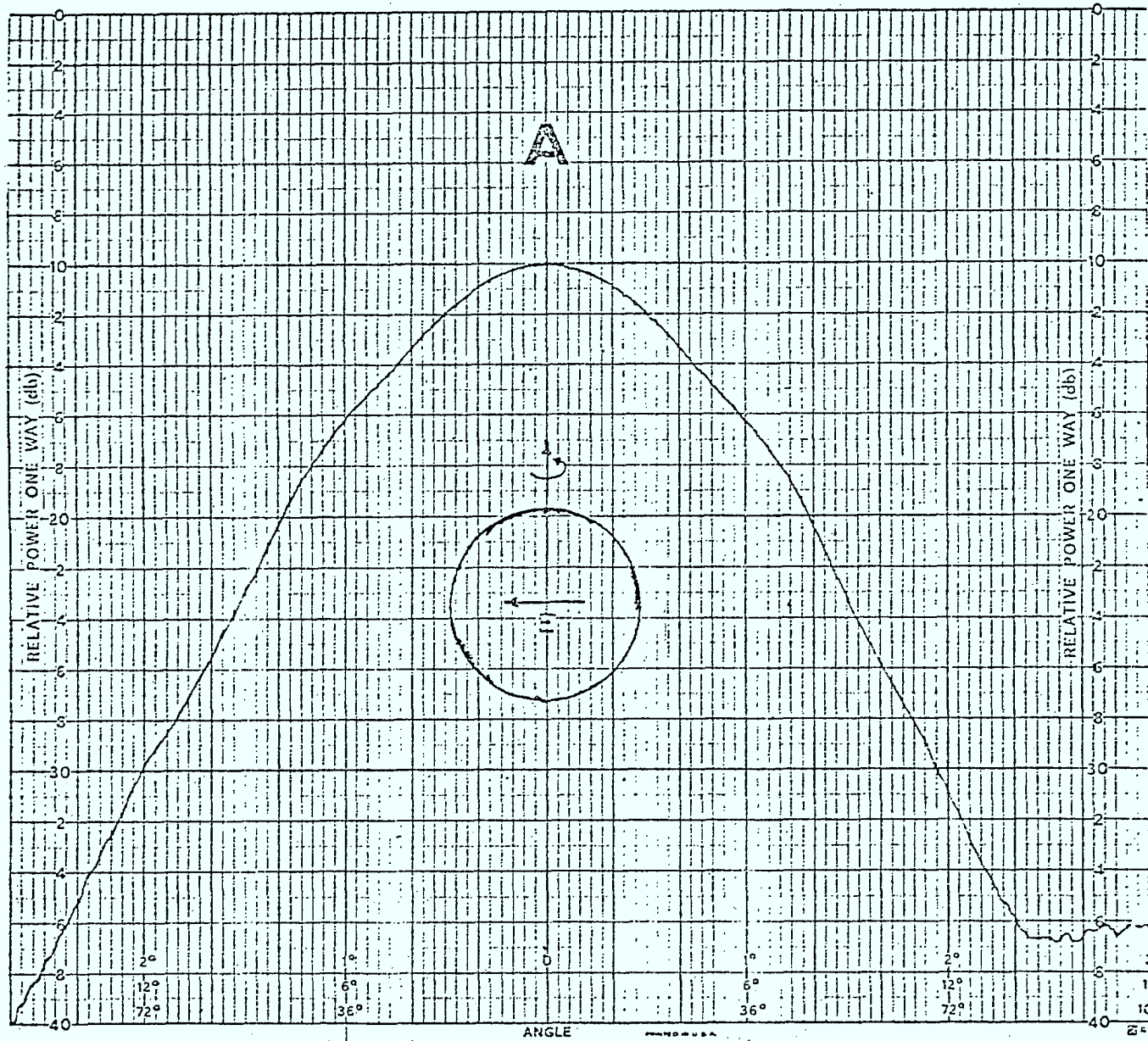
0.07

INPUT DATA

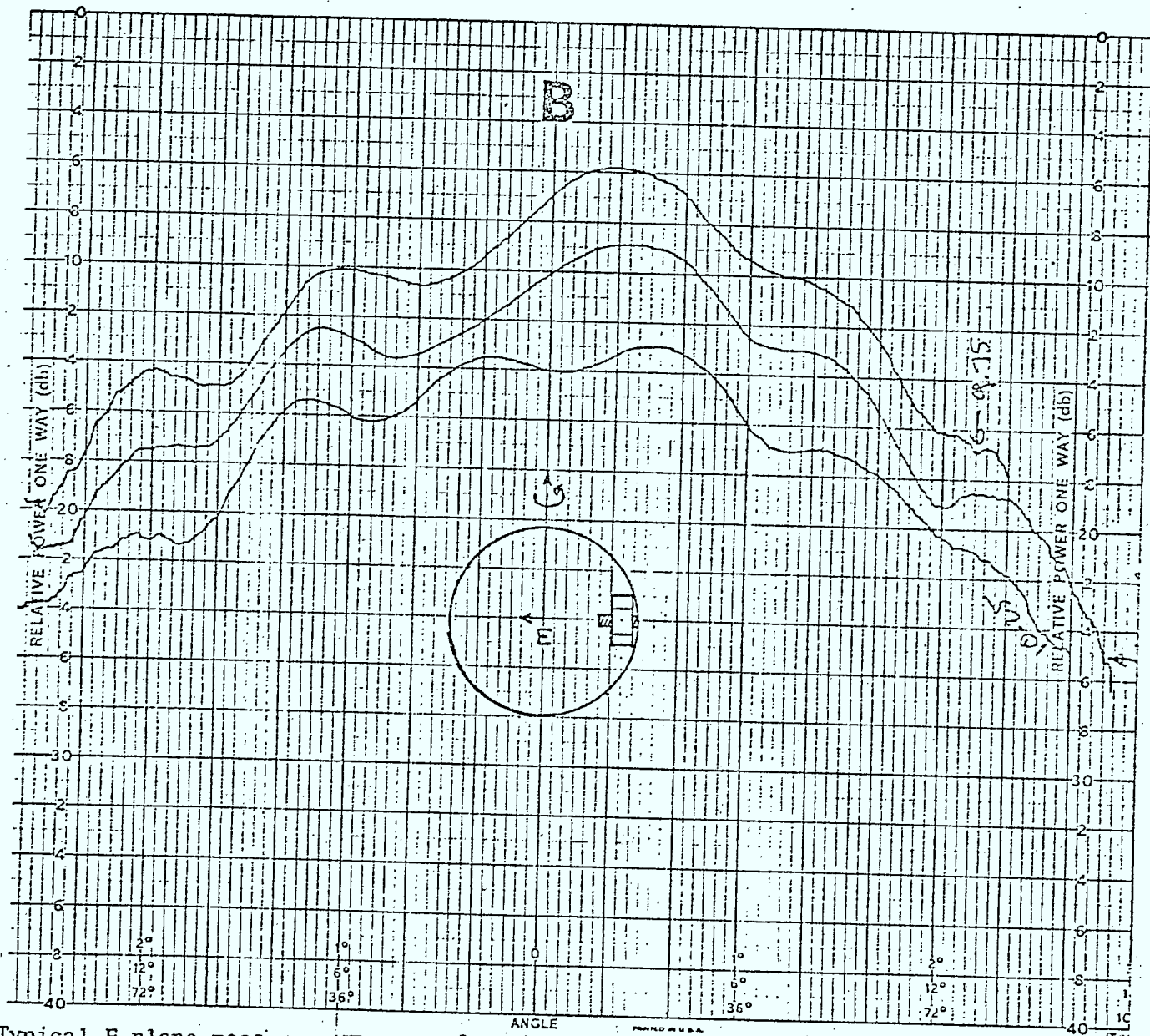
NO	DESCRIPTION	UNIT	VALUE
1	PERCENT		0.07
2	PERCENT		0.07
3	PERCENT		0.07
4	PERCENT		0.07
5	PERCENT		0.07
6	PERCENT		0.07
7	PERCENT		0.07
8	PERCENT		0.07
9	PERCENT		0.07
10	PERCENT		0.07
11	PERCENT		0.07
12	PERCENT		0.07
13	PERCENT		0.07
14	PERCENT		0.07
15	PERCENT		0.07
16	PERCENT		0.07
17	PERCENT		0.07
18	PERCENT		0.07
19	PERCENT		0.07
20	PERCENT		0.07
21	PERCENT		0.07
22	PERCENT		0.07
23	PERCENT		0.07
24	PERCENT		0.07
25	PERCENT		0.07
26	PERCENT		0.07
27	PERCENT		0.07
28	PERCENT		0.07
29	PERCENT		0.07
30	PERCENT		0.07
31	PERCENT		0.07
32	PERCENT		0.07
33	PERCENT		0.07
34	PERCENT		0.07
35	PERCENT		0.07
36	PERCENT		0.07
37	PERCENT		0.07
38	PERCENT		0.07
39	PERCENT		0.07
40	PERCENT		0.07
41	PERCENT		0.07
42	PERCENT		0.07
43	PERCENT		0.07
44	PERCENT		0.07
45	PERCENT		0.07
46	PERCENT		0.07
47	PERCENT		0.07
48	PERCENT		0.07
49	PERCENT		0.07
50	PERCENT		0.07



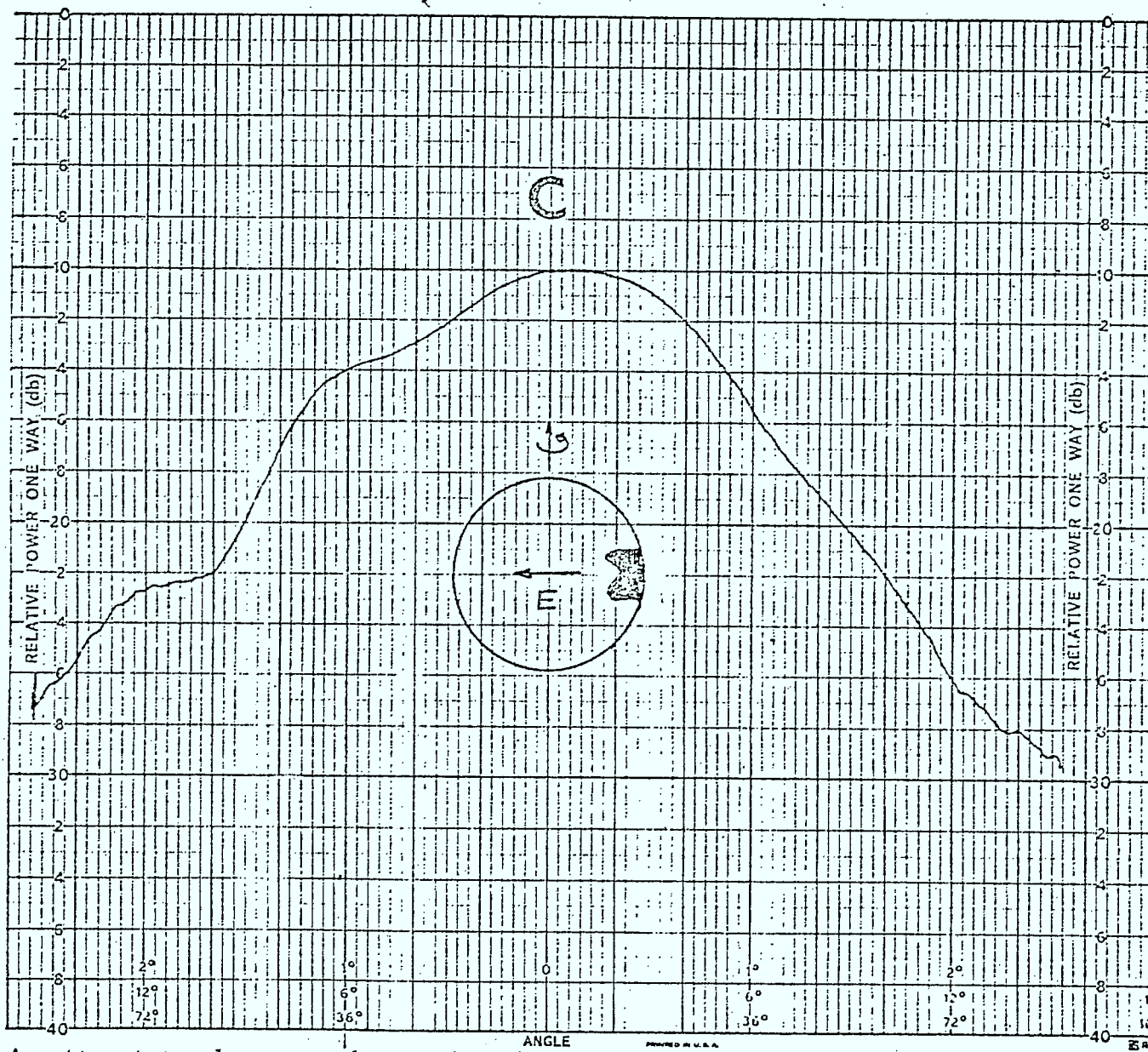
EXPERIMENTAL RESULTS



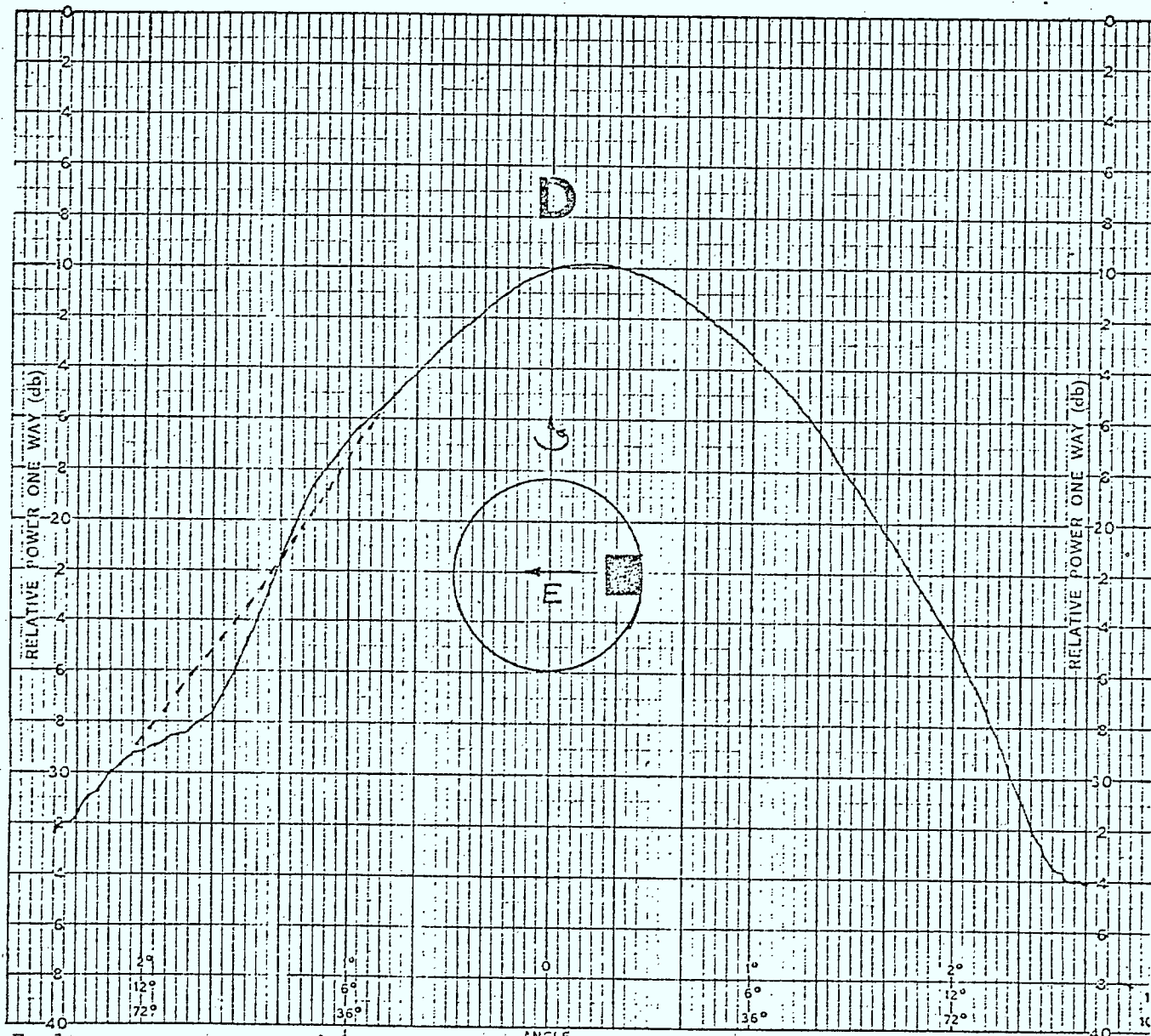
The E-plane measurements of the feed shown in Fig. 4 with no obstruction in the guide



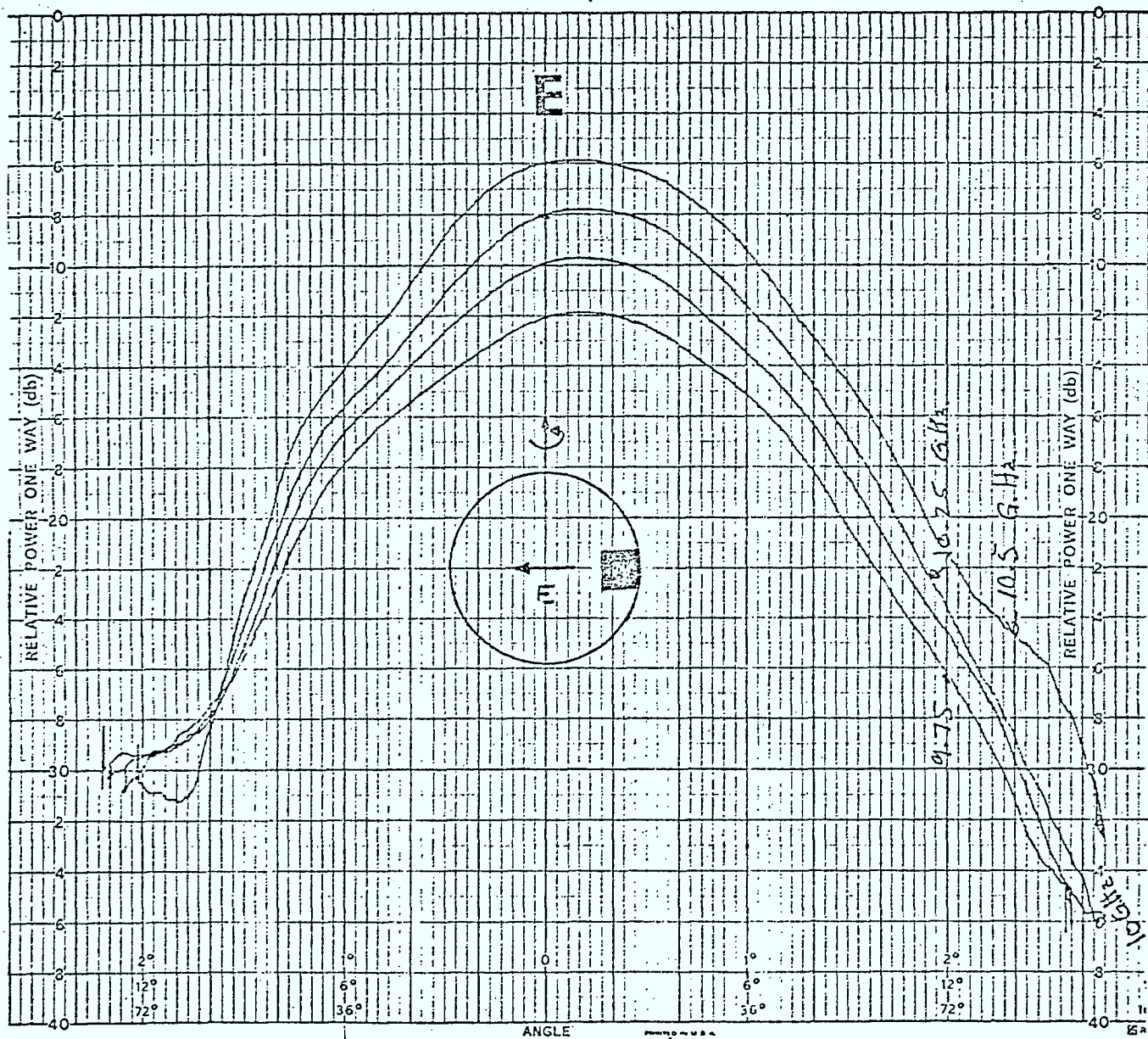
Typical E-plane measurements as a function of frequency of an arbitrary obstruction in the E-plane where the irregularities are attributed to the undesirable modes.



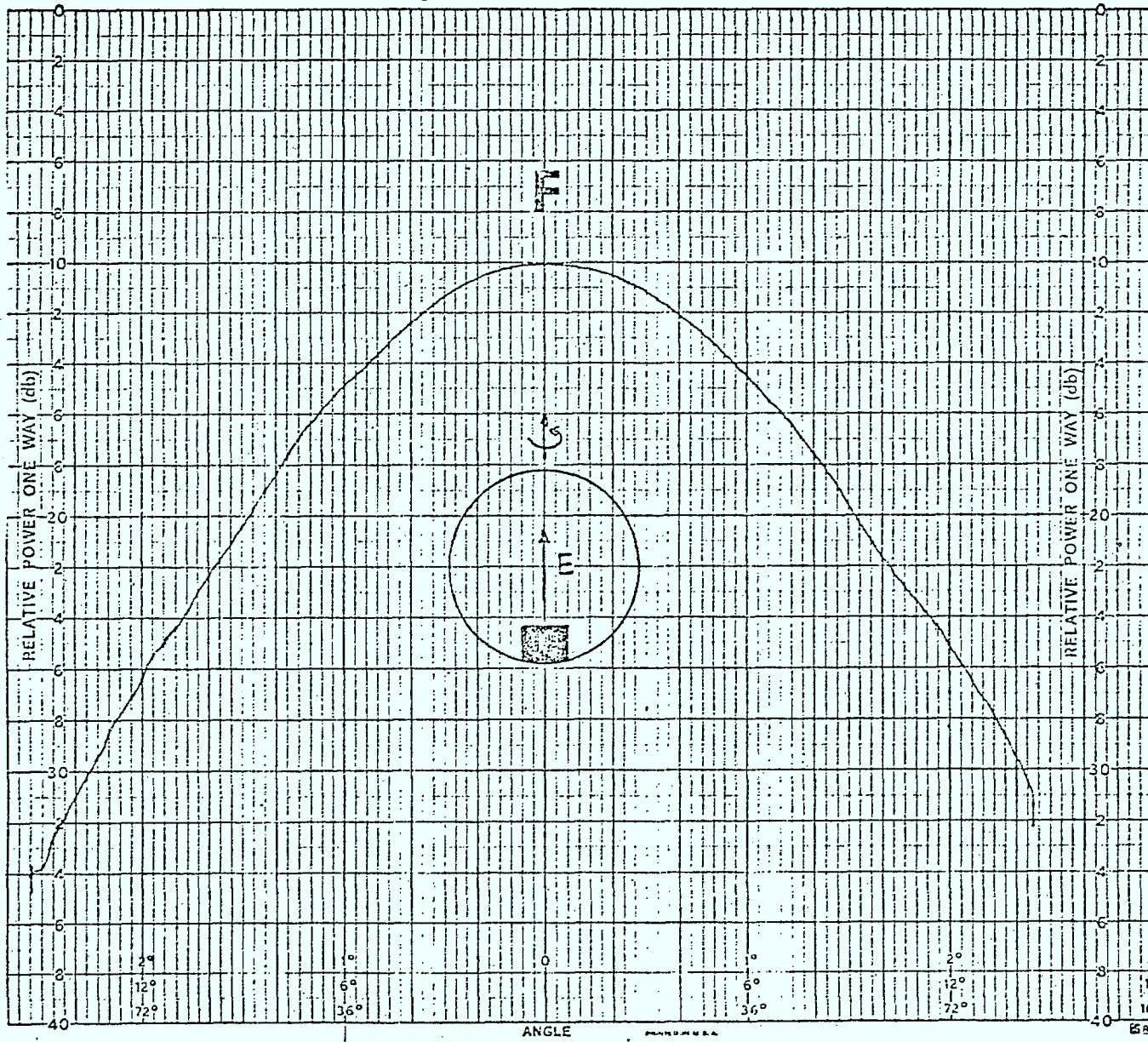
An attempt to choose an obstruction that minimizes the generation of the undesirable modes.



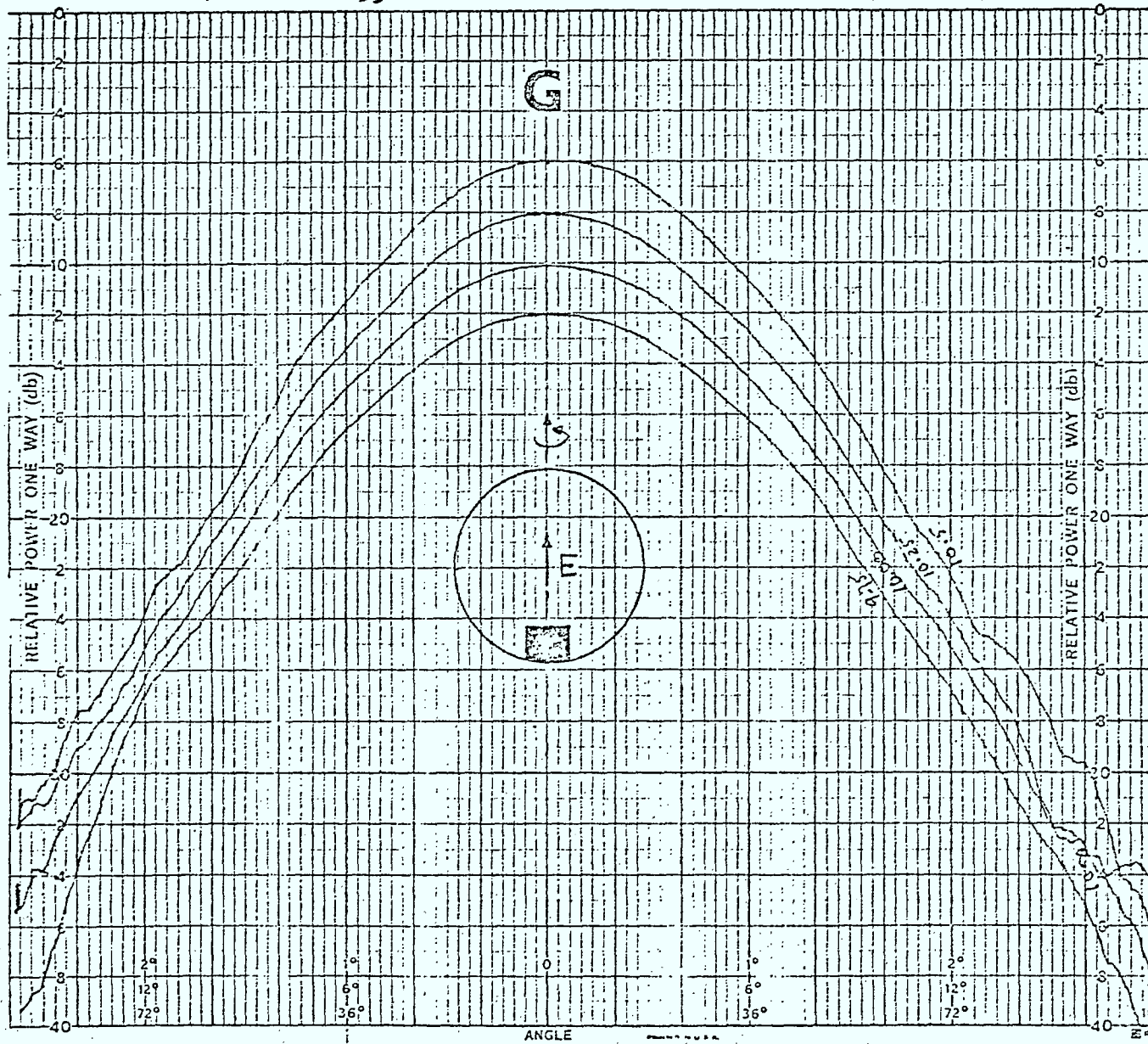
E-plane measurements with an obstruction in the E-plane after cleaning most of the irregularities due to the undesirable modes.



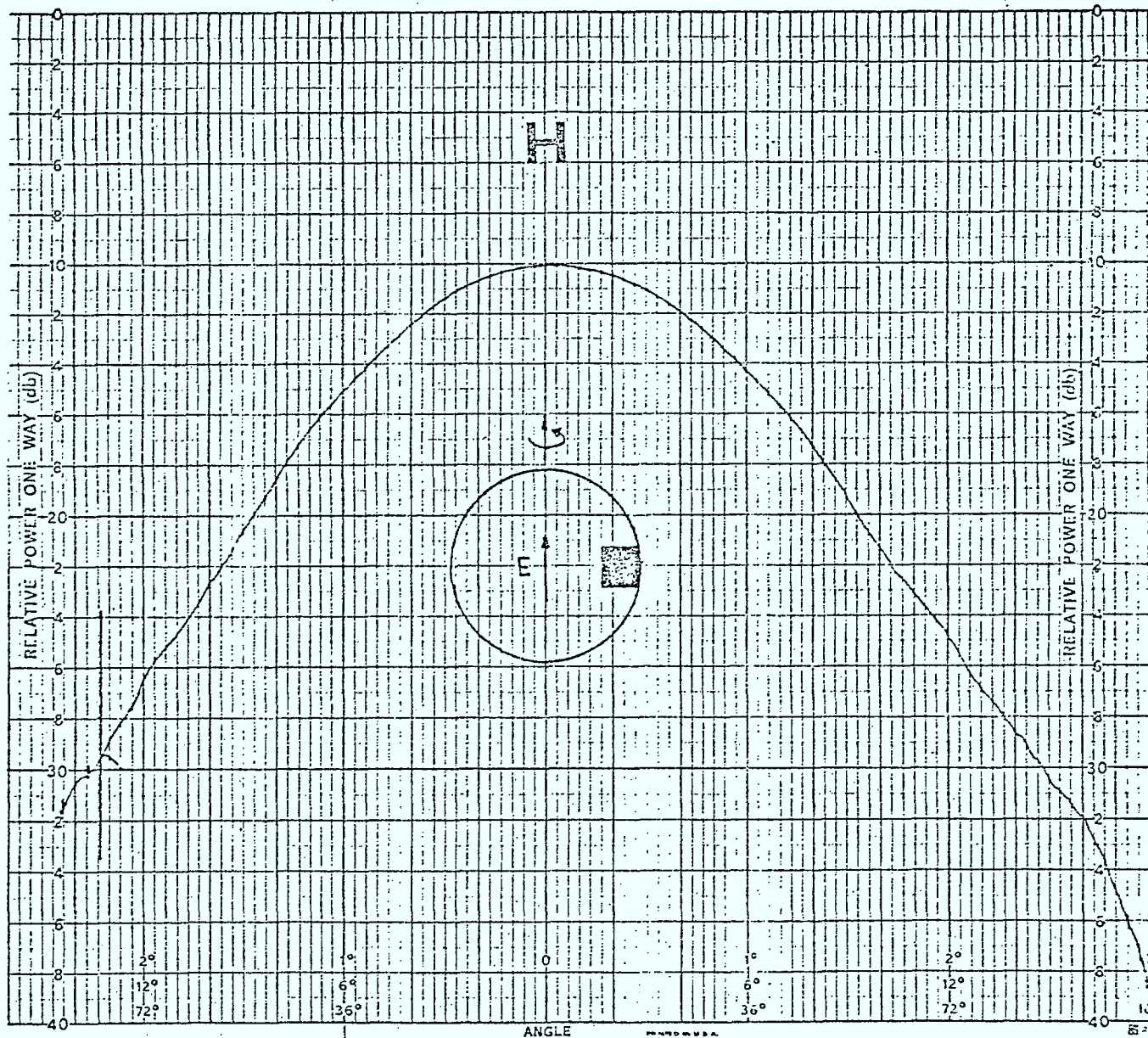
Asymmetry as a function of frequency when the obstruction of Fig. D is investigated.



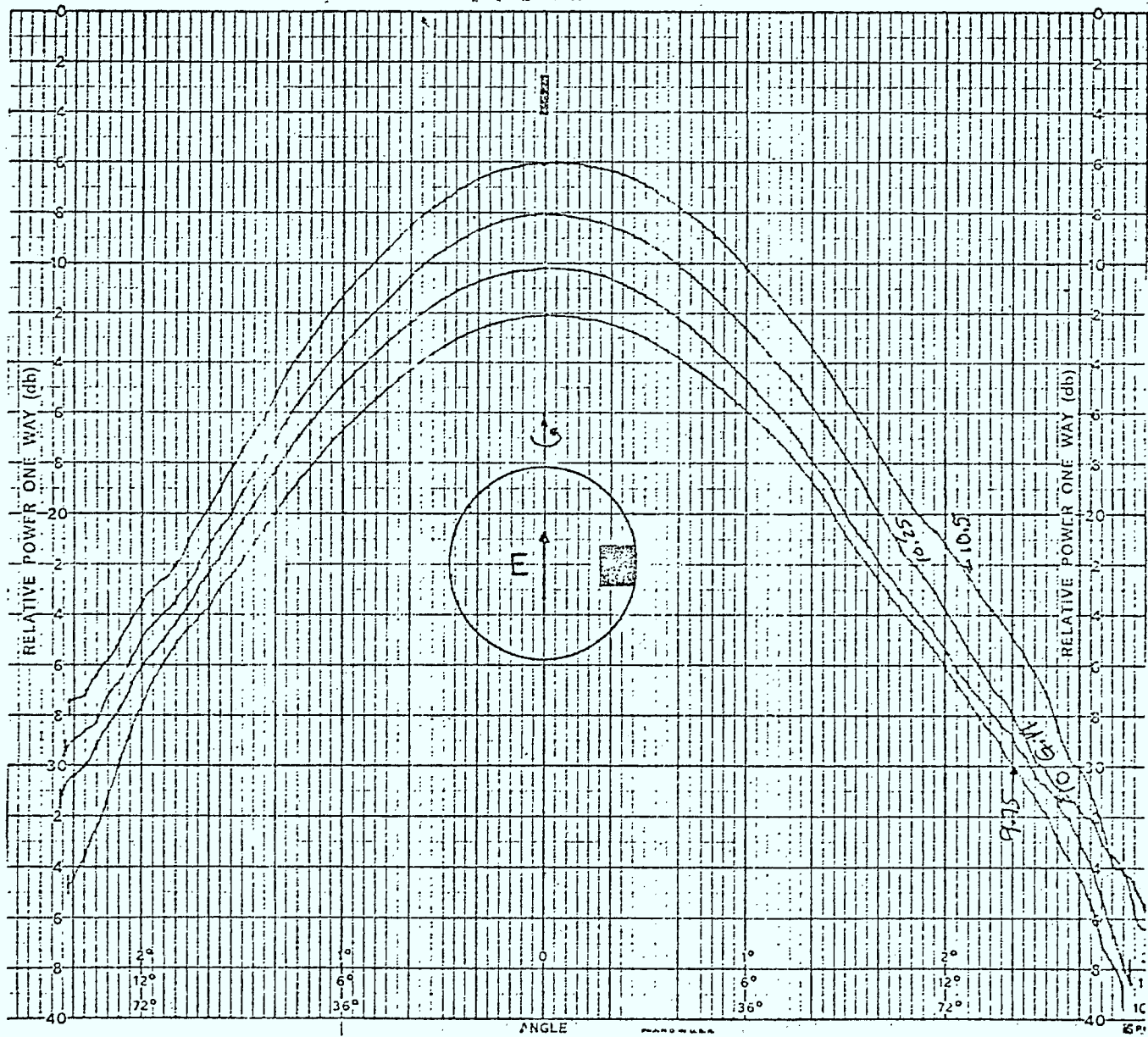
The H-plane measurements for the case of Fig. D.



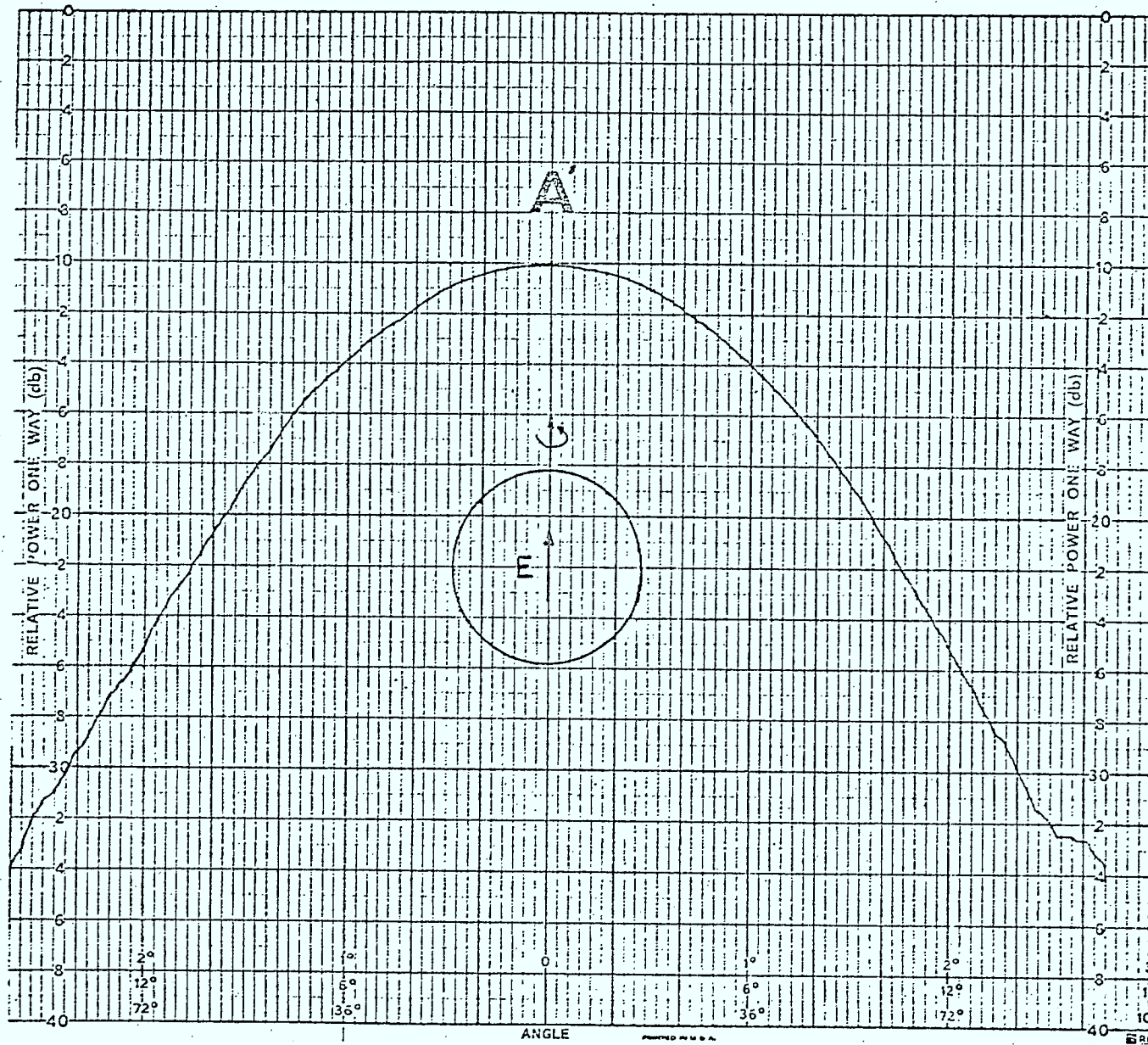
H-plane measurements for the obstruction of Fig. D as a function of frequency variation.



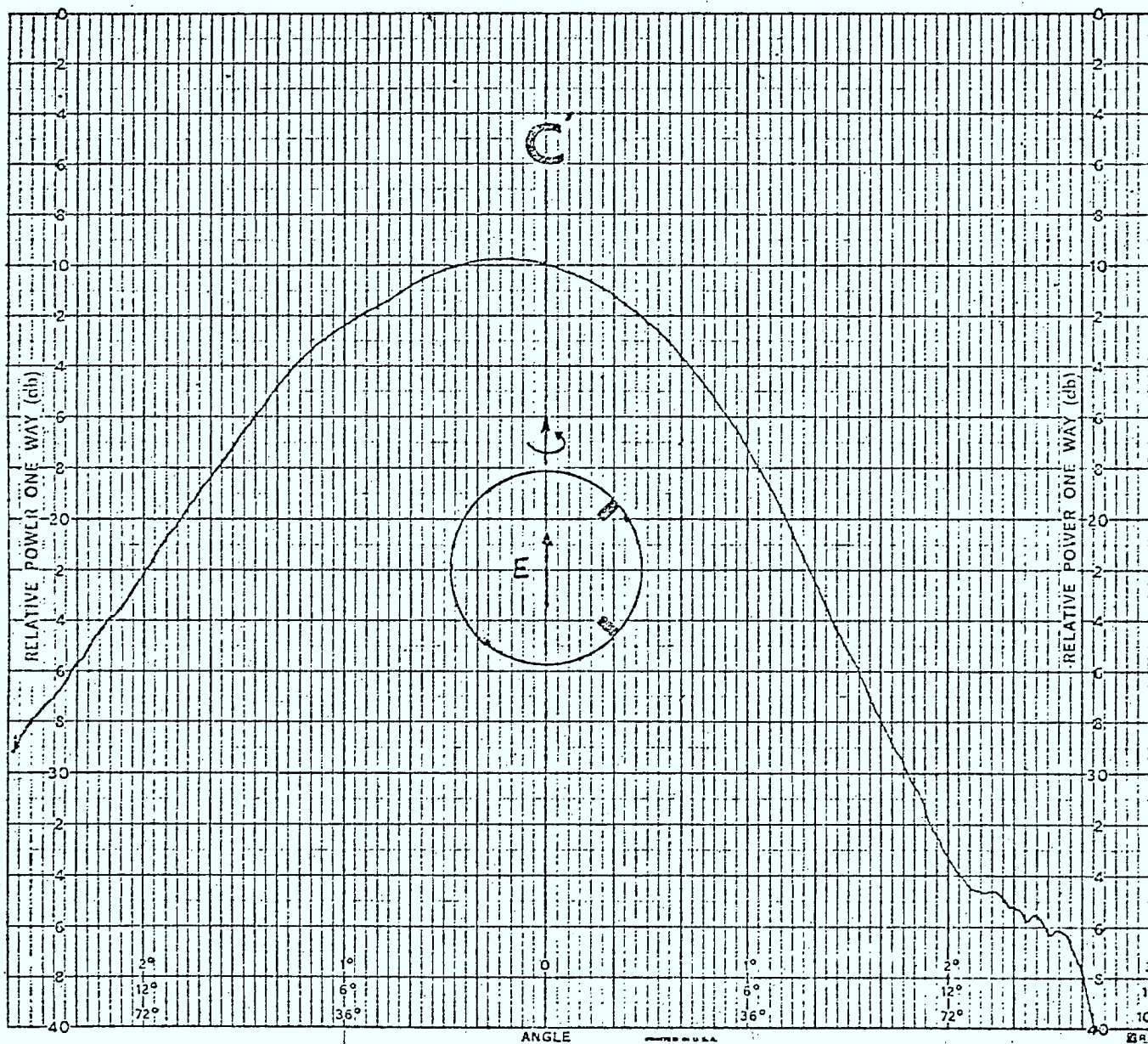
H-plane measurements for the previous obstruction when it is perpendicular to the main polarization. [Very slight asymmetry]



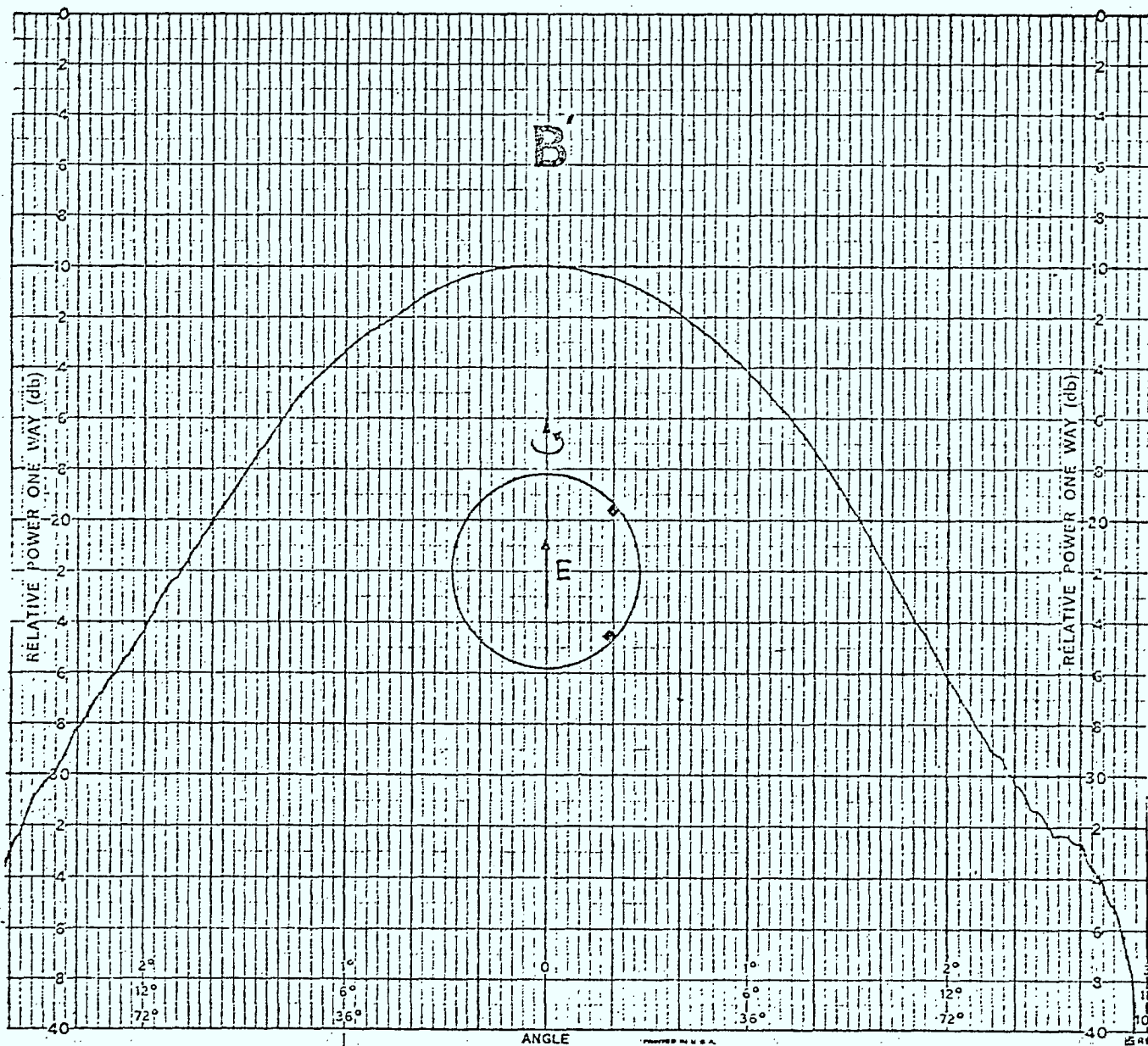
Asymmetry as a function of frequency for the same previous obstruction when it is perpendicular to the main polarization.



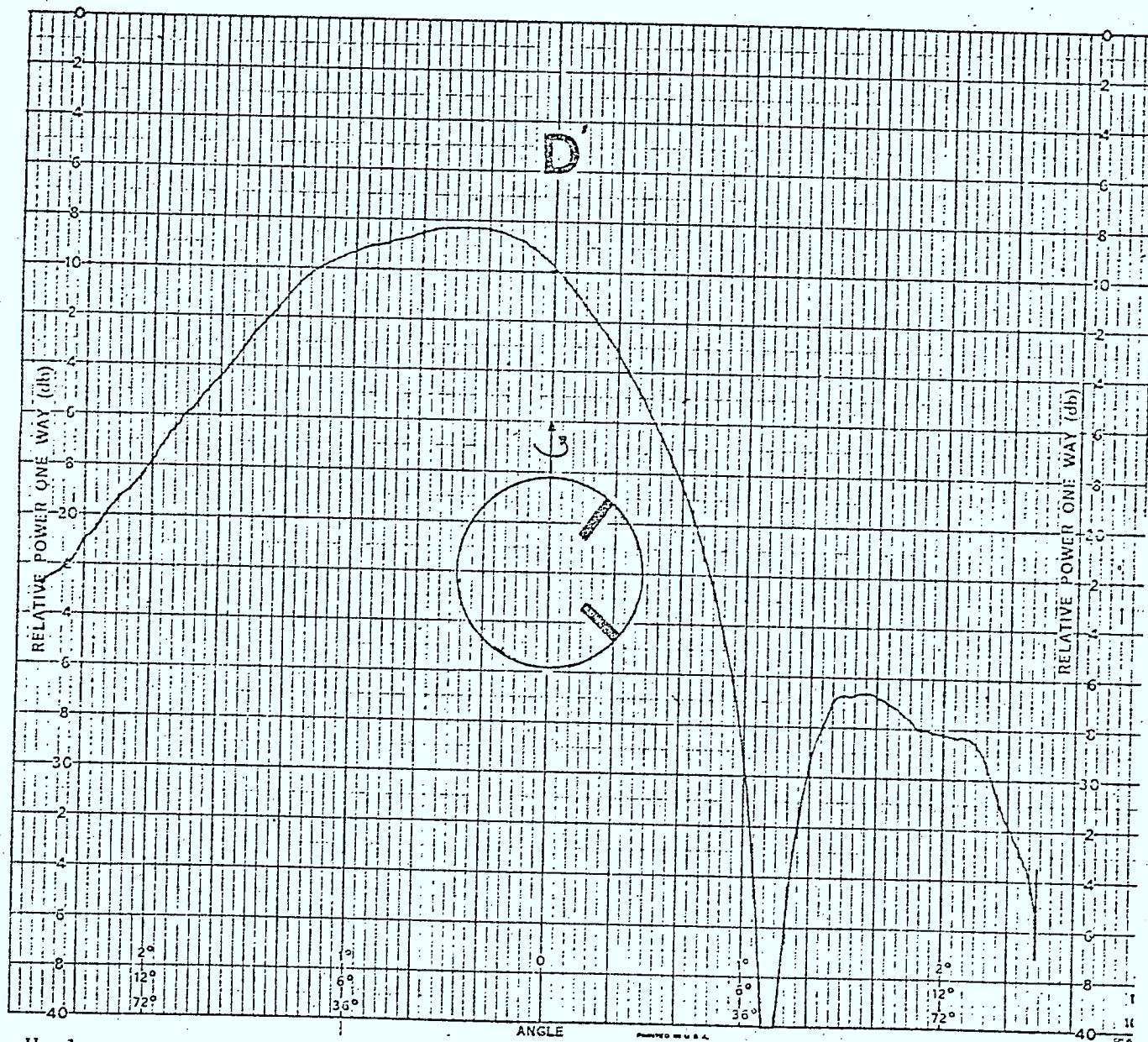
H-plane measurements of the feed in Fig. 4 with no obstruction in the guide



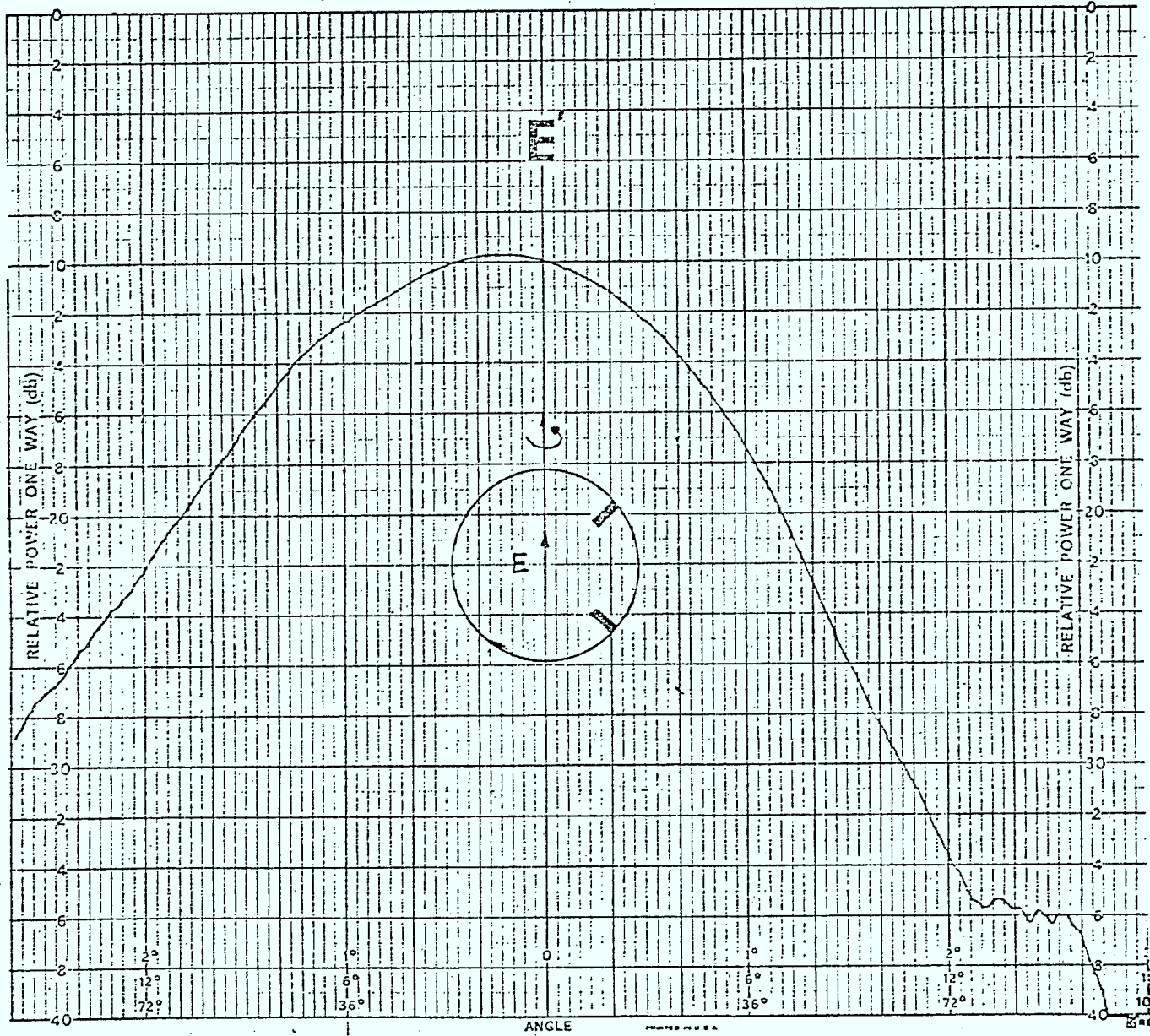
H-plane measurements with the two diagonal screws having about double the penetration of Fig. B'.



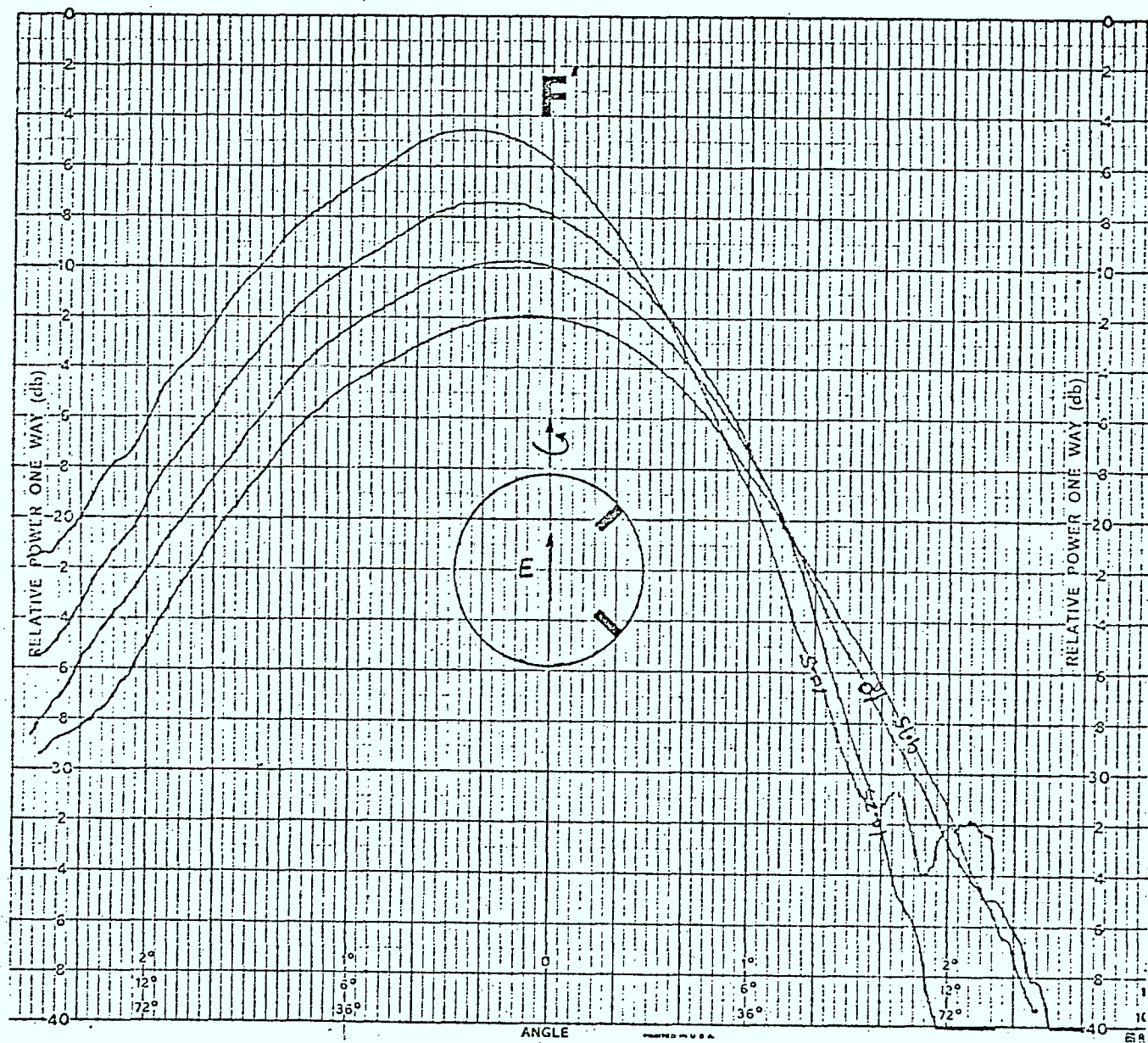
H-plane measurements with the two diagonal screws slightly protruding in the guide



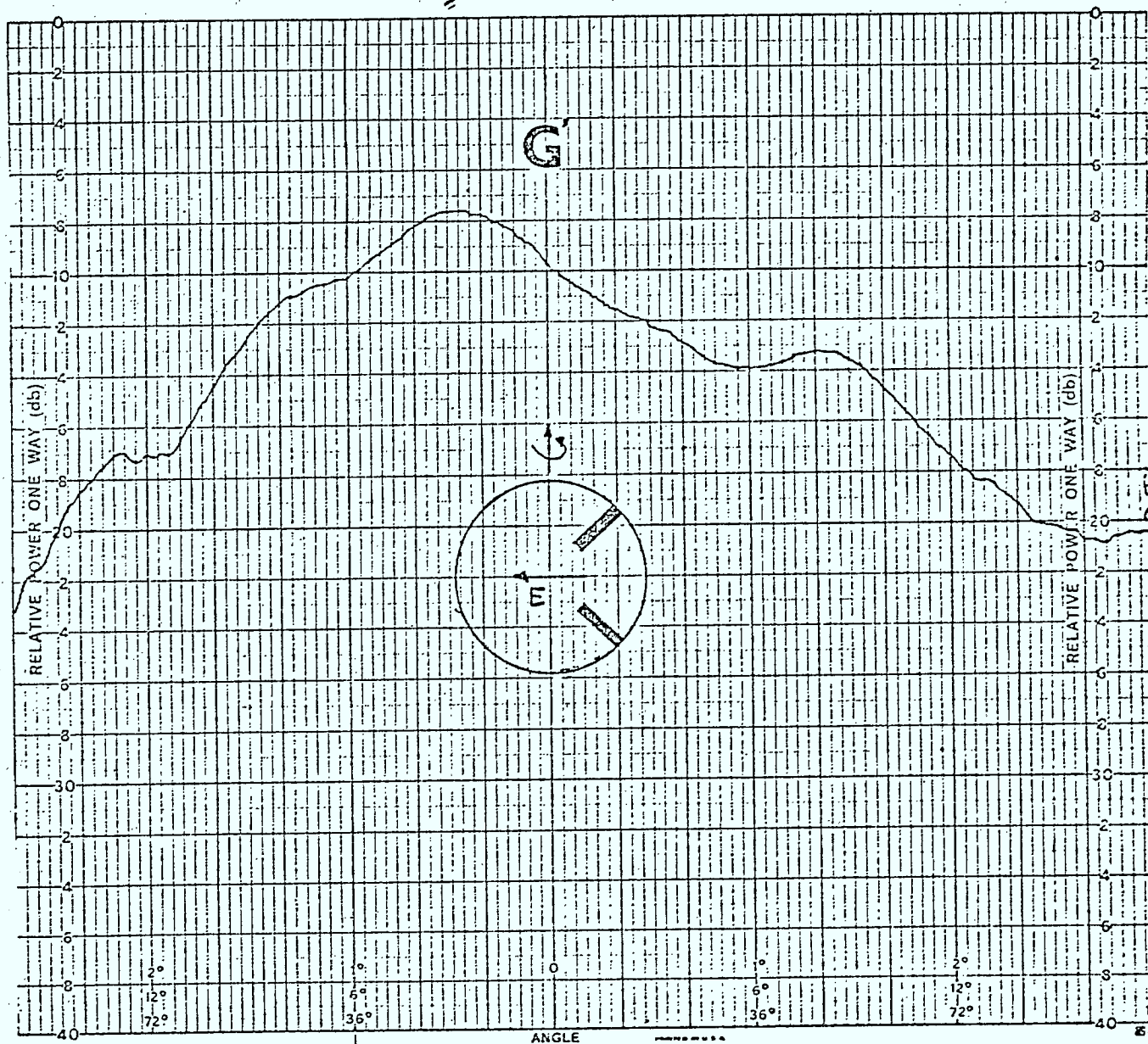
H-plane measurements with deep penetration of the two diagonal screws.



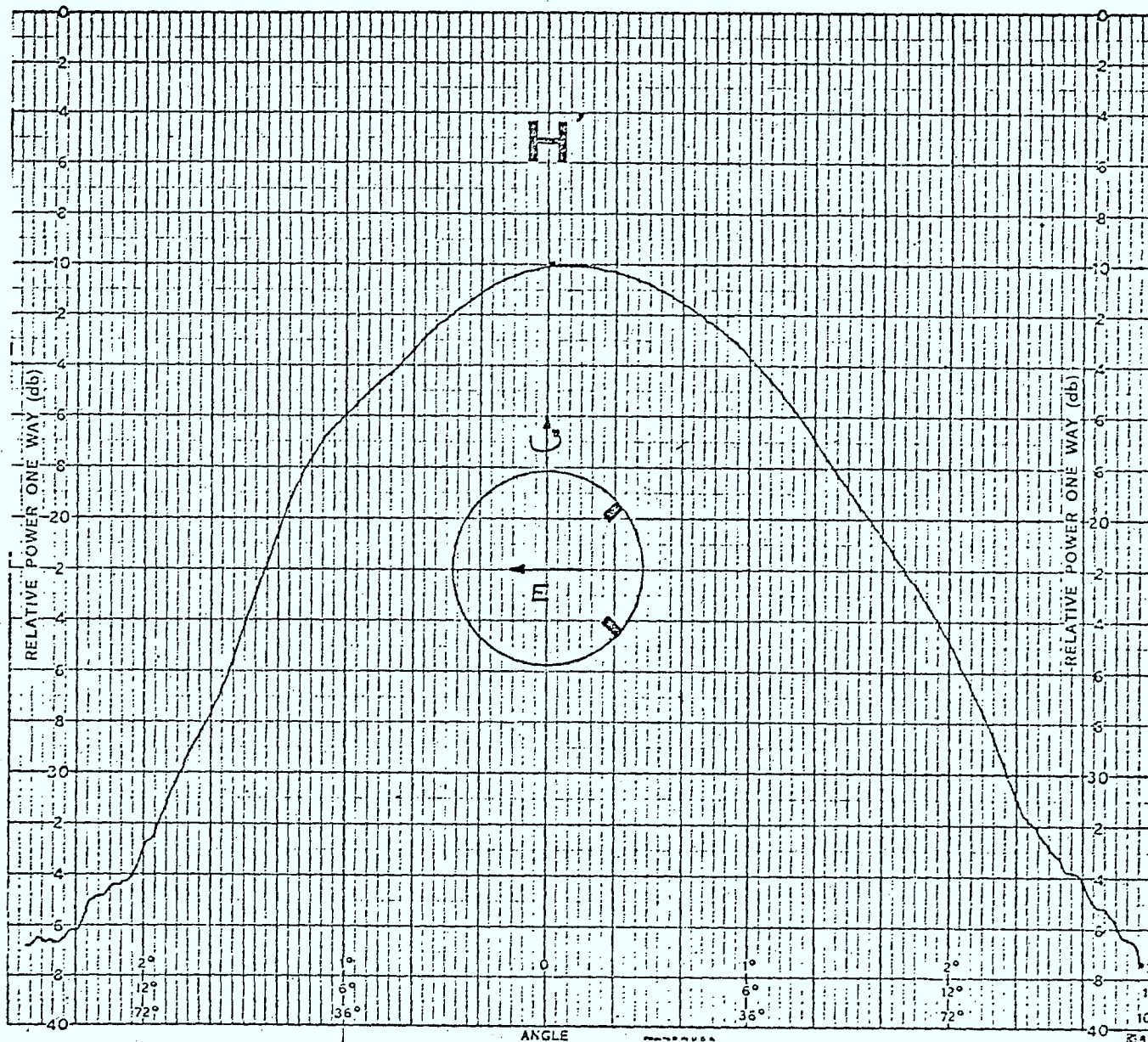
H-plane measurements with the two screws adjusted for asymmetry that corresponds to $\text{ALFA} = 0.2 - 0.25$.



Frequency dependence of the H-plane measurements for the case given in Fig. E'.



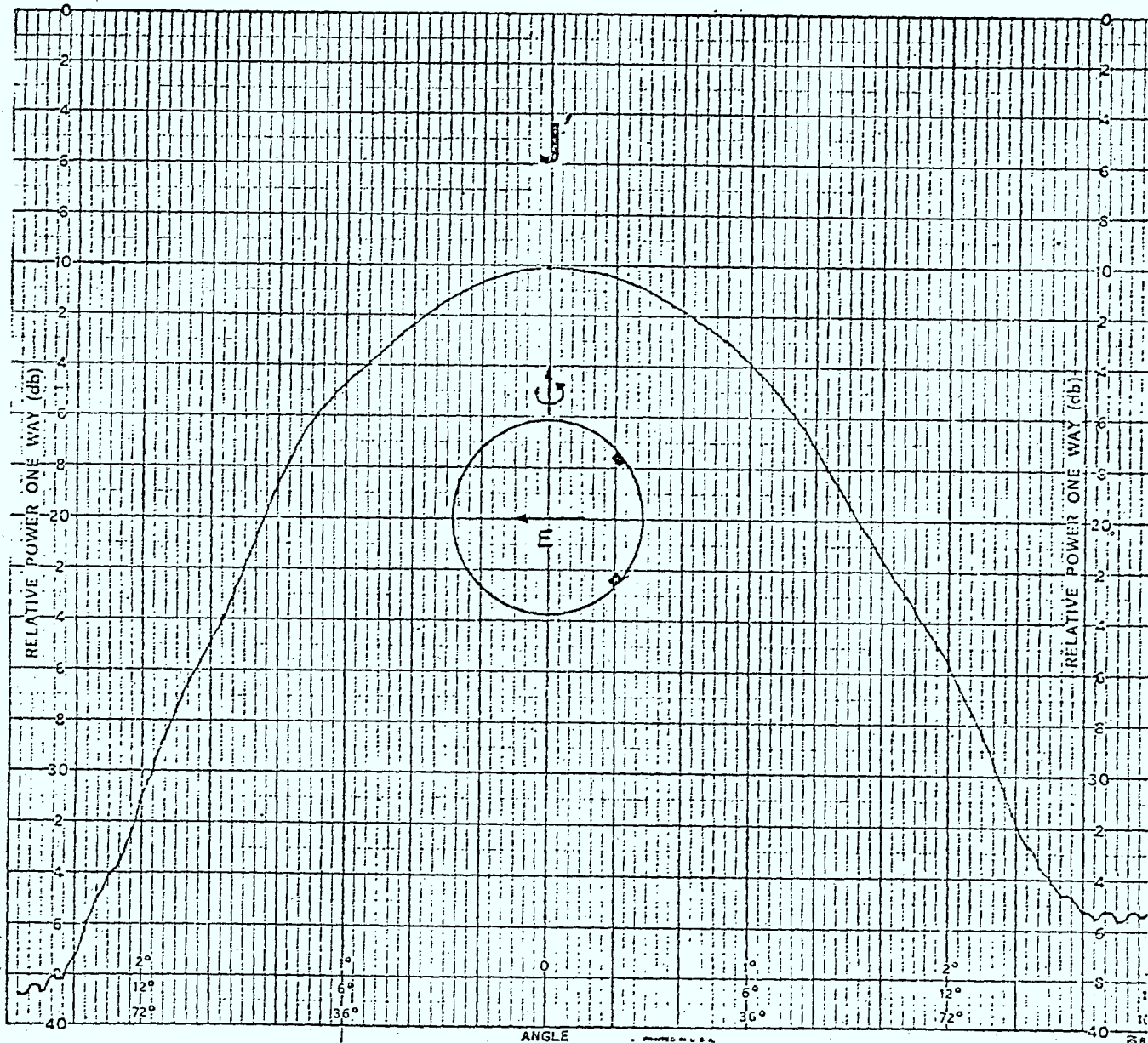
E-plane measurements for the diagonal screw with deep penetration and vertical polarization of the type of Fig. 2-a.



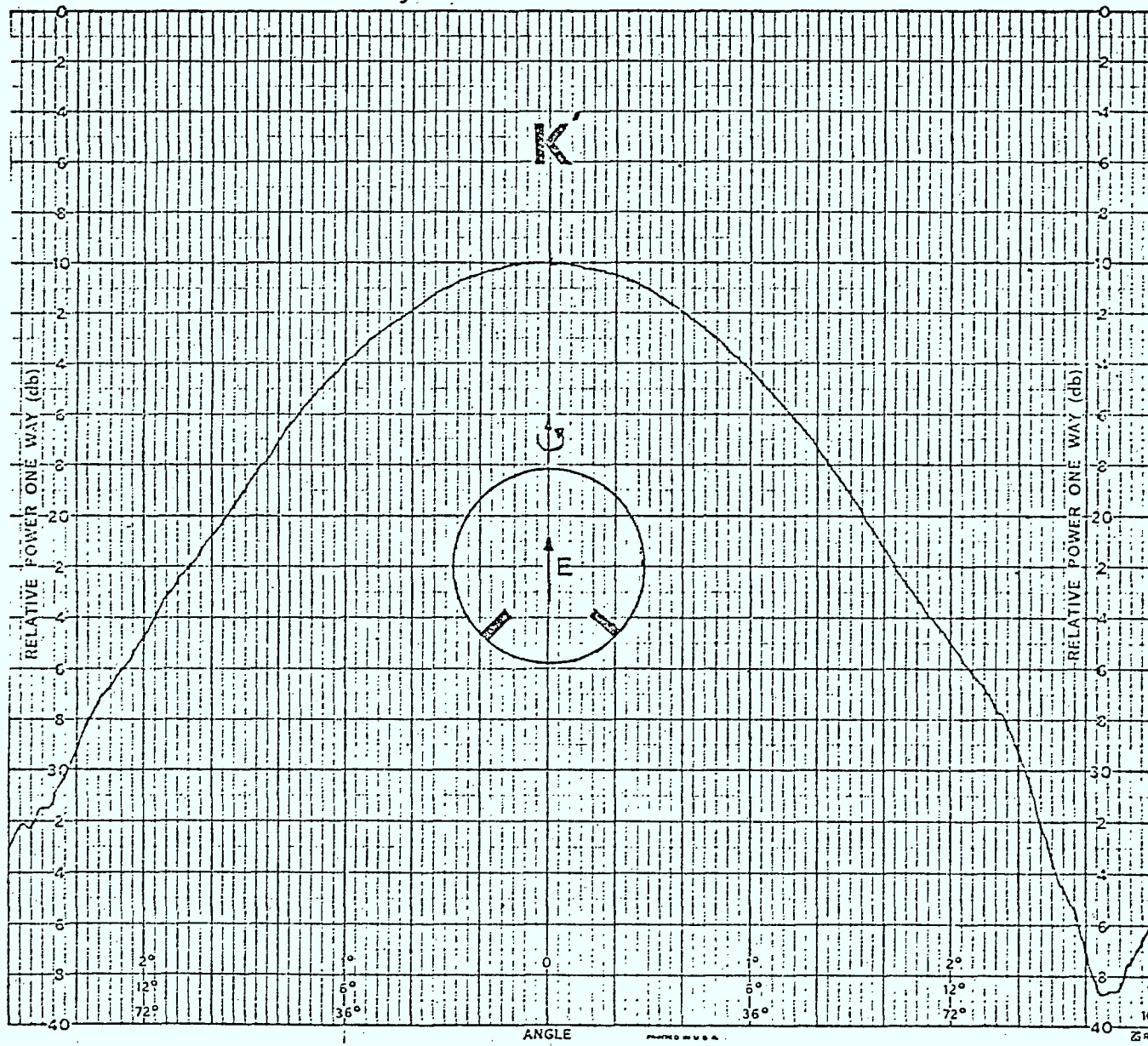
E-plane measurements for vertical polarization with varied positions of the two diagonal screws.



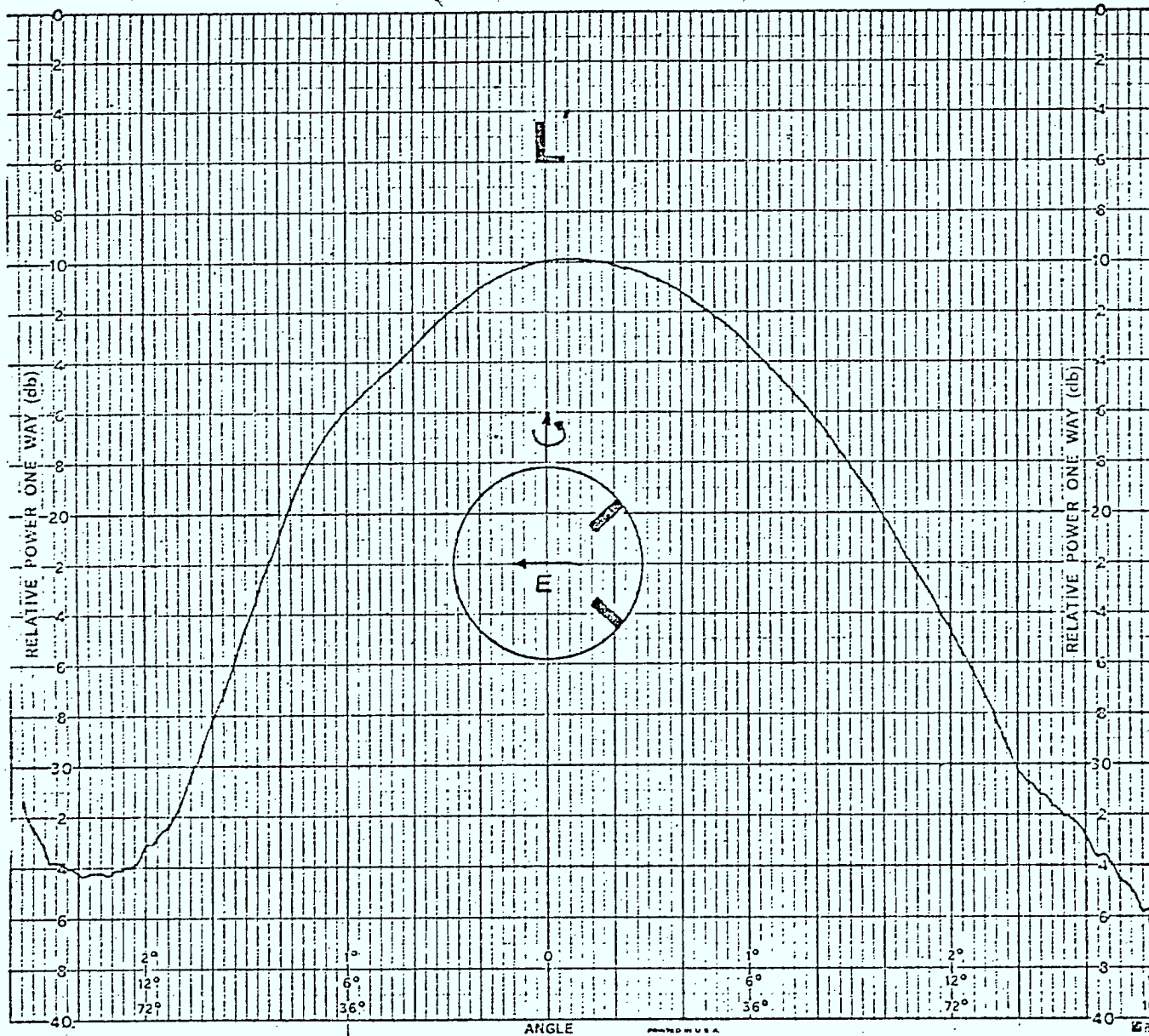
E-plane measurements for vertical polarization with the diagonal screws different from Fig. H'.



The same measurements as in Fig. 1' but different position for the diagonal screws.



H-plane measurements for the diagonal screws as used in conjunction with vertical polarization.



The corresponding E-plane measurements of the case of Fig. K'.

APPENDIXCOMPUTER PROGRAM FOR AN OFF-SET REFLECTORILLUMINATED BY A MATCHED FEEDPurpose:

This program computes the on-axis gain and the total directive gain pattern near the main axis of a front-Led paraboloid reflector of an off-set system that is illuminated with a matched primary-feed device.

Language:

WATFIV/FORTRAN IV

Author:

O. Aboul-Atta, Department of Electrical Engineering, Univeristy of Manitoba.

Description:

The on-axis antenna gain G_A is calculated according to

$$G_A = F \left(\frac{\pi d}{\lambda} \right)^2 \cot^2 \left(\frac{1}{2} \theta_c \right) \left| \int_0^{\theta_c} G^2(\theta') \tan \left(\frac{1}{2} \theta' \right) d\theta' \right|^2$$

where the factor F and feed gain function $G(\theta')$ are as defined in the report as well as the other parameters. The directive gain has been calculated for the vector radiation pattern according to the equation

$$g(\psi, \phi) = \left(\frac{1 + \cos \psi}{2} \right)^2 \left| \frac{1}{\lambda} \int_A \mathbf{E}_A \cdot \hat{\mathbf{R}} e^{jk\hat{\mathbf{r}} \cdot \hat{\mathbf{R}}} dA \right|^2$$

with the added access to the cross-polarization contribution to the total gain of the antenna.

Input Variables:

Eleven parameters are needed for the program to operate and are given in terms of only one data card (PHI, THETO, THETC, DLMDA, MKI,

MK2, MK3, DN, ALPHA, MM, M) which are defined in the comment statements documented at the beginning of the program (see program listing).

Output:

The existing output is a printout of the analytical primary feed with the desired mixing ratio of the compensating mode, the input data for checking, the output parameters which are ANTENNA GAIN, ANTENNA GAIN FACTOR, SPILL OVER POWER, APERTURE EFFICIENCY, and the TOTAL ANTENNA EFFICIENCY. Also a tabulation list of the relative radiation pattern of the antenna as well as the tabulation of the cross-polarization part of the radiation pattern, whenever it exists. A side output, that can be deleted if desired, is a punched card of these tabulations to be used with a plotter program listed after the main program in order to have a graphical display of the overall radiation pattern in the neighbourhood of the on-axis of the antenna.

\$JOB WATIV ABOLU-ATTA(MATCHED OFFSET ANTENNA)
 C-----PHI THE AZIMUTHAL ANGLE OF THE TOTAL RADIATION PATTERN OF THE
 C-----OFFSET ANTENNA SYSTEM.
 C-----EPSI THE POLAR ANGLE OF THE RADIATION PATTERN OF THE ANTENNA.
 C-----THETO THE ELEVATION ANGLE OF THE PRIMARY-FEED BORESIGHT AXIS.
 C-----THETC THE HALF ANGLE OF THE ILLUMINATION CONE.
 C-----FOVRD RATIO OF FOCAL DISTANCE TO THE DIAMETER OF THE ANTENNA.
 C-----DLMDA THE ANTENNA DIAMETER MEASURED IN WAVE LENGTH.
 C-----DN THE PRIMARY-FEED DIAMETER MEASURED IN WAVE LENGTH.
 C-----ALPHA RATIO OF THE COMPENSATING MODE TO THE FUNDAMENTAL FOR THE
 C-----MATCHED-FEED.
 C-----THTPR THE POLAR ANGLE OF THE PRIMARY-FEED RADIATION IN RADIANS.
 C-----MK1 IDENTIFY THE SPECIAL CASES OF PHI,C,PI/2, ELSE BY 1,2&3.
 C-----MK2 IDENTIFY THE LINEAR-POLARIZATION TO BE ONE FOR THE X'-AXIS
 C-----AND TWO FOR THE Y'-AXIS.
 C-----MK3 IDENTIFY THE CONVENTIONAL FEED BY ONE AND THE MATCHED-FEED
 C-----BY TWO.
 C-----PHIR, EPSIR, THTOR & THTCR ARE THE EQUIVALENT OF THE ABOVE ANGLES IN
 C-----RADIANS INSTEAD OF DEGREES.
 C-----MM AN INTEGER TO INDICATE THE RANGE OF EPSI TO BE CALCULATED
 C-----ACCORDING TO $EPSI = 0.05 * (102 * MM - 1)$ AND IS TO BE TAKEN AS 2
 C-----FOR THE FIRST TEN DEGREES.
 C-----M AN INTEGER TO BE TAKEN TO INDICATE THE NUMBER OF SUBDIVISI
 C-----ONS NEEDED FOR THE USE OF THE GAUSSIAN INTEGRATION OF 20
 C-----INTERVALS EACH, FOR THE NEAR AXIS CALCULATIONS IT IS TO BE
 C-----ONE.

1
 2
 3
 4
 5
 6
 7
 8
 9
 10
 11
 12
 13
 14
 15
 16
 17
 18
 19
 20
 21
 22
 23
 24
 25
 26
 27
 28
 29
 30
 31
 32
 33
 34
 35
 36
 37
 38
 39
 40
 41
 42
 43
 44
 45
 46
 47
 48
 49
 50
 51
 52
 53
 54
 55
 56
 57
 58
 59
 60
 61
 62
 63
 64
 65
 66
 67
 68
 69
 70
 71
 72
 73
 74
 75
 76
 77
 78
 79
 80
 81
 82
 83
 84
 85
 86
 87
 88
 89
 90
 91
 92
 93
 94
 95
 96
 97
 98
 99
 100

COMMON EPSIR, PHIR, THTOR, THTCR, FOVRD, DLMDA, PI, CR, CSTHC, SNTHO, CSTHC,
 SNTHC, CPSI, SNPSI, CSPHI, SNPHI, TWOKF, BETAN, ALFAN, MK1, MK2, MK3, ALPHA,
 DN, EI(361), HI(361), HII(361), HIII(361)
 DIMENSION GAINF(1000), PINOB(1000), CPOLR(1000), XPOLR(1000)
 COMPLEX A, B, CEXP, CMLPX, PISIN, QISIN, INTEG
 EXTERNAL PISIN, QISIN
 READ, PHI, THETO, THETC, DLMDA, MK1, MK2, MK3, DN, ALPHA, MM, M
 PRINT, ALPHA
 MMM = 102 * MM
 PI = 3.14159265
 CR = PI / 180.
 THTOR = THETO * CR
 THTCR = THETC * CR
 PHIR = PHI * CR
 SNTHO = SIN(THTOR)
 CSTHO = COS(THTOR)
 SNTHC = SIN(THTCR)
 CSTHC = COS(THTCR)
 SNPHI = SIN(PHIR)
 CSPHI = COS(PHIR)
 FOVRD = (CSTHC + CSTHC) / (4. * SNTHC)
 FLMDA = FOVRD * DLMDA
 TWOKF = 4. * PI * FLMDA
 CALL FKTR(FKT, SPILL, ANTG, GKTR, APEFF, ANTEF)
 SUBDS = .05 * CK
 DO 3 I = 1, MMM
 EPSIR = SUBDS * (I - 1)
 SNPSI = SIN(EPSIR)
 CPSI = COS(EPSIR)
 C = (1. + CPSI) ** 2
 ALFAN = TWOKF * SNPSI
 BETAN = TWOKF * SNPSI * CSPHI * SNTHO
 IF (PHIR .EQ. 0.) GO TO 1
 B = INTEG(0., THTCR, M, QISIN)
 GO TO 2
 A = (0., 0.)
 B = INTEG(0., THTCR, M, PISIN)
 CPOLR(I) = C * CABS(A * 1) / FKT
 XPOLR(I) = C * CABS(B * 3) / FKT
 GAINF(I) = CPOLR(I) + XPOLR(I)

```

39 DO 4 I=1,MMM
40 RATIO =CPOLE(I)/GAINF(I)
41 IF (RATIO.LT.1.E-10) RATIO=1.0E-10
42 CPOLR(I)=10.*ALOG10(RATIO)
43 RATIO =XPOLR(I)/GAINF(I)
44 IF (RATIO.LT.1.E-10) RATIO=1.0E-10
45 XPOLR(I)=10.*ALOG10(RATIO)
46 RATIO =GAINF(I)/GAINF(1)
47 IF (RATIO.LT.1.E-10) RATIO=1.0E-10
48 PINDB(I)=10.*ALOG10(RATIO)
49 4 FORMAT('1',//////////T2,'ANGLE RAD. PATTERN ANGLE
50 5 RAC. PATTERN ANGLE RAC. PATTERN')
51 6 FORMAT(' ',T2,'-----')
52 7 FORMAT(' ',F5.2,' ',F8.3,' *****',F5.2,' ',F8.3,' ****')
53 8 *',F5.2,' ',F8.3)
54 9 FORMAT('1',//////////T23,'*****')
55 10 FORMAT(' ',T23,'OFFSET REFLECTOR ANTENNA')
56 11 FORMAT(' ',T23,'*****')
57 12 FORMAT(' ',T11,'INPUT DATA')
58 13 FORMAT(' ',T11,'-----')
59 14 FORMAT(' ',T11,'OUTPUT DATA')
60 15 FORMAT(' ',T11,'-----')
61 16 FORMAT(' ',T11,'REFLECTOR DIAMETER IN WAVE LENGTH =',F6.2,' LAM
62 17 'DA')
63 17 FORMAT(' ',T11,'THE FOCAL DISTANCE IN WAVE LENGTH =',F6.2,' LAM
64 18 'DA')
65 18 FORMAT(' ',T11,'THE OFFSET ANGLE, THETA =',F6.2,' DEGRE
66 19 'ES')
67 19 FORMAT(' ',T11,'THE HALF ANGLE OF ILLUMINATION =',F6.2,' DEGRE
68 20 'ES')
69 20 FORMAT(' ',T11,'ANTENNA GAIN IN DECIBELS =',F6.3,' D
70 21 'BS')
71 21 FORMAT(' ',T11,'ANTENNA GAIN FACTOR =',F6.3,' RAT
72 22 'IO')
73 22 FORMAT(' ',T11,'THE SPILL OVER POWER IN PERCENT =',F6.3,'
74 23 'Z')
75 23 FORMAT(' ',T11,'THE APERTURE EFFICIENCY =',F6.3,'
76 24 'Z')
77 24 FORMAT('1',//////////T12,'ANGLE E1-PATTERN H1-PATTERN E2-PATTERN
78 25 'H2-PATTERN')
79 25 FORMAT(' ',T12,'-----')
80 26 FORMAT(' ',T12,F4.1,T20,F8.5,T32,F8.5,T44,F8.5,T56,F8.5)
81 DO 27 I=1,4
82 PRINT24
83 PRINT25
84 PRINT25
85 DO 27 J=1,45
86 K =J+(I-1)*45
87 ANGLE =0.5*(K-1)
88 VV1 =E1(K)
89 VV2 =H1(K)
90 VV3 =E11(K)
91 VV4 =H11(K)
92 27 WRITE(6,26)ANGLE,VV1,VV2,VV3,VV4
93 PRINT8
94 PRINT9
95 PRINT10
96 PRINT11
97 PRINT12
98 IF (MK2.EQ.1) PRINT34
99 IF (MK2.EQ.2) PRINT35
100 WRITE(6,15)CLMDA

```

```

91 WRITE(6,16) FLMDA
92 WRITE(6,17) THETAO
93 WRITE(6,18) THETC
94 WRITE(6,23) PHI
95 PRINT13
96 PRINT14
97 WRITE(6,19) ANTG
98 WRITE(6,20) GFKTR
99 WRITE(6,21) SPILL
100 WRITE(6,22) APEFF
101 WRITE(6,36) ANTEF
102 DO 28 I=1,MM
103 JBEG =1+102*(I-1)
104 JEND =JBEG+33
105 PRINT5
106 PRINT6
107 PRINT6
108 DO 28 J=JBEG,JEND
109 THT1 =0.05*(J-1)
110 THT2 =THT1+1.7
111 THT3 =THT1+3.4
112 JA =J
113 JB =JA+34
114 JC =JB+34
115 28 WRITE(6,7) THT1, PINDR(JA), THT2, PINDR(JB), THT3, PINDR(JC)
116 FORMAT(bF10.4)
117 30 FORMAT(F7.3)
118 PUNCH30,ANTG
119 DO 31 I=1,MMM,6
120 JBEG =I
121 JEND =JBEG+5
122 31 PUNCH29,(PINDR(K),K=JBEG,JEND)
123 IF (MK1.NE.2) GO TO 39
124 DO 32 I=1,MMM,6
125 JBEG =I
126 JEND =JBEG+5
127 32 PUNCH29,(XPCLR(K),K=JBEG,JEND)
128 CONTINUE
129 34 FORMAT(' ',T11,'LINEAR POLARIZATION IS IN THE PLANE OF SYMMETRY')
130 35 FORMAT(' ',T11,'POLARIZATION IS ORTHOGONAL TO PLANE OF SYMMETRY')
131 36 FORMAT(' ',T11,'THE TOTAL ANTENNA EFFICIENCY =',F6.3,'
7.1)
132 37 FORMAT('1',//////////T2,'ANGLE X-POLARIZATION ANGLE X
-POLARIZATION ANGLE X-POLARIZATION')
133 DO 38 I=1,MM
134 JBEG =1+102*(I-1)
135 JEND =JBEG+33
136 PRINT37
137 PRINT6
138 PRINT6
139 DO 38 J=JBEG,JEND
140 THT1 =0.05*(J-1)
141 THT2 =THT1+1.7
142 THT3 =THT1+3.4
143 JA =J
144 JB =JA+34
145 JC =JB+34
146 38 WRITE(6,7) THT1,XPCLR(JA),THT2,XPCLR(JB),THT3,XPCLR(JC)
147 39 RETURN
148 END

149 COMPLEX FUNCTION PISIN(THTPR)
150 COMPLEX S,CM,CMPLX,CEXP
151 COMMON EPSIP,PHIR,THTOR,THTCR,FOVRD,CLMDA,PI,CR,CSTFC,SNTHO,CSTHC,
SNTHC,CSPSI,SNPSI,CSPHI,SNPHI,TWQKF,BETAN,ALFAN,MK1,MK2,MK3,ALPHA,
DN,EI(361),HI(361),EI(361),HI(361)

```

```

152 SNTHP =SIN(THTPR)
153 CSTHP =COS(THTPR)
154 S = (0.,1.)
155 A =1.+CSTHP*CSTHO
156 B =SNTHP*SNTHO
157 C =CSTHP+CSTHO
158 AA =A*A
159 BB =B*B
160 CC =C*C
161 CCC =CC*C
162 D =CC*B/2.
163 F =1A-BB*(CSPHI**2)
164 ALFA =ALFAN*SNTHP/C
165 BETA =BETAN/C
166 CALL PERPT(THTPR, DN, ALPHA, E1, H1, E2, H2)
167 CALL BESSL( ALFA, BJJ, BJ1)
168 BJ2 =0.
169 BJ3 =0.
170 BJ4 =0.
171 BJ5 =0.
172 IF (ALFA.LT.1.0E-12) GO TO 0
173 RJZ =2./ALFA*BJ1-BJ0
174 BJ3 =4./ALFA*BJ2-BJ1
175 BJ4 =6.*BJ3/ALFA-BJ2
176 BJ5 =8.*BJ4/ALFA-BJ3.
177 0 CONTINUE
178 X1 =E1
179 Y1 =H1
180 X2 =E2
181 Y2 =H2
182 IF (MK2.EQ.1) GO TO 1
183 X1 =H1
184 Y1 =E1
185 X2 =H2
186 Y2 =E2
187 1 XX =A*Y1+C*X1
188 YY =A*X1-C*Y1
189 CO =CCC*XX
190 C1 =O*YY
191 C2 =CCC*YY
192 C3 =C1
193 CON =-2.*PI*FOVRD*DLMDA*SNTHP/(CCC*F)
194 IF (MK3.EQ.2) GO TO 6
195 IF (MK1-2)2,3,4
196 2 X =CO*BJ0+C2*BJ2
197 Y =C.*BJ1+C3*BJ3
198 GO TO 5
199 3 X =CO*BJC-C2*BJ2
200 Y =0.
201 GO TO 5
202 4 X =CO*BJ0+C2*BJ2*COS(2.*PHIR)
203 Y =C1*BJ.*CSPHI+C3*BJ3*COS(3.*PHIR)
204 5 CMPLX(X,Y)
205 PISIN =CON*CM*CEXP(S*(BETA-TWOKF))
206 RETURN
207 6 Z = (6.*AA*AA-7.*AA*BB+4.*BB*BB)/F
208 CO = (4.*AA-Z)*(A*B/2.)*X2+(4.*(AA+CC)-Z)*(B*C/2.)*Y2
209 Z =AA+3.*CC-(6.*AA*BB-7.*AA*BB+2.*BB*BB)
210 C1 = (BB*(6.*CC+BB)/2.+AA*Z/2.)*X2+A*C/2.*(AA+3.*CC+Z)*Y2
211 Z =BB-(CC*CC-(A*BB)/F)
212 C2 =C2+2.*A*BB*(CC-Z)*X2+2.*B*C*Z*Y2
213 Z =2.*BB+(4.*AA*AA-12.*AA*BB+12.*BB*BB)/(2.*F)
214 C3 =C3-(BB*CC/2.+AA*Z/2.)*X2+A*C/2.*Z*Y2
215 C4 = (AA*BB*(BB-2.*CC)/2.*F)*(A*X2-C*Y2)
216 C5 = (A*AA/(4.*F))*(A*X2-C*Y2)
217 IF (MK1-2)7,8,9.

```

```

218 7 X =C0*BJ0+C2*BJ2+C4*BJ4
219 Y =C1*BJ1+C3*BJ3+C5*BJ5
220 GO TO 10
221 8 X =C0*BJ0-C2*BJ2+C4*BJ4
222 Y =0.
223 GO TO 10
224 9 X =C0*BJ0+C2*BJ2*CCS(2.*PHIR)+C4*BJ4*CCS(4.*PHIR)
225 Y =C1*BJ1+C3*SPHI+C3*BJ3*CCS(3.*PHIR)+C5*BJ5*CCS(5.*PHIR)
226 10 CH =CMPLX(X,Y)
227 PISIN =CON*CM*CEXP(S*(BETA-TWOKF))
228 RETURN
229 END

230 COMPLEX FUNCTION QISIN(THTPR)
231 COMPLEX S,CM,CMPLX,CEXP
232 COMMON EPSIF,PHIR,THTOR,THTCR,FQVRD,DLMDA,PI,CR,CSTHC,SNTHO,CSTHC,
SNTHC,CSPSI,SNPSI,CSPHI,SNPHI,TWOKF,BETAN,ALFAN,MK1,MK2,MK3,ALPHA,
DN,EI(361),HI(361),II(361),HII(361)
= (0.,1.)
S = SIN(THTPR)
SNTHP = COS(THTPR)
CSTHP = 1.+CSTHP*CSTHO
A = SNTHP*SNTHO
B = CSTHP+CSTHO
AA = A*A
BB = B*B
CC = C*C
CCC = CC*C
C = CC*B/2.
F = AA-BB*(CSPHI**2)
ALFA = ALFAN*SNTHP/C
BETA = BETAN/C
CALL PERPT(THTPR,DN,ALPHA,E1,H1,E2,H2)
CALL BESSL( ALFA,BJ0,BJ1)
BJ2 = 0.
BJ3 = 0.
BJ4 = 0.
BJ5 = 0.
IF (ALFA.LT.1.0E-12) GO TO 0
BJ2 = 2./ALFA*BJ1-BJ1
BJ3 = 4./ALFA*BJ2-BJ1
BJ4 = 6.*BJ3/ALFA-BJ2
BJ5 = 8.*BJ4/ALFA-BJ3
0 CONTINUE
X1 = E1
Y1 = H1
X2 = E2
Y2 = H2
IF (MK2.EQ.1) GO TO 1
X1 = H1
Y1 = E1
X2 = H2
Y2 = E2
1 XX = 3.*A*X1+C*Y1
YY = A*Y1-C*X1
ZZ = A*X1-C*Y1
S1 = B*XX/2.
S2 = C*YY
S3 = B*ZZ/2.
CON = -2.*PI*FQVRD*DLMDA*SNTHP/(C*F)
IF (MK3.EQ.2) GO TO 6
IF (MK1-2)2,3,4
2 X = 0.
Y = 0.
GO TO 5
3 X = 0.

```

```

281 Y =S1*BJ1-S3*BJ3
282 GO TO 5
283 X =S2*BJ2*SIN(2.*PHIR)
284 Y =S1*BJ1*SINPHI+S3*BJ3*SIN(3.*PHIR)
285 5 CM =CMPLX(X,Y)
286 OPISIN =CON*CM*CEXP(S*(BETA-TWOKF))
287 RETURN
288 6 Z =(.6.*AA+BB)/(2.*F)
289 S1 =S1-4.*A+C*(1.-Z/4.)*Y2+(.5*(3.*AA+CC)-CC+Z)*X2
290 S2 =S2-2.*B*C*(1.-4A/F)*Y2+AVC/F*X2
291 Z =(.3.*AA+CC)/(4.*F)
292 S3 =S3+2.*C*Z*Y2+(BB/2.-CC*Z)*X2
293 S4 =S4+A*B*C/F*(A*Y2-C*X2)
294 S5 =S5-B*B*C/F*(A*Y2-C*X2)/4.
295 IF (MK1-2)7,8,9
296 X =0.
297 Y =0.
298 GO TO 10
299 8 X =0.
300 Y =S1*BJ1-S3*BJ3+S5*BJ5
301 GO TO 10
302 9 X =S2*BJ2*SIN(3.*PHIR)+S4*BJ4*SIN(4.*PHIR)
303 Y =S1*BJ1*SINPHI+S3*BJ3*SIN(3.*PHIR)+S5*BJ5*SIN(5.*PHIR)
304 10 CM =CMPLX(X,Y)
305 OPISIN =CON*CM*CEXP(S*(BETA-TWOKF))
306 RETURN
307 END

308 SUBROUTINE BESSL(ALFA,BJO,BJ1)
309 REAL*8 POLY(4),LAMBDA(20),A(4,7)/-.78539816,.79789456,-2.35619449,
.79789456,-4.1663970-2,-7.70-7,1.24990120-1,1.566-6,-3.9540-5,-5.5
.2740-3,5.650-5,1.6576670-2,2.625730-3,-9.5120-5,-6.378750-3,1.7105
.0-4,-3.41250-4,1.372370-3,7.43480-4,-2.495110-3,-2.93330-4,-7.2805
.0-4,-7.98240-4,1.136530-3,1.35580-4,1.44760-4,-2.91660-4,-2.00330-4
./,Y,VR
SOLFA =SQRT(ALFA)
IF (ALFA.LT.2.0) GO TO 2
VF =3./ALFA
DO 1 I=1,4
POLY(I) =A(I,6)+A(I,7)*VF
DO 1 J=1,5
POLY(I) =POLY(I)+VR+A(I,6-J)
CS1 =POLY(1)+ALFA
CS2 =POLY(2)+ALFA
CS3 =POLY(3)+ALFA
BJ0 =POLY(4)*COS(CS1)/SOLFA
BJ1 =POLY(4)*COS(CS3)/SOLFA
GO TO 3
2 Y =ALFA/3.0)**2
BJ0 =1.+Y*(-2.249997+Y*(1.2656208+Y*(-.3163866+Y*(.0444479+Y*
(-.00394444+Y*.00021))))))
BJ1 =ALFA*(.5+Y*(-.56249985+Y*(.21093573+Y*(-.03954289+Y*(.004
.43319+Y*(-.00021761+Y*.0001109))))))
3 RETURN
END

327 COMPLEX FUNCT(ON INTEG(B,E,M,FUNKT)
328 COMPLEX Z,ZZ,SUM,FUNKT
329 REAL*8 X(20),n(20)
330 DATA X/,387724180-1,.11608407,.19269758,.26815215,C.34199409,
.41277920,.48307530,.54945713,.61255359,.67195668,
.72731826,.77830586,.82461223,.86395950,.90205881,
.93231281,.95791682,.97725993,.99073624,.99823771,
DATA W/,775059480-1,.770398160-1,.761103620-1,.747221690-1,
.728865820-1,.70616470-1,.679120460-1,.643040130-1,
.613062420-1,.574397690-1,.532278470-1,.486958080-1,
.438709080-1,.387821680-1,.334601950-1,.275370070-1,

```

```

332      ,22245349D-1,.16421058D-1,.10498285D-1,.45212771C-2/
333      SUM      =(0.,0.)
334      D        =(E-B)/M
335      DD 1     I=1,M
336      BI      =B+(I-1)*D
337      BI      =BI+E
338      C        =(E1-BI)/2.
339      CC      =(E1+BI)/2.
340      CD 1     J=1,20
341      Y        =CC+C*X(J)
342      YY       =CC-C*X(J)
343      Z        =FUNKT(Y)
344      ZZ       =FUNKT(YY)
345      SUM      =SUM+C*W(J)*(Z+ZZ)
346      INTEG
347      RETURN
348      ENO
349
350      SUBROUTINE PFRPT(THTPR, DN, ALFA, E1, H1, E2, H2)
351      PI      =3.14159265
352      U        =PI*DN*SIN(THTPR)
353      IF (U.GT.0.001) GO TO 1
354      E1       =1.
355      H1       =1.
356      E2       =0.
357      H2       =0.
358      GO TO 2
359      1
360      F        =1.+COS(THTPR)
361      A1       =1.-(U/1.841)**2
362      A2       =1.-(U/3.0541)**2
363      CALL BESSEL(U, BJO, BJ1)
364      X1       =BJ1/U
365      Y1       =BJ0-X1
366      BJ2      =2.*X1-BJO
367      E1       =F*X1
368      H1       =F*Y1/A1
369      X2       =2.*BJ2/U
370      Y2       =BJ1-X2
371      E2       =ALFA*F*X2
372      H2       =ALFA*F*Y2/A2
373      RETURN
374      ENO
375
376      SUBROUTINE FKTR(SFKT, SPILL, ANTG, GFKTR, APEFF, ANTEF)
377      COMMON EPSIP, PHIR, THTOP, THTKR, FOVRD, DLMDA, PI, CR, CS1, C, SNTHO, CSTHC,
378      SNTHC, CSPSI, SNPSI, CSPHI, SNPHI, THCKF, BETAN, ALFAN, MK1, MK2, MK3, ALPHA,
379      DN, EI(361), HI(361), EII(361), HII(361)
380      DIMENSION SP(361), SM(361)
381      FLMDA   =FOVRD*DLMDA
382      CD 1     I=1,361
383      THTPR   =0.5*CR*(I-1)
384      SNTHP   =SIN(THTPR)
385      CSTHP   =COS(THTPR)
386      BS      =SNTHP*SNTHO
387      APLSC   =(1.+CSTHO)*(1.+CSTHP)
388      CALL PFRPT(THTPR, DN, ALFA, A, B, C, D)
389      EI(I)   =A
390      HI(I)   =B
391      EII(I)  =C
392      HII(I)  =D
393      SM(I)   =((A+B)+2.*BS*(C+D)/APLSC)*SNTHP/APLSC
394      SM(I)   =(A*A+B*B+C*C+D*D)*SNTHP
395      FKTR    =0.
396      ANTG    =0.
397      DD 2     I=2,360,2
398      FKTR    =FKTR+SM(I-1)+4.*SM(I)+SM(I+1)

```

```

393 THETC =THTCR*180./PI
394 I =THETC
395 DELTA =THETC-I
396 J =2*I
397 CAPT =0.
398 DO 3 K=2,J,2
399 ANTG =ANTG+SMM(K-1)+4.*SMM(K)+SMM(K+1)
400 3 CAPT =CAPT+SM(K-1)+4.*SM(K)+SM(K+1)
401 AUX =SM(J+1)+4.*SM(J+2)+SM(J+3)
402 CDRF =SMV(J+1)+4.*SMV(J+2)+SMV(J+3)
403 CAPT =CAPT+DELTA*AUX
404 ANTG =(ANTG+DELTA*CDRF)*CR/6.
405 CAPEF =CAPT/FKT
406 FKT =CR*FKT/6.
407 ANTG =((8.*PI*FL*DA*ANTG)**2)/FKT
408 GFKTR =ANTG/((PI*DL*DA)**2)
409 ANTG =10.*ALOGLO(ANTG)
410 SPILL =(1.-CAPEF)*100.
411 APEFF =GFKTR/CAPEF*100.
412 ANTEF =GFKTR*100.
413 RETURN
414 END

```

ENTRY

PLOT PROGRAM

UNIVERSITY OF MANITOBA COMPUTER CENTER ***

DATE= 2/22/78 TIME=11:17 AM

```
//STEP1 EXEC FORTHCLG,USERLIB='SYS2.VPLOTLIB'.SIZE=256K
//FOPR.SYSIN DD *
```

```
DIMENSION IBUF(6000),X(203),Y1(203),Y2(203),Y3(203)
DATA ANGINC,NO/0.05,201/
```

```
1 FORMAT (F7.3)
2 FORMAT (6F10.4)
5 FORMAT (6(2X,F10.4))
7 FORMAT (' .....*****.....')

READ 1,ANTG
READ 2,Y1
PRINT 5, Y1
PRINT 7
READ 2,Y2
PRINT 5, Y2
PRINT 7
READ 2,Y3
PRINT 5, Y3
PRINT 7

DO 3 I= 1,NO
3 X(I)= (I-1)*ANGINC
DO 4 I= 1,NO
IF (Y1(I).LT.-50.0) Y1(I)= -50.0
IF (Y2(I).LT.-50.0) Y2(I)= -50.0
IF (Y3(I).LT.-50.0) Y3(I)= -50.0
4 CONTINUE
Y1(NP+1)= -50.0
Y2(NP+1)= -50.0
Y3(NP+1)= -50.0
Y1(NP+2)= 5.0
Y2(NP+2)= 5.0
Y3(NP+2)= 5.0
X(NP+1)= 0.0
X(NP+2)= 1.0
CALL PLOTS (IBUF,6000)
CALL PLOT (0.0,-11.0,23)
CALL PLOT(3.0,2.0,-3)
CALL FACTOR (0.5)
CALL AXIS (0.0,0.0,7HGAIN,DB,+7,10.0,90.0,-50.0,5.0)
CALL AXIS (0.0,0.0,13HANGLE,DEGREES,-13,10.0,0.0,0.0,1.0)
CALL GRID (0.0,0.0,1.0,1.0,10,10)
CALL SYMBOL (6.5,6.5,0.14,10HANT.GAIN =,0.0,10)
CALL NUMBER (999.,6.5,0.14,ANTG,0.0,3)
CALL SYMBOL (6.1,6.1,0.14,3H DB,0.0,3)
CALL SYMBOL (6.1,6.1,0.14,1,0.0,-1)
CALL SYMBOL (6.5,6.1,0.14,13H E-PLANE RAD.,0.0,13)
CALL SYMBOL (6.1,6.6,0.14,2,0.0,-1)
CALL SYMBOL (6.5,6.6,0.14,13H H-PLANE RAD.,0.0,13)
CALL SYMBOL (6.1,6.1,0.14,4,0.0,-1)
CALL SYMBOL (6.5,6.1,0.14,19H CROSS POLORIZATION,0.0,19)
CALL LINE (X,Y1,NP,1,7,1)
CALL LINE (X,Y2,NP,1,5,2)
CALL LINE (X,Y3,NP,1,0,4)
CALL PLOT (14.0,0.0,999)
STOP
END
```